INFLUENCE OF RAW MATERIALS AND BINDING AGENTS ON ENGINEERING PROPERTIES OF FLY ASH BASED PELLETIZED AGGREGATES

Thesis

Submitted in partial fulfilment of the requirements for the degree of

DOCTOR OF PHILOSOPHY

by

B P SHARATH

(187CV501)

DEPARTMENT OF CIVIL ENGINEERING

NATIONAL INSTITUTE OF TECHNOLOGY

KARNATAKA, SURATHKAL, MANGALORE - 575 025

MAY 2024

INFLUENCE OF RAW MATERIALS AND BINDING AGENTS ON ENGINEERING PROPERTIES OF FLY ASH BASED PELLETIZED AGGREGATES

Thesis

Submitted in partial fulfilment of the requirements for the degree of

DOCTOR OF PHILOSOPHY

by

B P SHARATH

(187CV501)

Under the Guidance of

Dr. BIBHUTI BHUSAN DAS

Professor

DEPARTMENT OF CIVIL ENGINEERING

NATIONAL INSTITUTE OF TECHNOLOGY KARNATAKA,

SURATHKAL, MANGALORE - 575 025

MAY 2024

DECLARATION

I hereby declare that the Research Thesis entitled **"Influence of Raw Materials and Binding Agents on Engineering Properties of Fly ash Based Pelletized Aggregates"** which is being submitted to the **National Institute of Technology Karnataka, Surathkal** in partial fulfilment of the requirements for the award of the Degree of **Doctor of Philosophy** in **Civil Engineering** is a bonafide report of the research work carried out by me. The material contained in this Research Thesis has not been submitted to any University or Institution for the award of any degree.

Place: NITK, SURATHKAL
Date: 30/05/24

B P SHARATH
187CV501
Research Scholar
Department of Civil Engineering

CERTIFICATE

This is to certify that the Research Thesis entitled **"Influence of Raw Materials and Binding Agents on Engineering Properties of Fly ash Based Pelletized Aggregates"** submitted by **B P SHARATH** (Registration number: 187CV501) as the record of research work carried out by him, is accepted as Research Thesis submission in partial fulfilment of the requirements for the award of degree of **Doctor of Philosophy**.

Dr. BIBHUTI BHUSAN DAS
Department of Civil Engineering
Research Supervisor

Dr. SUBHASH C YARAGAL
Department of Civil Engineering
Chairman - DRPC

NATIONAL INSTITUTE OF TECHNOLOGY KARNATAKA, SURATHKAL
DEPT. OF CIVIL ENGG.

Chairman (DRPC)
Department of Civil Engineering
National Institute of Technology Karnataka
Surathkal, Mangalore - 575 025, Karnataka, INDIA

Dedicated to

My Beloved Parents

and

Professors

ACKNOWLEDGEMENT

I take this opportunity to express my sincere gratitude and profound thanks to my guide and Dr. Bibhuti Bhusan Das, Professor, Department of Civil Engineering. His keen engineering and scientific insight have helped me tremendously in improving the technical content and practical relevance of the thesis. Working with him has been a great learning experience to me. This research would not have been possible without his constant support and guidance. More than anything, he looked after me as a guardian and helped me immensely. To accomplish my doctorate thesis under his supervision has been both a great privilege and honor for me. I acknowledge, the time spent in technical discussions with him as immensely interesting and profoundly knowledge enhancing, for which I am greatly indebted to.

I wish to extend my sincere thanks to Prof. Gangadhar Mahesh, Professor, Department of Civil Engineering, and Dr. Saumen Mandal, Associate Professor, Department of Metallurgical and Materials Engineering for being the Research Progress Assessment Committee (RPAC) members and their valuable suggestions at various stages of this research work.

I wish to thank Prof. Subhash C Yaragal., Head of the Department of Civil Engineering and Prof. B R Jayalekshmi, former Head of the Department of Civil Engineering, for their support and encouragement throughout the journey of my research. I am grateful to the course instructors during my course work Prof. Bibhuti Bhusan Das, Prof. Suresha S N, Prof. Murulidhar N N, through whom I have learnt a lot.

I would also like to thank the support and facilities extended by Prof. Bibhuti Bhusan Das, faculty-in-charge of Materials and Testing Laboratory, Dr. T Palanisamy faculty-in-charge of Industrial Structures Laboratory and Dr. Babloo Chaudhary, faculty-in-charge of Geotechnical Laboratory

My thanks are also due to the office staff of Civil Engineering Department, especially Mr. Monnappanna Mrs. Anvitha Shanbhogue, Mrs. Tara Devadiga and Mrs. Prabhavathi Kolla for their constant administrative help at different stages of my research.

This research work would not have been possible without the support and cooperation of the Foremen of Materials and Testing Laboratory Mr. Geetesh Shetty. and other supporting

staff of civil engineering laboratory members, Mr. Ramanath Acharaya, Mr. Shashikanth M Devadiga, Mr. Ranjith, Mr. Prasad Suvarna, Mr. Yatheesha Kumar, Mr. Pawan Kumar and Mr. Subhas, humbly acknowledged.

I would like to express my sincere gratitude to the authorities of NITK Surathkal, for providing me excellent facilities inside the campus. And also, I would like to thank all the teaching and non-teaching staff of Department of Civil Engineering, National Institute of Technology Karnataka, Surathkal, for their co-operation and help during the project work.

I am extremely thankful to Mr. Roque D Souza and Mr. Ramakrishna Rao, retired general managers, KIOCL Limited for permitting me to conduct a part of my research at the organization. Additionally, I would also like extend my deep gratitude to Mr. Salam M A, head of the department (retired), Mr. Balakrishna and Mr. Shastri, deputy managers (retired), in the process control department, KIOCL Limited for their support and help in conducting experiments in the departmental laboratory.

Without the support and help of my seniors Dr. Shivaprasad K N, Dr. Sharan Kumar Goudar, Dr. Snehal K, Dr. Raghuram K C, Dr. Prasanna K M and present research scholars Mr. Sumukh E P, Mr. Anil Sagar S, Mr. Rakesh P, Mr. Shiv Sai Trivedi and Mr. Sanjeet Kumar Mishra and Mrs. Shwetha K G, this research work would not have seen the light of the day.

I acknowledge the help received from the former M.Tech students of construction technology and management engineering Mr. Neeraj Kumar Bharathi, Mr. Anuj Kumar, Mr. Nikunj P, Sreehari M, Mr. Akhilesh Kumar and Ms. Kanupriya in the conduction of laboratory experiments.

I am thankful to my beloved parents, without whose encouragement and support this work would not have been possible. Above all I thank almighty for guiding me and showering blessings to complete this thesis successfully.

B P SHARATH

ABSTRACT

This experimental research investigates the influence of geopolymerization factors on the engineering properties of ambiently cured binary blended pelletized aggregates containing fly ash (FA), bentonite (BT), burnt lime (BL), ground granulated blast furnace slag (GGBS), iron ore tailings (IOT) and copper ore tailings (COT). Additionally, this research also demonstrated the production of multi-blended pelletized aggregates with ultrafine fly ash addition (UFA) in the optimized proportions of binary blended pelletized aggregates cured in ambient temperature conditions. In the first phase of this study, governing parameters of geopolymerization, like the dosage contents of Na_2O and water and the ratio of SiO_2/Na_2O, were coupled with the dosage contents of additive admixtures, that is, BT, BL and GGBS for producing and assessing the properties of binary blended pelletized FA-BT, FA-BL and FA-GGBS aggregates. Furthermore, in order to further improve the engineering properties of binary blended pelletized aggregates, the admixing of IOT and COT was conducted to produce FAIOT and FACOT aggregates. The concept of design of experiments was used for jointly investigating the influence of governing factors of geopolymerization and dosage contents of BT, BL, GGBS, IOT and COT. In the second phase of this study, to produce superior quality multi-blended pelletized aggregates, UFA was substituted in the optimized mixes identified from the binary blended pelletized aggregates. The engineering properties of pelletized aggregates, like specific gravity, aggregate impact value, aggregate crushing value, water absorption and individual crushing strength, were assessed in compliance with the respective testing standards. Microstructural, thermal and identification of chemical bonds were carried out through advanced characterization techniques such as scanning electron microscopy coupled with energy dispersive X-ray spectroscopy (SEM-EDS), thermogravimetric analysis (TGA) and Fourier transform infrared spectroscopy (FTIR).

The experimental test results revealed that higher dosages of Na_2O and mineral admixture BT, GGBS were to be more influential factors in pelletized FA-BT and FAGGBS aggregates. However, Na_2O and water content were found to be the principal factors in pelletized FA-BL aggregates. The inclusion of IOT and COT addition has considerably affected the engineering characteristics of pelletized FAIOT and FACOT aggregates. The admixing of UFA in the production of multi-blended pelletized aggregates has resulted in the attainment of superior characteristics. The quantified amount of hydration products in binary and multi-blended pelletized aggregates that is, N-A-S-H, C-S-H and C-H,

intensified with increasing dosages of Na_2O, mineral admixtures IOT and COT. The FTIR spectrum showed strong and broadened bands of Si-O terminal for all types of blended aggregates, representing the conversion of unreacted minerals to chains of aluminosilicate gel (geopolymerized hydration product).

CONTENTS

LIST OF TABLES

LIST OF FIGURES

NOMENCLATURE

Abbreviations

FA	Fly ash
PPC	Portland pozzolana cement
MT	Metric tonnes
PCS	Particle crushing strength
PS	Particle crushing load
BS	Bulk crushing strength
SSD	Saturated surface dry particle density
OD	Oven dry particle density
TPFV	Ten percent fines value
WA	Water absorption
BA	Bottom ash
SF	Silica fume
GGBS	Ground granulated blast furnace slag
RHA	Rice husk ash
MSWI	Municipal solid waste incinerator fly ash
WAS	Washing aggregate sludge
MK	Metakaolin
UFA	Ultrafine fly ash
BT	Bentonite
BL	Burnt lime
IOT	Iron ore tailings
COT	Copper ore tailings
RPM	Revolutions per minute
SEM	Scanning electron microscopy
AIV	Aggregate impact value
ACV	Aggregate crushing value
IPS	Individual crushing strength of pellets
GRG	Grey relational grade
EDS	Energy dispersive spectroscopy
TGA	Thermogravimetric analysis
DTG	Derivative of thermogravimetry
EN	European standards
IS	Indian standards
FTIR	Fourier transform infrared spectroscopy

CHAPTER – 1

INTRODUCTION

1.1 GENERAL

Cement production is responsible for 8-9% of all anthropogenic CO_2 emissions (Brinkman and Miller 2021). Hence, specific importance is being given to the inclusion of various industrial by-products and industrial wastes, such as fly ash, GGBS, and silica fume, as a substitute for cement and concrete production. Utilization of these by-products helps in reducing the excessive usage of OPC and the rising CO_2 emissions associated with its production (Mannan and Neglo 2010). One of the significant ingredients of concrete, i.e., aggregates, consists of about 70-80% of the volume of concrete (Oktay et al. 2015). A recently published report stated that, in 2018, the global market for construction aggregates was valued at approximately $ 360 billion, which is likely to increase to more than $ 490 billion by 2025, at a multiple-yearly growth rate of 4.6% between 2019 and 2025 (Zion 2019). Consequently, with the increase in urbanization, finding sources for these large amounts of construction aggregates has led to the exhaustion of natural aggregates.

Nowadays, the fulfilment of primary energy requirements has become more complicated as a result of industrialization. So, coal-based energy production systems have attracted significant attention in providing large-scaled energy production facilities. During the process of energy extraction, power plants utilize pulverized coal as a fuel source, resulting in the production of fly ash. It is identified as one among the various wastes which causes an impact on the environment, especially polluting air and water. As per the recent available reports, the world's FA market size was valued at USD 12.25 billion in 2021, which is projected to grow from USD 12.70 billion in 2022 to USD 19.19 billion by 2029, exhibiting a compound annual growth rate of 6.1 % during the forecasted period (Insights 2021). Hence, efficient use of fly ash can bring down the coal combustion amounts, which need to disposed of in landfills; otherwise, it can pose dangerous consequences to the environment as well as to human health (Sharath et al. 2023a).

In addition, there is a need to use anthropogenic wastes, such as mine wastes (Ahmari and Zhang 2012). Mining and ore upgradation operations generates enormous quantities of solid wastes and by-products consisting chiefly of mine waste rocks, tailings, ashes, slags

and sludges (Palmer et al. 2010). Presently, the challenge of sustainable disposal of these mine tailings and mine waste landfills has become considerably critical (Dong et al. 2019; Nurcholis et al. 2017; Vickers 2017; Zhou et al. 2020). On one side, the tailings may comprise little amounts of target material with previously unclaimed elements, which can be restored back with the adoption of a suitable mining techniques (Kaze et al. 2021; Rico et al. 2008; Zhang et al. 2021), and on the other side, chemical compositions of mine tailings formation mostly consists of silica, alumina, and calcium oxide, with a content ranging from 60-90% (Lazorenko et al. 2021). Because of this reason, these tailing materials are having a strong potential to be used as an alternative source which can fulfil the wide range of construction and other industries requirements (Divvala 2021; Dold 2020; Eugênio et al. 2021; Kinnunen et al. 2018; Rico et al. 2008).

Iron ore tailings are solid wastes which are generated after the completion of beneficiation process of iron ores. Similarly, copper ore tailings are a waste rock that remains after the accomplishment of ore processing in removing the copper. Due to complexity of ores, the generation amount of iron ore tailings differs from region by region. In the year 2019, the worldwide output of iron ore, based on useable ore, reached to around 2.5 billion tons, containing an estimated 1.5 billion tons of iron. Notably, this upsurge in production was recorded in the countries like Australia, Brazil, China, and India. Furthermore, as per the report 'Monthly Summary on Non-Ferrous Minerals and Metals, April 2022: Govt. of India', the global copper mine production from April 2021 – January 2022 was about 17,862 MT, wherein India's alone share in worldwide production of copper was 21.126 thousand MT during April 2021 – January 2022. Prolonged disposal of mine tailings that contains radioactive materials such as Pb, Hg, and other mine tailings related toxins in the open environment builds-up tailings (Li et al. 2019; Salam et al. 2021), pollutes soils, air (Csavina et al. 2012; Moradi et al. 2021; Zhang et al. 2020) and water (Hageman and Briggs 2000; Nguyen et al. 2022; Zhai et al. 2022). This clearly indicates the need of the hour for sustainable utilization of these mine tailings i.e., iron ore and copper ore tailings, into valuable resources like artificially producing coarse aggregates.

Recent years have witnessed a significant development in the area of cementitious materials, viz. geopolymer, a novel inorganic material all around the globe. These geopolymer materials was originally introduced by Davidovits in 1970's in the field of inorganic cementitious materials (Davidovits 1991). Its synthesis consists of admixing aluminosilicate-rich materials with a combination of strong alkaline solutions that are cured under ambient temperature conditions (Sharath et al. 2023a).

Enough literature is available that states that artificial aggregates were being produced by adopting a well-known metallurgical process called agglomeration, where finer particles are converted into fresh agglomerates (often called pellets) of varied shapes and sizes (Nor et al. 2016). Literature reports that the whole process of pelletization is influenced by several factors such as (i) fineness of raw materials, (ii) water content, (iii) type, nature, and dosage of binding agent, and (iv) duration of pelletization (Gomathi and Sivakumar 2014a; Kockal and Ozturan 2011; Manikandan and Ramamurthy 2007; Priyadharshini et al. 2011; Ramamurthy and Harikrishnan 2006). It is understood from past literature that production of aggregates using class-C FA was stronger and more stable as compared to those produced using class-F fly ash (Bijen 1986a; Manikandan and Ramamurthy 2008). This could be attributed to the existence of calcium-rich FA interferes with the process of polymerization, resulting in flash setting and also altering the microstructure (Zhao et al. 2019). However, it is reported that utilisation of low calcium FA (i.e., ASTM class-F fly ash) is found to be more beneficial compared to that of high calcium FA (i.e., ASTM class-C fly ash) especially from the shrinkage and durability aspects when incorporated in the geopolymeric system (Hardjito and Rangan 2005). It is also reported that the existence of silica and alumina rich precursors such as class-F fly ash undergoes a glass transition phase leading to the fusion of Si-O-Al chains (aluminosilicate gel), which aids in improving the hardened properties of aggregates like aggregate impact value, aggregate crushing value, individual pellet strength, and abrasion of the produced aggregates (Bui et al. 2012a). Various researchers have stated that regardless of the positive aspects of class-F fly ash in the process of geopolymerization, fly ash added mixes showed a slow rate of strength gain (Sumer 2012), delayed setting time (Nath et al. 2015), possessing less specific gravity, lightweight as per EN 13055-1 (DIN 2015), and with lower individual pellet strength values (Chi et al. 2003).

It is for these reasons that researchers started adding several additive admixtures such as GGBS (Bui et al. 2012b), lime (Reddy et al. 2016; Videla and Martinez 2002), clay binders (Geetha and Ramamurthy 2010a; Ramamurthy and Harikrishnan 2006), bentonite (Gomathi and Sivakumar 2012; Manikandan and Ramamurthy 2009) alkali activators like NaOH, KOH etc., (Geetha and Ramamurthy 2013; Shivaprasad and Das 2018; Terzić et al. 2015) in the production of fly ash based pelletized aggregates (especially with class-F fly ash) for enhancing the engineering properties of the produced aggregates (Wasserman and Bentur 1997; Yang et al. 2011). Additionally, for producing pelletized aggregates with superior characteristics like reduced water absorption, specific gravity, density, etc.,

incorporation of mine tailings is also a viable option since high in specific gravity of mine tailings (iron and copper ore tailings) would facilitate in achieving characteristics in comparison to that of natural aggregates (Sharath et al. 2023a).

Nevertheless, utilizing an alkaline solution in conjunction with precursor (fly ash), additive admixtures, and mine tailings in the production of pelletized aggregates is complicated and challenging process. In order to combinedly understand the complexity of the relative influence of geopolymerization factors (mineral as well as chemical) with additive admixtures and mine tailings on the properties of produced aggregates, the concept of experimental design plays an important role at this stage (Cavazzuti 2013a; Krishnan and Purushothaman 2017; Montgomery 2017; Soudki et al. 2001). Various other experimental designs such as factorial designs (Cavazzuti 2013a; Krishnan and Purushothaman 2017; Soudki et al. 2001), response surface methodology (Cavazzuti 2013b; Hanrahan and Lu 2006; Vasugi and Ramamurthy 2014) and other methodologies are available for formulating and optimizing the production process of pelletized aggregates. Among all of these experimental design methodologies, it is reported that by using Taguchi's experimental design methodology, a suitable understanding can be developed between the evaluated responses and considered governing factors through the response indices concept (Shivaprasad and Das 2018) with the conduction of a minimum number of experimental trials. Further, for obtaining a clear understanding of the response indices altogether, the researchers adopted grey relational analysis as it benefitted by converting a multi-objective problem into a single objective function (Sahoo et al. 2017; Shivaprasad and Das 2018).

Regardless of the fact that sufficient information is available in the literature, the production of FA based pelletized aggregates admixed with additive admixtures and mine tailings in conjuncture with alkaline solution as a binding medium will have the strong potential to significantly reduce the need for large quantities of aggregate in concrete, thereby mitigating the dependency on mining operations for aggregate extraction from the quarries.

1.2 NEED OF THE PRESENT RESEARCH WORK

Sustainable usage of industrial by-products in the production of blended cement has formulated the idea of the sustainable production and development of construction materials. As per the current scenario, the consumption of artificially recreated materials using industrial by-products in cement and concrete has drawn considerable attention. The utilisation of natural aggregates in concrete production is increasing day by day, making it one of the scarce resources in the near future. Hence, there is a need for alternative building

materials for construction industries which can be a substitution for natural aggregates. Producing such alternative materials by utilising the maximum number of industrial by-products such as fly ash with additive admixtures (mineral and chemical) and mine tailings is the need of the hour that can be achieved through a retrospective approach. Since curing regime plays a vital role it is also essential to make the production process less energy intensive and in this scenario production of fly ash pelletized based aggregates through ambient curing pays a vital contribution.

1.3 THESIS STRUCTURE

The present thesis is structured into six different chapters. The chapter one discusses a generalized introduction and necessity of the present research work is presented. The chapter two discusses a complete literature review and a critical review for identification of research gap/problem. The third chapter consists of all the source materials utilized in this experimental research, methodology adopted for the production of binary and multi-blended pelletized aggregates is presented and standard testing methods applicable for testing of the produced aggregates is presented. The results and discussions on the impact of governing factors on the production of binary and multi-blended pelletized aggregates are presented in chapter four. The attained results for multi-blended pelletized aggregates are presented in chapter five. The concluding remarks as well as major findings of this experimental research with the scope for further research is presented in chapter six.

CHAPTER – 2

LITERATURE REVIEW

2.1 GENERAL

This chapter provides a detailed assessment of relevant literature on the production of pelletized aggregates using various industrial by-products along with binding agents. Further, the viability of utilizing geopolymer binder in the manufacturing of pelletized aggregates is also discussed in this chapter.

2.2 THEORY OF PELLETIZATION

The principle of pelletization was formulated during the 1940's. The process of pelletization for fine powders has undergone significant growth in relevance, particularly within the metallurgical industry (Ramamurthy and Harikrishnan 2006). Although this method has been widely employed in the manufacturing of pelletized aggregates, it is not yet widely implemented in the construction industry. The rationale for this was the ample availability of natural resources and the comparatively high production costs of pelletized aggregates in contrast to natural aggregates (Baykal and Döven 2000).

2.2.1 Process of pelletization

The pelletization process can be described as the method that produces larger spherical units by rolling the moistened fine particles in the absence of any external pressures. The desired particle size distribution of pelletized aggregates can be achieved by two methods: crushing larger aggregates or by agglomerating the cementitious fines either by themselves or blending those with any binding agents. The process of pelletization refers to the aggregation of particles that have been moistened within a revolving drum or disc. The final output of the pelletization process is commonly known as a "fresh/green pellet." The crushing strength of the green pellet should be sufficient enough to facilitate their transportation and storage. Depending on the characteristics of the fines used in the pelletization process and the intended purpose of usage, the pellets may be sintered for a predetermined period of time after manufacturing to optimize their engineering performance (Baykal and Döven 2000).

2.2.2 Sequential steps involved in producing pellets

1. Selecting a precursor for production followed by fixing the appropriate mixing dosage.
2. Agglomeration of precursors either by agitation or by pressure for the formation of pellets
3. The fresh agglomerates undergo through the process of hardening wherein these weak agglomerates get bonded more firmly. The commonly used hardening techniques are sintering, autoclaving and cold bonding.
4. Finally, these firm, strong, well bonded pellets are sieved in order to classify from undesirable and undersized pellets.

The sequential steps discussed above are represented below in Figure 2.1.

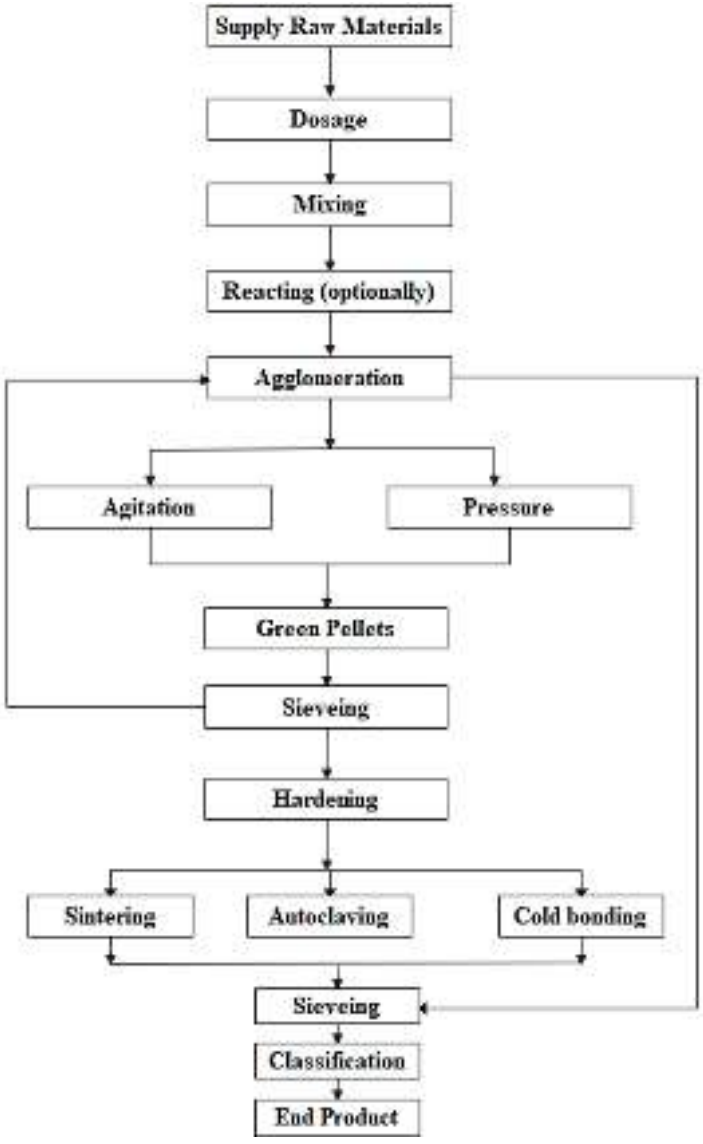

Figure 2.1: Sequential steps involved in producing pellets (Source: Bijen 1986a)

2.2.3 Green pellet formation mechanism

The production of agglomerates is influenced by two phenomena, with the major one being dependent upon the specific location and method employed for feeding the ingredients/precursors and binding agents or binders. One method for the formation of pellets might be referred to as "rolling of shells" or the "snowball effect" as illustrated in Figure 2.2.

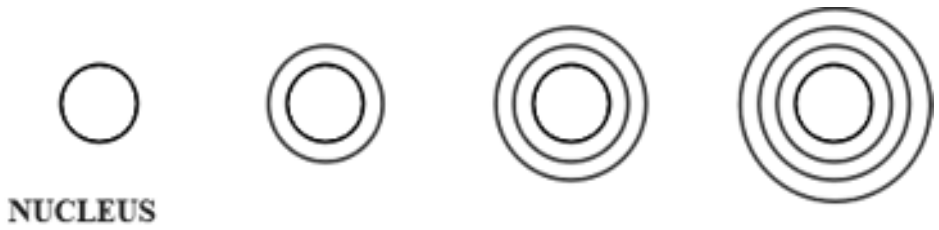

Figure 2.2: Influence of 'snowball' phenomenon on green pellet formation (Rao 1994)

As previously stated, under the influence of the second phenomenon that is, addition of a/any binding agent, the pores fill up with water, and the entire system of a pellet behaves like a capillary tube filled with water, where an attractive force is developed that operates on the fines and thus holds these moistened particles together in the form of pellets (Rao 1994). In the early phases, the bond between the particles is caused by a water bridge and will be insufficiently strong (Figure 2.3). As the binder dosage increases, the liquid film atop the particles begins to combine, and the spaces between the particles fill up with air (Figure 2.3). Surface forces from the meniscus traveling between individual particles affect particle coherence (Rao 1994). As more wet particles are coated onto the nucleus, the ball expands. Mechanical forces produced by bumping balls against each other and against the walls of the revolving device in which they are enclosed expel the air enveloped in the balls, resulting in the full capillary stage (Figure 2.3). At this point, the liquid has filled the open space between the particles, resulting in particle coherence throughout the ball due to capillary forces (Rao 1994).

Figure 2.3: Mechanism of ball formation (Rao 1994)

Both behaviors exist in the case of larger pellets. Surface tension causes the formation of the initial nucleus, which develops in size as more succeeding layers are deposited on top of it. More fines moistening leads to large, uneven balls, as illustrated in Figure 2.4.

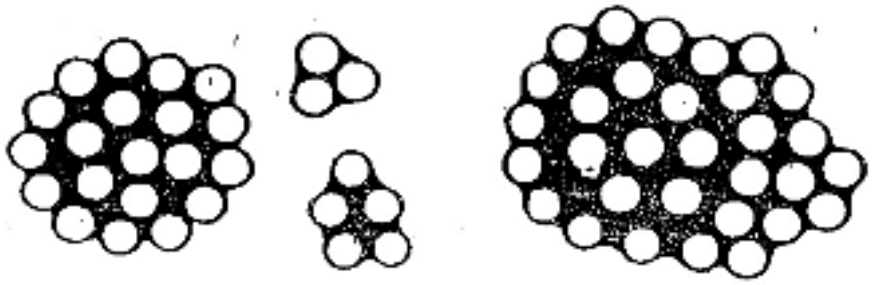

Figure 2.4: Formation of irregular shaped balls (Rao 1994)

2.2.4 Parameters governing the process of pelletization

Many researchers indicated that raw materials, moisture content, binder type, dosage, and pelletization duration are all the parameters that govern the pelletization process in producing pellets from finer particles (Ramamurthy and Harikrishnan 2006; Tajra et al. 2019), as well as some of the parameters that should be considered for the efficiency of pellet production i.e., specifically, the type of pelletizer used in the pelletization process. Furthermore, it is stated that the hardening procedures used to produce pellets are sintering, conventional water curing, autoclaving, and steam curing (Harikrishnan and Ramamurthy 2006). However, the energy required for the processes used which produce the agglomerated material (i.e., curing regime and sintering) is significant and the engineering performance of the resultant pellets is primarily determined by the binder employed in the process (Baykal and Döven 2000; Harikrishnan and Ramamurthy 2006).

For the production of pellets, various types of pelletizers were employed, including disc or pan type, drum type, cone type, and mixer type (Sastry et al. 2021; Sivakumar and Gomathi 2012). Among these pelletizers, the disc type pelletizer has a more controllable pellet size distribution than the drum type pelletizer. In the disc pelletization, the formation of green pellets takes place in two phases. In the very first phase, the initially formed pellets (termed as seeds), grow larger in size. Figure 2.5 depicts the growing path of pellets in a disc pelletizer with an adjustment in its inclination. As mentioned above, the grain size distribution of pellets can be controlled with ease by using a disc pelletizer rather than using a drum pelletizer (Bijen 1986b).

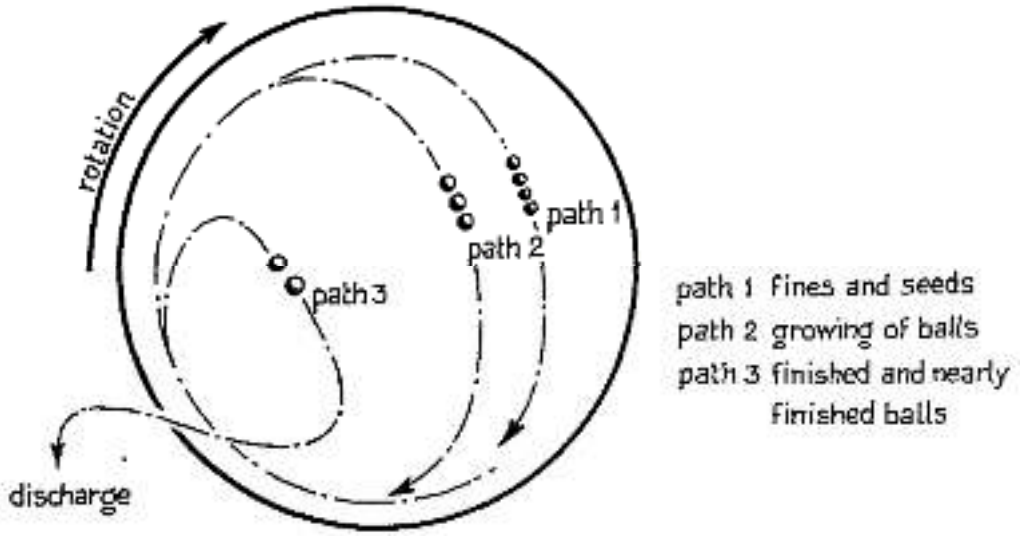

Figure 2.5: Growing paths of green pellets in a disc pelletizer (Source: Bijen 1986b)

2.3 REVIEW OF RAW MATERIALS, BINDERS, PRODUCTION PROCESS PARAMETERS, AND CHARACRTERISTICS OF PELLETIZED AGGREGATES

Table 2.1 displays the variety of raw materials, binders, production process parameters and characteristics of the pelletized aggregates reported by the researchers.

Table 2.1: Production process parameters, binders and characteristic properties explored by various researchers for producing pelletized aggregates

Reference	Composition of pelletized aggregates		Production process parameters used in disc pelletization						Characteristics of pelletized aggregates (Designation by ranking*)						
											Density (g/cc)		Crushing strength		
	Base materials; supplement	Binders	Diameter (mm)	Depth (mm)	Water content (%)	Angle (°)	Speed (rpm)	Duration (min)	Size (mm)	WA (%)	SSD	OD	PCS (MPa)	PS (N)	BS (MPa)
(Tajra et al. 2018)	FA and perlite	OPC	400	100	12	35	30	15	2-8	High	-	Less	-	-	III
(Güneyisi et al. 2015)	FA and OPC	OPC	800	350	-	-	-	20	0.25 to 4	High	Less	-	-	-	-
(Reddy et al. 2016)	FA	OPC and lime	550	250	-	55	40	-	10 to 12.5	Medium	-	-	-	-	-
(Videla and Martinez 2002)	FA	PPC, OPC and lime	1500	250		-	-	-							
(Geetha and Ramamurthy 2010b)	FA and BA; Na_2SO_4	OPC and lime	-	-	31	-	-	14 to 7	10 to 12.5	High	-	-	-	-	-
(Kockal and Ozturan 2011)	FA; SF	OPC, bentonite and glass powder	400	150	-	43	45	20	4.75 to 19	-	Less	Less	-	III	-
(Gomathi and Sivakumar 2012)	FA; NaOH	OPC and lime	500	250	25	36	55	10 to 15	-	Medium to high	Less to more	Less	II to III	-	-
(Kockal and Ozturan 2011)	FA	Bentonite and glass powder	400	150	22-25	43	45	20							

(Terzić et al. 2015)	FA	Na_2SiO_3	-	-	-	-	-	-	0.5 to 14	Medium to high	-	-	-	III	-
(Gesoğlu et al. 2007)	FA	OPC	-	-	24-30	35	43	20	4 to 14	High	-	Less	-	I to III	-
(Vasugi and Ramamurthy 2014)	Pond ash; Na_2SO_4	OPC and lime	-	-	28-33			14 to 7	-	Medium to high	-	-	-	-	-
(Baykal and Döven 2000)	FA	OPC and lime	400	60		43	45	20	4.75 to 19	High	-	Less	-	I to III	-
(Manikandan and Ramamurthy 2009)	FA	Bentonite (medium and high swelling)	-	-	31-35	50-55	47-54	14-15	-	-	-	-	-	-	-
(Geetha and Ramamurthy 2010b)	BA	Kaolinite, metakaolin and OPC	-	250	30-33	-	-	-	-	-	-	-	-	-	-
(Manikandan and Ramamurthy 2007)	FA	Bentonite and kaolinite	-	-	33-35	-	35-55	15	-	-	-	-	-	-	-
(Ramamurthy and Harikrishnan 2006)	FA	OPC, Lime and bentonite	570	250	-	55	40	-	-	-	-	-	-	-	-
(Thomas and Harilal 2015)	Quarry dust and FA	OPC	600	100		25	26	-	6.5 to 20	Medium to high	Less to more	Less to more	II to III	-	-

(Hwang and Tran 2015)	FA and GGBS	PC, NaOH and Na_2SiO_3	800	300	-	-	-	-	4-10	Medium to high	Less to more	Less	III	-	II
(Gesoğlu et al. 2012)	FA and GGBS	OPC	800	350	-	45	42	-	4-14	Low to medium	Less to more	Less to more	-	I to III	-
(Bui et al. 2012c)	FA, GGBS and RHA	NaOH and Na_2SiO_3	800	300	-	53	35	-	4.75-9.5	Low to medium	-	-	-	II	-
(Bui et al. 2012c)	FA, GGBS and RHA	OPC	800	300	-	-	-	-	-	Low to high	-	-	-	-	I to III
(Tang et al. 2017)	MSWI Bottom Ash, FA and Paper Sludge Ash	OPC	100	150	-	45	15	-	2-8	Medium	Less	Less			II
(Colangelo et al. 2015)	MSWI FA	OPC and lime	800	160		45	40	-	4-18	Low to medium	Less	-			I to II
(Tang and Brouwers 2018)	FA, WAS, MSWI, BA; Nano silica, Polypropylene Fibre	OPC	100	150	20	45	15	-	-	Medium to high	-	-	-	-	I
(Geetha and Ramamurthy 2013)	BA and Lime	NaOH and Na_2SiO_3	-	-	-	-	-	-	4.75 to 12.5	Medium	-	-	-	-	-

(Gomathi et al. 2013)	FA	GGBS and NaOH			25	36	55	10-15	6 to 20	-	-	-	I to III		
(Ramamurthy and Harikrishnan 2006)	FA	-	570	250		40 and 70	20 and 40	10 and 20	5 to 16	High	-	-	-	-	-
(Cioffi et al. 2011)	MSWI and BA	OPC	-	-	-	-	-	-	5 to 20	Medium	Less	-	-	-	III
(Shivaprasad and Das 2018)	FA	NaOH and Na_2SiO_3	450	100	19	45	-	15	-	-	-	-	-	-	-
(Gomathi and Sivakumar 2015a)	FA and bentonite	NaOH	500	270	-	36	55	15	-	-	-	-	-	-	-
(Manikandan and Ramamurthy 2008)	FA	-	560	250	31	55	55	-	-	-	-	-	-	-	-

The data shown in the Table 2.1 clearly indicates that fly ash is the predominant material utilized in the production of pelletized aggregates. The reason for this commonality is the widespread availability of this type of waste material, as well as the urgent need to recycle it into a value product (Ahmaruzzaman 2010). In conjunction with fly ash, other indigenous industrial waste materials were also been utilized in the manufacturing of pelletized aggregates, as depicted in Table 2.1, that comprise GGBS, rice husk ash, MSWI, and WAS. The utilization of a binder is a crucial component in the pelletization process, particularly when dealing with a raw material that possesses limited or negligible cementitious characteristics. As indicated in Table 2.1, in addition to OPC which has been extensively employed in the literature, other binders such as bentonite, glass powder, lime, and clay have been employed. Furthermore, the environmental impact of cement production has encouraged researchers to use alternate binders. As a result, an alkaline activator composed of sodium silicate (Na_2SiO_3) and sodium hydroxide (NaOH) has been added into production of geopolymer based pelletized aggregates.

2.3.1 Characteristics of pelletized aggregates

The physical and mechanical characteristics of pelletized aggregates obtained by various researchers throughout their experimental investigations are ranked in the Table 2.1. The range of the obtained values for the characteristic properties based on which the designation of ranking is

For WA → Low – 0 to 9%; Medium – 10 to 20%; High – More than 20%

For Density → Less – 0 to 2 g/cc; More – greater than 2 g/cc

For crushing strength → PCS – I: > 10 MPa; II: 5 to 10 MPa; III: < 5 MPa; PS – I: > 500 N; II: 100 to 500 N; III: < 100 N; BS – I: > 10 MPa; II:5 to 10 MPa; III: < 5 MPa

The Table 2.1 illustrates that the particle sizes, particle density, loose bulk density, and water absorption of pelletized aggregates as reported in the literature (presented in Table 2.1) fall within the ranges of 4 to 20 mm, 0.88 to 21.2 g/cm^3, 510 to 1247 kg/m^3, and 2.5 to 77%, respectively. The presented data in Table 2.1 clearly indicates that the majority of the aggregates that has been produced demonstrates an oven dry particle density of less than 2 g/cm^3 or a loose bulk density of less < 1200 kg/m^3. As a result, they can be categorized as lightweight aggregates, as per the guidelines outlined in EN 13055-1 (DIN 2013). Individual crushing strengths of pelletized aggregates ranged from 30 to 2210 N, and 0.4

to 22.8 MPa, with bulk crushing strength ranging from 0.2 to 15.7 MPa. The observed variations in crushing strength of pellets, even within a single research, can be directly related to the specific characteristics of the raw materials, such as their form, particle size, and density (Li et al. 2000).

2.3.2 Influence of production process parameters

According to the reported literature presented in Table 2.1, there has been limited study conducted on the impact of production process parameters on the pelletization efficiency of the produced pelletized aggregates. According to the findings of Manikandan and Ramamurthy, the utilization of low angles and speeds in the pelletizer results in a reduction in particle movement paths and a decrease in particle collisions. Consequently, this leads to the production of smaller aggregates with inadequate efficiency (Manikandan and Ramamurthy 2009).

In addition to aggregate size, it has been noted that other properties of pelletized aggregates are significantly influenced by production process parameters, as illustrated in Table 2.1. Colangelo and Cioffi produced pelletized aggregates at varied revolution speeds (35, 45, and 55 rpm) at a constant angle of 50°, revealing that the highest density and strength of pelletized aggregates are attained at 45 RPM rather than the maximum speed of 55 RPM. The association between angle and speed contributes considerably to achieving optimal particle movement and collision, thereby increasing the structure of the aggregate formed (Colangelo and Cioffi 2013). Tajra et al. investigated three speeds (20, 30, and 40 RPM) and two angles (35° and 40°). Researchers discovered that as the speed of rotation increased, the particle density and bulk crushing strength of the aggregates formed increased at any fixed angle. As a result, they determined that the faster the rotation, the denser the pelletized aggregate's structure. It was also established that increasing the angle speed, and duration of pelletization results in a longer pellet path and hence a rise in tumbling forces, resulting in the formation of compacted aggregates with reduced water absorption and higher strengths (Vasugi and Ramamurthy 2014).

2.3.3 Influence of raw materials and binding agents

Table 2.1 presents an assessment of the viability of several by-products as well as various types of binders, in relation to the manufacturing of pelletized aggregates. The properties of the raw materials and their compatibility play a crucial role in determining the production efficiency and properties of the resulting aggregates (Chiou et al. 2006). According to Gesoğlu et al., the fineness of the raw materials has the greatest influence on pelletization

efficiency. They found that crushed fly ash with a fineness of 570 m^2/kg pelletized more efficiently than fly ash with a specific area of 287 m^2/kg (Gesoğlu et al. 2012). Geetha and Ramamurthy investigated the impact of several binders on the productivity of low calcium bottom ash based aggregate (Geetha and Ramamurthy 2010a), obtaining a pelletization efficiency of 98% with cement, lime, and high swelling bentonite as binders at a 14% weight content. The same efficiency was obtained using 25 % medium swelling bentonite and 30% weight of clay binders like kaolin and metakaolin. Many researchers have been pushing for the use of additives to improve pelletization efficiency, and it has been established in the literature that the use of $Ca(OH)_2$ reduces pelletization time by accelerating agglomeration, thereby improving productivity of pelletized aggregates (Geetha and Ramamurthy 2010a; Priyadharshini et al. 2012; Vasugi and Ramamurthy 2014; Vijay 2015).

Multiple studies have been conducted to evaluate the effect of the binder employed on the qualities of pelletized aggregates, as shown in Table 2.1. Gomathi and Sivakumar compared the performance of fly ash aggregates produced with OPC and lime. They found that the oven dry particle density, loose bulk density, and particle crushing strength of OPC containing aggregates were approximately 34%, 37%, and 50% greater, respectively, than aggregates generated with lime (Gomathi and Sivakumar 2012). This is due to the creation of an extra hydration product, which in the case of OPC as a binder occurs from the reaction between $Ca(OH)_2$, which is generated during cement hydration, and the pozzolanic compounds of fly ash (Vasugi and Ramamurthy 2014). Manikandan and Ramamurthy observed that the effect of bentonite concentration as a binder is related to duration of pelletization. The authors showed that increasing the bentonite concentration leads in a significant improvement in formation of aggregate shape (spherical form) during an 8-minute duration of pelletization. When this period was increased to 16 minutes due to the expansive nature of bentonite, flaky aggregates with less strength were formed (Manikandan and Ramamurthy 2009).

The reactivity of raw materials utilized in the production process was also found to have role in the characteristics of pelletized aggregates. In this field, researchers observed the qualities of pelletized aggregates manufactured with GGBS, rice husk ash, etc. The pelletized aggregates produced from GGBS and OPC had higher particle density and crushing resistance than aggregates made from OPC and fly ash. This tendency is mostly due to raw material reactivity, as illustrated by the presence of reactive SiO_2, which combines with the $Ca(OH)_2$ generated during cement hydration to produce additional

hydration product, resulting in the creation of denser and stronger aggregates (Gesoğlu et al. 2007, 2012).

Overall, the physical and mechanical characteristics of the raw materials and binders used in production have a significant impact on manufacturing productivity and pelletized aggregate properties.

2.3.4 Influence of water content

Water content, in addition to production process parameters and raw material characteristics, is an important aspect in the effective production of pelletized aggregates. It also has a direct impact on pelletized aggregates productivity and properties. Meanwhile, the characteristics of the raw materials utilized influence the amount of water required in production. It is obvious that less amount of water leads to an effective agglomeration, whereas excessive water results in the formation of irregular balls (Chiou et al. 2006). As a result, the optimal amount of water has been identified in most of research through many production trials in order to achieve high pelletization efficiency. According to the findings of Baykal and Döven, it is necessary to utilize an enough amount of water to completely fill the intergranular spaces within fresh pellets, while ensuring the absence of a water film on the surface of the pellets. This approach is crucial for attaining size coherence in the pellets (Baykal and Döven 2000). In contrast, the formation of entrapped air voids occurs within the newly formed pellets, resulting in a reduction of the overall strength of the aggregate (Gesoğlu et al. 2012). According to the findings of Harikrishnan and Ramamurthy (Harikrishnan and Ramamurthy 2006), the water content has been identified as the predominant element influencing the size of the aggregate produced. The investigation necessitated water contents of 15 and 35% weight in order to generate pelletized aggregates with a size range of 5 to 8 mm and 10 to 20 mm, respectively.

2.4 EXPERIMENTAL DESIGN METHODOLOGIES

A number of trials are required in an experimental study to identify the effects of various elements influencing the experiment results. Experimental design techniques are becoming increasingly significant in research to effectively develop new goods and processes. There are various experimental design approaches available in the design of experiments, including full factorial, fractional factorial, Taguchi's orthogonal arrays, response surface method, and central composites (Cavazzuti 2013a).

Harikrishnan and Ramamurthy used statistically designed experiments to study the effect of the pelletization process on the characteristics of the pelletized aggregates. The research was carried out utilizing fractional factorial experiments and Taguchi's orthogonal array approach (Harikrishnan and Ramamurthy 2006). The authors reported that the moisture content is the most important parameter, followed by the angle, which impacts the size of the pellets and has the greatest influence on the strength of the pellet. The speed of the pelletizer, followed by the moisture content, has a major influence on the water absorption of sintered aggregates. Among the parameter interactions, the angle and moisture content interaction have a significant influence on the size growth and strength of the pellets.

Manikandan and Ramamurthy evaluated the effect of fly ash fineness for producing pelletized aggregates (Manikandan and Ramamurthy 2007). The effect of fly ash fineness was investigated by collecting various samples of fly ash from two thermal power plants. Using a fractional factorial design, the important influencing parameters in the production of pelletized aggregates were statistically established. For fly ash with fineness of 414 m^2/kg and 257 m^2/kg, respectively, a fractional factorial design of 2^4 and 2^5 was utilized. The researchers stated that using clay binders such as bentonite and kaolinite into the pelletization process improves the pelletization efficiency of coarser fly ash, and that the amount of binder and moisture content varies depending on the kind of binder utilized. Only angle and speed have a significant influence on the pelletization of fly ash with a fineness of 414 m^2/kg, according to statistically designed experiments using a fractional factorial design. All of the parameters, however, had a substantial impact on the pelletization process for fly ash with a fineness of 257 m^2/kg.

Geetha and Ramamurthy used central composite design of response surface methodology with five parameters at five levels to investigate the properties of sintered low calcium bottom ash aggregates with clay binders (Geetha and Ramamurthy 2011). Moisture content, binder, $Ca(OH)_2$ dosage, sintering temperature, and duration were the parameters considered in their experimental research. According to the researchers, the engineering characteristics of the produced aggregates were primarily affected by the sintering temperature, the binding ability of the binders, and the internal pore structure of the material. The properties of produced aggregates varied depending on the binder employed, and it was observed that increasing the binder dose and sintering temperature led in aggregates with a greater 10% fines value and low water absorption.

Vasugi and Ramamurthy investigated the production and characteristics of pelletized pond ash aggregates (Vasugi and Ramamurthy 2014). A statistical technique called central

composite design under response surface methodology was used to design the experimental runs with different parameters such as moisture content, binder dosage, pelletization and strength enhancer dosage with a variable range. For the influence of factors, the engineering characteristics of produced aggregates like bulk density, water absorption, and aggregate strength have been determined. The dosage of binder, strength, and pelletization enhancing admixture improved the engineering characteristics of aggregates, as observed by the researchers.

2.5 THEORY OF GEOPOLYMERIZATION

Glukhovsky first identified alkaline activated aluminosilicates in the 1950s, which makes them to function as a binding agent comparable to cement-like construction material. The term "geopolymer" was preferred by the vast majority of researchers to describe all alkaline activated aluminosilicate binders. According to Davidovits, geopolymers novel type of binding agents that varies from alkaline activated aluminosilicates.

2.5.1 Process of geopolymerization

The process of geopolymerization, also known as geo-synthesis, hold the involvement of the occurrence of a quick chemical reaction with the incorporation of minerals. Fly ash, GGBS, metakaolin, and other aluminosilicate minerals are exposed to high-alkaline environments, undergoes through geopolymerization process, resulting in the geopolymer formation. They are inorganic, with Al and Si ions serving as the backbone on which the chain structures are developed. The resulting geopolymer's chemical composition is comparable to that of natural zeolitic materials, but the microstructure is amorphous rather than crystalline. In the polymerization process, when the materials constituting with Si-Al minerals are subjected to a strong alkaline environment result in formation of a 3-D chain ring structured polymer, consisting of Si-O-Al-O bonds, as described are undergoes through a significantly quick chemical reaction under strong alkaline environment, a 3-D polymeric chain and ringed structure of Si-O-Al-O linkages results, described below (Davidovits 1999; Nikolić et al. 2015)

$$M_n [-(SiO_2)_z-AlO_2]_n . wH_2O \qquad \text{(Eqn. 2.1)}$$

where, M represents alkaline element (K, Na or Ca); z can be 1, 2, or 3; n represents polycondensation/polymerisation degree. The geopolymer structure is a linear 2-D network, and its properties rely greatly on value of z (z = 1–15, up to 300). When the value

of z is low (z properties and across-linked 3-D network), the geopolymer exhibits adhesive properties.

Geopolymerisation process can be better understood with the help of diagrammatic explanation presented in Figure 2.6, proposed by Duxson et al. 2007.

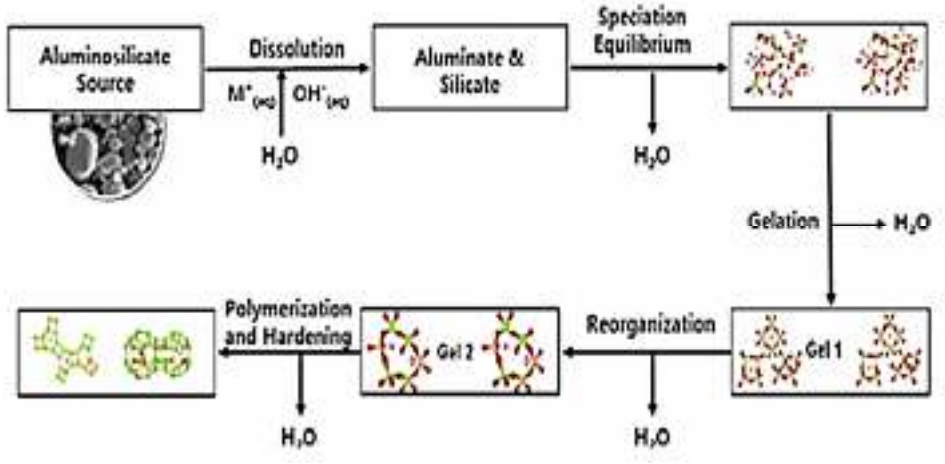

Figure 2.6: Geopolymerization theoretical model representation (Source: Duxson et al. 2007)

A geopolymer can take one of the three basic forms as shown in the Figure 2.6, i.e.:

- Poly (sialate), which has [-Si-O-Al-O-] as the recurring unit.
- Poly (sialate - siloxo), which has [-Si-O-Al-O-Si-O-] as the recurring unit.
- Poly (sialate - di-siloxo), which has [-Si-O-Al-O-Si-O-Si-O-] as the recurring unit.

The various terminologies used in geopolymerization concept according to Davidovits is presented in Figure 2.7. Davidovits also suggested various possibilities for geopolymer materials; Figure 2.8 briefly describes the possible applications of geopolymeric materials.

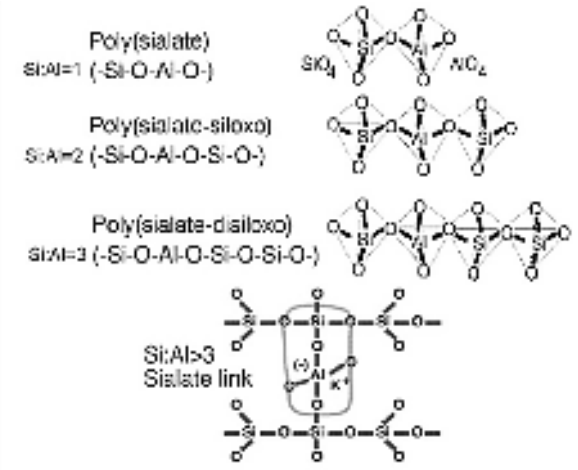

Figure 2.7: Terminologies used in geopolymerization concept (Source: Davidovits 1999)

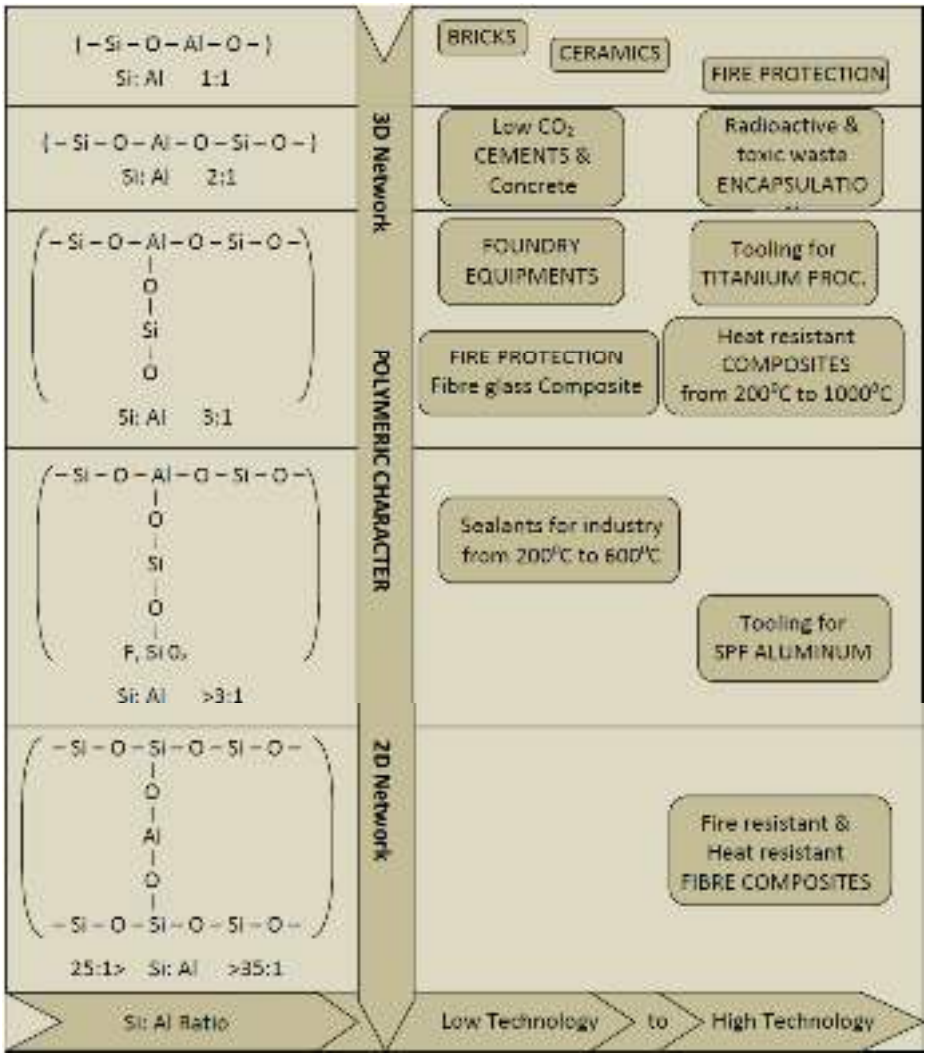

Figure 2.8: Various applications of geopolymeric materials (Source: Davidovits 1999)

2.5.2 Elements of geopolymer

(a) Aluminosilicate materials

Materials primarily composing of amorphous Si and Al are potential sources for geopolymers (Shuaibu 2014). In comparison to products derived from non-calcined materials like kaolin clay, mine tailings, and naturally occurring minerals, demonstrated that calcined source materials such fly ash, GGBS and calcined kaolin displayed a greater compressive strength and reduction in reaction time. Metakaolin, ASTM Class F fly ash natural Al-Si minerals, combination of calcined material and non-calcined materials, combination of fly ash and metakaolin, and combination GGBS and metakaolin were investigated as source materials in the past (Fifinatasha et al. 2013). Because of its high

dissolving rate, ease of control of the Si/Al ratio, and white colour, metakaolin is chosen by geopolymer product developers.

(b) Alkaline based activators

In the process of geopolymerization, NaOH or KOH and Na_2SiO_3 or K_2SiO_3 solution are the most frequently utilised alkaline based activators (Barbosa et al. 2000; Davidovits 1999; Palomo et al. 1999). Some studies also conducted using single alkaline based activator (Teixeira-Pinto et al. 2002). Type of activator plays an important role in the polymerization process. Compared to using solely alkaline hydroxides, reactions happen much more quickly when the alkaline-based activator also contains soluble silicate (either Na_2SiO_3 or K_2SiO_3). The addition of Na_2SiO_3 solution to the K_2SiO_3 as the alkaline based activator enhanced the reaction of source material (Palomo et al. 1999).

2.6 PARAMETERS AFFECTING THE PROPERTIES OF FLY ASH BASED GEOPOLYMERS

Alkaline activator or chemical activator solution plays an essential role in the beginning of surface hydrolysis of the particles present in aluminosilicate materials as the precursors in geopolymerization. A high alkaline media is generally required to promote the surface hydrolysis of fly ash. A variety of parameters influence the geopolymerization's process outcome, including the type of alkaline activator used, the concentration of the alkaline solution, the binder to alkaline ratio, the curing regime, and so on (Rangan et al. 2005; Ridtirud et al. 2011).

2.6.1 Chemical activator type

Strong alkaline, such as NaOH, Na_2SO_4, Na_2SiO_3, Na_2CO_3, K_2CO_3, KOH, K_2SO_4, $Ca(OH)_2$, are required in the geopolymerization mechanism to activate the Si and Al containing in fly ash. Furthermore, a small amount of cement clinker or an alkaline solution mixture can also be employed in the geopolymerization process (Khale and Chaudhary 2007; Komljenovic et al. 2010; Leong et al. 2016; de Vargas et al. 2014). The type and concentration of alkaline activator, according to researchers, is the most critical parameter in the geopolymerization process.

Phoongernkham et al. used NaOH and Na_2SiO_3 for fly ash based geopolymer and observed that this combination of solutions results in attaining good mechanical properties due to the formation of crystalline Ca_2SiO_4 hydrates that co-existed with amorphous gel (Phoo-ngernkham et al. 2015). However, Leong et al. explored the combination of alkaline

hydroxides (i.e. NaOH, KOH, or $Ca(OH)_2$) and Na_2SiO_3. The compressive strength and workability of $Ca(OH)_2$-based geopolymers were found to be the weakest when compared to NaOH and KOH-based geopolymers (Leong et al. 2016). This was attributed to the difference in ionic diameter between K and Na that caused KOH to have a lower activation potential than NaOH.

2.6.2 Alkaline activators concentration

Many researchers demonstrated that the dissolution of Si and Al species during geopolymer synthesis is strongly dependent on alkaline solution concentration (Khale and Chaudhary 2007; Rattanasak and Chindaprasirt 2009; Singh et al. 2005). Khale and Rubina reported on the influence of NaOH concentration in geopolymerization mechanism on the release of silicate and aluminate monomers from aluminosilicate sources and observed that as the concentration increases, so does the release of silicate and aluminate monomers from those aluminosilicate sources (Khale and Chaudhary 2007). Rattanasak and Prinya investigated the leaching of fly ash admixed with NaOH solution (Rattanasak and Chindaprasirt 2009). The leaching of SiO_2 and Al_2O_3 was studied by mixing fly ash with different concentrations of NaOH solution for varied time periods and it was found that when fly ash came into contact with NaOH solution, leaching of Si, Al, and other minor ions began. The optimal leaching period is determined by the concentration of the NaOH solution. The leaching time of 5 to 10 minutes is stated to be adequate, as increasing the leaching time to 20 to 30 minutes did not result in an increase in the concentration of Si^{4+} and Al^{3+} ions.

Al-Bakri et al studied the influence of NaOH concentration on the compressive strength of a fly ash based geopolymer paste. While fly ash to alkaline activator and Na_2SiO_3 to NaOH ratios remained fixed, different concentrations of NaOH were utilized (Mustafa Al Bakri et al. 2011). Based on the compressive strength (cured at 60°C for 24 hours) and tested for 7 days, the optimum NaOH concentration of 12M contributed a high compressive strength of 94.59 MPa. Somna et al, on the other hand, evaluated the effect of NaOH concentration on the ground fly ash based geopolymers cured at room temperature (Somna et al. 2011). As an alkaline activator, NaOH concentrations ranging from 4.5 to 16.5 M were utilized. It was observed that increasing the NaOH concentration from 4.5 to 14.0 M enhanced the strength of fly ash based geopolymeric pastes. Microstructure investigations revealed that at higher NaOH concentrations (12.0-14.0 M), new crystalline sodium aluminosilicate products were formed. The compressive strengths of geopolymeric paste at 28 days were 20.0-23.0 MPa with NaOH concentrations ranging from 9.5-14.0 M. Increasing the NaOH

concentration above this point, however, resulted in a loss in paste strength due to early precipitation of aluminosilicate compounds.

Further research into the effect of NaOH content on fly ash based geopolymeric mortar or concrete was also been conducted (Atiş et al. 2015; Görhan and Kürklü 2014; Hardjito et al. 2008; Mishra et al. 2008; Patankar et al. 2014; Ridtirud et al. 2011). The compressive strength of geopolymer mortar or concrete is dramatically affected by an increase in NaOH solution concentration from 3M to 16M.

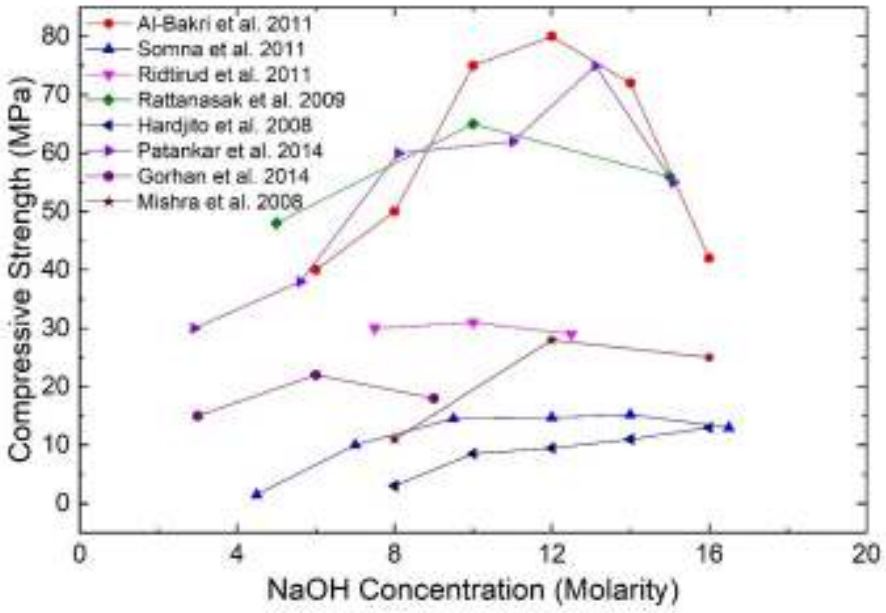

Figure 2.9: Influence of molarity of alkaline on fly ash based geopolymers compressive load carrying capacity (compiled results from various researchers)

Figure 2.9 shows that increasing the concentration of alkaline activator increases the mechanical characteristics of the geopolymers up to a certain point, after which it decreases. However, the workability of the geopolymers demonstrates that the flow increases with increasing concentration of NaOH solution and that the density of geopolymers does not depend on NaOH solution concentration.

2.6.3 Ratio of Na_2SiO_3/NaOH

It was observed that utilizing either Na_2SiO_3 or NaOH resulted in decreased aluminosilicate material activation. As per Phoongernkham et al. the use of both NaOH and Na_2SiO_3 in combination for the production of fly ash based geopolymer resulted in the synthesis of crystalline structures that co-existed with amorphous gel (Phoo-ngernkham et al. 2015). However, using only Na_2SiO_3 solution, on the other hand, resulted in the formation of

largely amorphous products. NaOH or Na_2SiO_3 solution alone yielded low strengths when cured at ambient temperature conditions. For best strength development, a combination of NaOH and Na_2SiO_3 solutions is recommended.

Mustafa et al. examined the effects of varying ratios of Na_2SiO_3 to NaOH on the compressive strength of fly ash based geopolymeric paste (Al Bakri et al. 2012). The ratios were kept constant throughout the experimental work at 0.5, 1, 1.5, 2, 2.5, and 3. The concentration of NaOH was kept at 10 M. According to the compressive strength results, (cured for 24 hours at 60°C and evaluated for 7 days) a high compressive strength of 57 MPa may be attributed to the ideal ratio of 2.5 for Na_2SiO_3 to NaOH. Because of the high concentration of hydroxyl ions in the combination, geopolymeric paste with a Na_2SiO_3 to NaOH ratio of 3.0 is said to have low compressive strength results.

Nevertheless, a thorough analysis of the compressive strength of fly ash based geopolymers with different Na_2SiO_3 to NaOH ratios by numerous researchers revealed that the ratio significantly affects fly ash based geopolymers. M^+ (alkaline ions), which acts as charge-balancing ions and are crucial to the formation of geopolymers, were found to be present in higher concentrations in the mixture when the ratio of Na_2SiO_3 to NaOH increased (Hardjito et al. 2008; Leong et al. 2016; Morsy et al. 2014; Ridtirud et al. 2011; Risdanareni et al. 2015). Furthermore, compared to other ratios with the Na_2SiO_3 to NaOH of 0.3 - 1.5, the researchers reported that fly ash based geopolymer with a high Na_2SiO_3 to NaOH of 3.0 produces reduced drying shrinkage. This can be ascribed to high silicate content the reaction or condensation is fairly quick (Ridtirud et al. 2011).

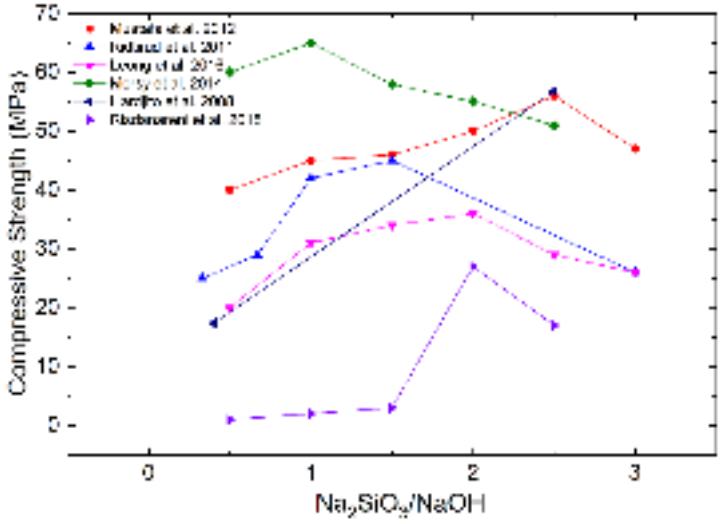

Figure 2.10: Influence of the ratio of NaOH to Na_2SiO_3 on the compressive load carrying capacity of fly ash based geopolymers (compilation of obtained results from various researchers)

Figure 2.10 shows that the ratio of Na_2SiO_3 to NaOH increases the mechanical characteristics of the geopolymers up to a certain point, after which it decreases. Leong et al. investigated the fly ash based geopolymeric mortar and observed that the workability decreases as the Na_2SiO_3/NaOH ratio increases, and commercial grade Na_2SiO_3 significantly increases the workability of fly ash based geopolymers when compared to industrial grade Na_2SiO_3. The compressive strength of geopolymers made with commercial grade Na_2SiO_3 is much higher than that of geopolymers made with industrial grade Na_2SiO_3, and it increases as the Na_2SiO_3/NaOH ratio increases.

2.6.4 NaOH to binder ratio

The fresh mixture characteristics, particularly flowability or workability and setting rate, are critical for the practical application of cementitious materials. The alkaline activator to binder ratio is critical for understanding the behaviour of the geopolymerization process, as well as the fresh and hardened properties of the geopolymers. So, the fresh characteristics of geopolymer mixes, such as workability and setting, are substantially influenced by the amount of water added and the alkaline content of the solution. The amount of water used, or the water to binder ratio, has a considerable impact on the workability of the mixes, their setting, and the engineering characteristics of the hardened products. The water-to-binder ratio is critical in geopolymer combinations because it acts as the water-to-cement ratio in Portland cement mixtures.

The researchers observed that the binder to alkaline activator ratio was the most important parameter in the development of geopolymers (Kong et al. 2007; Leong et al. 2016; Patankar et al. 2014). Experimental studies by various researchers have shown that fly ash based geopolymers with different binder to alkaline activator ratios with other parameters have constant workability and it increases with increasing alkaline to binder ratio. Leong et al. evaluated the effect of alkaline activator to fly ash ratio on the workability of geopolymer mortar by altering the ratio from 0.3 to 0.6 and observed that the workability of the geopolymer mortar increases as the alkaline activator to fly ash ratio increases (Leong et al. 2016). It has been reported that at an alkaline activator to binder ratio of 0.3, workability cannot be measured since the mixture collapses instead of flowing when exposed to a flow table test. At an alkaline activator to fly ash ratio of 0.6, the maximum workability (about 250 mm) was observed. The water content in the mix increases as the alkaline activator to fly ash ratio increases, indicating high workability. However, as the solution to binder ratio increases, the rate of flow gain becomes less important. The

spherical morphologies and fineness of the fly ahs particles, which dramatically boosts workability, resulted in much higher alkaline to binder ratios for the fly ash based geopolymers. The alkali activator to binder ratio influences numerous essential geopolymer characteristics. This parameter, however, has a considerable impact on overall strength. Many researchers investigated the effect of the alkali activator to binder to ratio, which ranged from 1 to 5, and test results on the compressive load carrying capacity of geopolymers revealed that an optimum range of 2 to 4 was used in their studies, depending on the properties of raw materials, chemical composition of alkali activator, and water content in the alkali activator (Abdul Rahim et al. 2014; Abdullah et al. 2011; Kong et al. 2007). Figure 2.11 depicts the effect of alkaline activator to binder ratio on compressive strength of geopolymer paste.

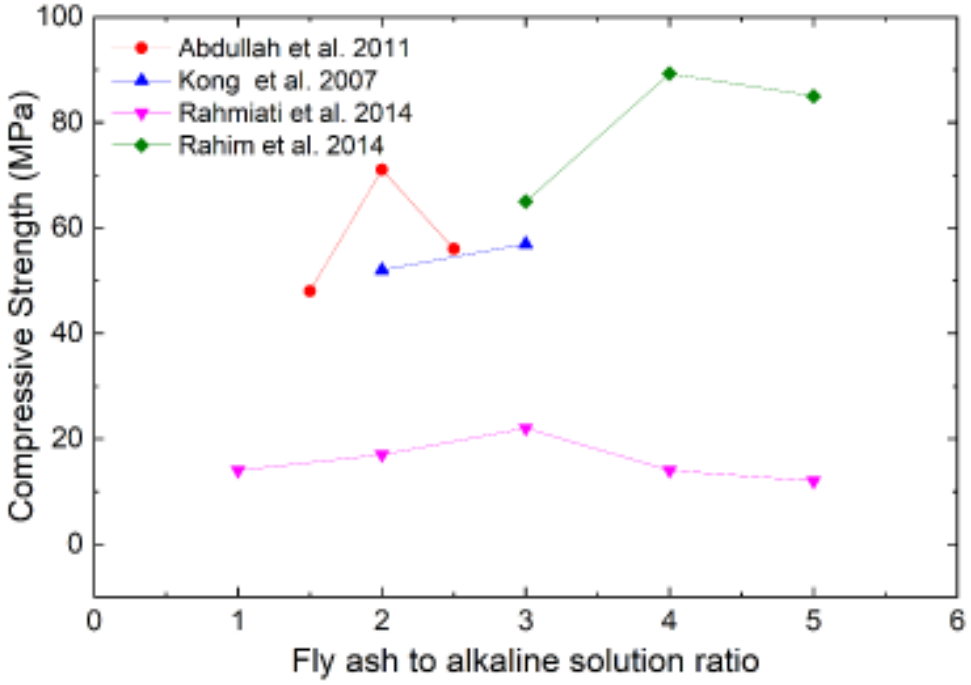

Figure 2.11: Influence of the ratio of NaOH to binder on the compressive load carrying capacity of geopolymers (compilation of obtained results from various researchers)

2.7 REVIEW OF PELLETIZED AGGREGATES PRODUCTION USING ALKALINE ACTIVATION

The following table (Table 2.2) summarizes the production of pelletized aggregates using a combination of alkaline activators using various precursors such as fly ash, bottom ash, GGBS, bentonite, pond ash, and rice husk ash etc.

Table 2.2: Production of pelletized aggregates using alkaline activation

Reference	Composition of pelletized aggregates		Production process parameters used in disc pelletization						Characteristics of pelletized aggregates							
	Base material; Supplement	Binding agent	Diameter (mm)	Depth (mm)	Water content (%)	Angle (°)	Speed (rpm)	Duration (min)	Size (mm)	WA (%)	TPFV	Density (g/cc)		Crushing Strength		
												SSD	OD	PCS (MPa)	PS (N)	BS (MPa)
Geetha and Ramamurthy 2010a	FA and BA; Na_2SO_4	OPC and lime	-	-	31	-	-	14 to 7	10 to 12.5	19 to 23	2.5 to 3	-	-	-		
Gomathi and Sivakumar 2012	FA; NaOH	OPC and lime	500	250	25	36	55	10 to 15	-	12 to 77	-	1.64 to 2.12	1.17 to 1.79	0.25 to 13.72	-	-
Terzić et al. 2015	FA	Na_2SiO_3	-	-	-	-	-	-	0.5 to 14	17 to 22	-	-	-	-	119 to 159	-
Vasugi and Ramamurthy 2014	Pond Ash; Na_2SO_4	OPC and lime	-	-	28-33			14 to 7	-	22 to 52	0.25 to 5	-	-	-	-	-
Bui et al. 2012b	FA and GGBS	OPC, NaOH and Na_2SiO_3	800	300	-	-	-	-	4-10	13.7 to 25.6	-	1.84 to 2.09	1.26 to 1.51	4.73 to 8	-	-
Bui et al. 2012c	FA, GGBS and RHA	NaOH and Na_2SiO_3	800	300	-	53	35	-	4.75-9.5	7.08 to 20.5	-				148 to 306	5.7 to 15.7
Geetha and Ramamurthy 2013	BA; lime	NaOH Na_2SiO_3	-	-	-	-	-	-	4.75 to 12.5	10 to 12	2.5 to 4	-	-	-	-	-
Gomathi et al. 2013	FA	GGBS and NaOH			25	36	55	10-15	6 to 20		-			0.8 to 22.8		
Shivaprasad and Das 2018	FA	NaOH and Na_2SiO_3	450	100	19	45	-	15	5 to 20	4.3 to 17.8	-	-	-	-	-	-

The aforementioned raw materials discussed in Section 2.3 have been utilized collectively in combination with OPC as a binding agent. In recent years, there has been a significant study focus on the utilization of alkaline activators as a binder in the production of alkaline activated pelletized aggregates (Geetha and Ramamurthy 2013; Gomathi and Sivakumar 2015b; Shivaprasad and Das 2018). This is primarily attributed to the remarkable performance exhibited by cement-free matrices generated through alkaline activation. Geopolymer aggregates were produced by activating low-calcium bottom ash with a mixture of Na_2SiO_3 and NaOH at a molarity of 8-12 mol/l (Geetha and Ramamurthy 2013). The bulk density and ten percent fines value of the aggregates were found to be 7 to 20% and 12 to 93% greater, respectively, than that of cement-activated aggregates, according to their research findings. A similar solution was also employed as an alkaline activator to activate fly ash, GGBS, and rice husk ash. Gomathi and Sivakumar conducted a research to assess the efficacy of NaOH with a molarity of 10 mol/l in stimulating the activation of fly ash and bentonite (Gomathi and Sivakumar 2015b). The researchers came to the conclusion that the utilization of an alkaline activator significantly enhances the mechanical and microstructural characteristics of the produced pelletized aggregates.

2.8 REVIEW OF USAGE OF MINE TAILINGS FOR PRODUCING VALUED ADDED PRODUCTS

2.8.1 General

Mine tailings refer to the residual materials that remain subsequently after the extraction of precious minerals from the non-valuable portion of an ore. The quantity of tailings produced can vary significantly, with certain copper ores yielding between 90% and 98%, while other mineral deposits may generate between 20% and 50% of tailings (Nagaraj 2000). Waste generated during the extraction and processing of mineral resources is one of the main waste streams that has yet to be accounted for. Topsoil, overburden, waste rock, and tailings are typical materials that must be removed in order to obtain access to mineral deposits. The massive amounts of mine tailings produced by mining operations have raised concern about the ecological and environmental consequences, such as the encroachment of enormous areas of land, the formation of windblown dust, and the poisoning of surface and subsurface water. Iron ores frequently contain so few metals that about 32% of the ore mined ends up as tailings. (Sunil et al. 2015). In terms of chemical composition, these mine tailings is mostly composed of Si, Al, and CaO, with a percentage ranging from 60% to 90% (Lazorenko et al. 2021). Consequently, tailings possess the potential to serve as an

alternate resource for fulfilling various construction and industrial needs (Divvala 2021; Dold 2020; Eugênio et al. 2021; Kinnunen et al. 2018; Rico et al. 2008). As discussed previously, the geopolymer network consists of tetrahedra comprised of AlO_4 and SiO_4, which are interconnected by oxygen atoms (Provis and Van Deventer 2009). The negative charge inside the network is counterbalanced by the presence of positively charged ions (such as $Ca^{2+,}$ Na^+, K^+, and Li^+) within the framework's cavities. The utilization of mine tailings as a general practice approach may have the potential to mitigate the accumulation of these tailings and reduce ecological contamination. Additionally, this approach can offer the combined benefits of geopolymer technology, including a decrease in CO_2 emissions, the utilization of other techniques for alumino-silicate waste, and the versatile characteristics of geopolymers as a construction adhesive (Chau-Khun et al. 2018; Lazorenko et al. 2020b; a).

2.8.2 Review of techniques available for disposal of mine tailings

Disposal of MT is a major contributor to environmental degradation in the mining industry. Such a result is highly anticipated, considering that the quantity of mine tailings that require storage frequently exceeds the capacity of on-site ore extraction. In the last century, there has been a significant increase in the quantity of mine tailings due to the rising need for metals and minerals, as well as the implementation of improved mining and processing techniques to effectively employ low-grade minerals and enhance their value extraction.

Figure 2.12: Available techniques for converting mine tailings into value added products (Source: Qaidi et al. 2022)

Figure 2.12 illustrates the various techniques available/explored by researchers for disposing mine tailings in a sustainable manner. A major portion of prior research has focused on the utilization of mine tailings for the purpose of backfilling cement paste (Zhao et al. 2021). The surface based mine tailings are frequently blended with a binder in a small backfill plant before pumping to subterranean slopes through gravity (Qi and Fourie 2019). This method reduces the amount of mine tailings that must be stored in tailings ponds (Lottermoser 2011). It is feasible to mitigate the problems associated with mine tailings, such as dust production, landslides, surface water contamination, and acquisition agricultural land by these tailings. Furthermore, essential elements can be recovered from previously deposited mine tailings like Ag and Li containing minerals can be recovered from Au and micaceous tailings, respectively (Qaidi et al. 2022). Many types of mine tailings can be recycled and used again like Mn rich tailings can be used to make building materials, ceramics, glass, and coatings; clay-rich tailings can be used to make bricks, sanitary wares, porcelain, and cements; iron ore tailings admixed with other materials like FA and sewage; and $Al_2O_3.2H_2O$ containing tailings can be used as aluminium resources (Qaidi et al. 2022). These disposal techniques help mining industries to clean up the accumulated mine tailings and convert it into something valuable to the construction industry.

2.8.3 Review of usage of mine tailings in conjunction with geopolymers

As previously stated in the Section 2.8.1, the process of geopolymerization or alkali-activation of mine tailings is a viable option for the sustainable management of these mining wastes. This strategy holds significant potential for utilizing large quantities of hazardous mining wastes to produce value-added products while simultaneously mitigating environmental consequences. A review of the past research pertaining to the utilization of mine tailings in the synthesis of geopolymers/alkali activated materials is discussed in the subsequent sections.

2.8.3.1 Copper ore tailings and gold ore tailings

Using an alkaline solution of NaOH and aqueous Na_2SiO_3, Ahmari et al. produced geopolymer materials from copper ore tailings (Ahmari et al. 2012). The results stated that the addition of Na_2SiO_3 increases compressive strength while maintaining the SiO_2/Na_2O ratio between 1 and 1.26. In a similar way, it has been observed that the NaOH concentration of 15 M significantly enhances the compressive strength of the material. This

enhancement is most pronounced when the curing temperature is elevated to 90 °C, resulting in a denser microstructure.

In a study conducted by Zhang et al., it was observed that the incorporation of fly ash into mine tailings resulted in enhanced mechanical characteristics and the development of a denser structure (Zhang et al. 2011), wherein the percentage of fly ash added ranged from 0% to 75%. This favourable effect was primarily due to a drop in the Si/Al ratio. Furthermore, an increase of NaOH concentration had a significant role in facilitating the rapid dissolving of Si and Al particles. Consequently, this led to the subsequent formation of geopolymeric gels exhibiting enhanced compressive strength in the resultant geopolymers derived from copper ore tailings. Copper ore tailings were also utilized to make geopolymer bricks (Ahmari and Zhang 2012). The geopolymeric bricks achieved higher unconfined compressive strength with 15 M NaOH, slightly higher curing temperature, and higher forming pressure, resulting in a compact microstructure.

The study conducted by Caballero et al. examined the utilization of gold ore tailings waste as a precursor for geopolymeric sources in the production of alkaline activated binders (Caballero et al. 2014). The compressive load carrying capacity values of the alkaline activated geopolymers, which were subjected to a curing temperature of 70 °C for a duration of 12 hours, exhibited greater values compared to those of commercial OPC. The combination of NaOH with a concentration of 15 M with sulphidic mine tailings and GGBS resulted in the solidification of materials exhibiting compressive load carrying capacity value of up to 3.5 MPa. The incorporation of 5% of GGBS activated by a 5M NaOH solution results in a notable enhancement of the unconfined compressive strength, with a maximum value of 4.4 MPa. According to Kiventerä et al., the compressive load carrying capacity values reached 20 MPa as the GGBS content increased and was activated by 5M NaOH (Kiventerä et al. 2016).

It was observed that the utilization of gold ore tailings as a precursor for geopolymers resulted in the development of materials with a compressive load carrying capacity value of around 5.48 MPa. This was achieved by employing lime sludge in combination with NaOH 5 M as the activators, as reported by Aseniero et al. 2019. The unconfined compressive strength of the resultant geopolymers were determined to be 18.10 MPa after a curing period of 5 days at a temperature of 100 °C. This result was achieved through the activation process using KOH and $K[Al(OH)_4]$. The activator ratio employed was around 2.8, resulting in a Si/Al ratio of 1.02. Another study conducted by Huang et al. shown that

the compressive load carrying capacity values of compressed geopolymers, initially at 10 MPa, significantly increased to 40 MPa through the activation of mine tailings with NaOH at a temperature of 170 °C for a duration of 1 hour (Huang et al. 2020).

2.8.3.2 Iron ore tailings and tungsten ore tailings

In a study, Niu et al. employed Na_2SiO_3 and NaOH to activate iron ore tailings admixed with GGBS (Niu et al. 2011). The researches explored the effects of varied synthesis parameters on the activation process. The study demonstrated that the addition of 80% GGBS resulted in an increase in compressive strength carrying capacity values, reaching 45.10 MPa. Furthermore, when a Na_2SiO_3 to NaOH ratio of 0.5 was employed, the compressive strength carrying capacity values further improved to 63.79 MPa after 7 days of curing. Subsequently, after 14 days, the unconfined compressive strength was around 71.25 MPa. The tailings were utilized in the production of geopolymer bricks. The key factors for achieving favourable mechanical characteristics were determined to be a Na_2SiO_3 content of 31%, an initial setting time of 15 minutes, and a curing temperature of 80°C. By adhering to these parameters, a compressive strength carrying capacity values of 50.35 MPa was attained after 7 days of curing. Furthermore, the researchers of this study noted that these bricks offer certain advantages over commercial alternatives in relation to energy usage, achieved by the utilization of low temperature oven drying (Kuranchie et al. 2016).

Furthermore, the utilization of iron ore tailings was employed as a substitute for quartz aggregates in the development of metakaolin-based geopolymeric mortar, in conjunction with NaOH and Na_2SiO_3. The prepared samples exhibited a higher density and a more compact structure in comparison to those containing quartz aggregates. The water absorption and porosity exhibited greater values in comparison to the quartz formulation containing quartz aggregate, as reported by Borges et al. 2019. The aforementioned findings were validated in the context of geopolymers utilizing a combination of class-C fly ash and 20% iron ore tailings. Analysis of SEM images revealed a decrease in apparent porosity and microcracking, accompanied by a notable high compressive strength carrying capacity values of approximately 50 MPa (Duan et al. 2016b).

Another study by Sharath et al. stated that the utilization of iron ore tailings as fine aggregates in the production of class-F fly ash geopolymer mortars, activated with NaOH and Na_2SiO_3 solution, resulted in a compressive strength carrying capacity values of 8.27

MPa. This value was found to be greater than that of mortars containing natural sand (Sharath et al. 2018).

Adding red clay brick wastes to tungsten ore tailings cured at 60°C for 24 hours enhanced compressive strength carrying capacity values up to 59 MP after 28 days, forming three gels (N-A-S-H, C-A-S-H, and K-A-S-H)(Sedira et al. 2018). Using GGBS at various percentages with tungsten ore tailings resulted in alkali-activated materials with a compressive strength carrying capacity values of 23.5 MPa after 28 days of curing. The reduction of porosity and average pore diameter caused by CaO hydration led to the formation of C-A-S-H gel (Sedira and Castro-Gomes 2019). Tungsten ore tailings with 40% waste glass activated by NaOH and Na_2SiO_3 solution increased amorphous phase by 21%. Samples cured at 20°C achieved compressive strength capacity values only up to 2.6 MPa after 28 days. After 28 days at 80°C, it reached up to 22 MPa (Kastiukas et al. 2016).

2.8.3.3 Vanadium ore tailings and bauxite ore tailings

Jiao et al. employed vanadium ore tailings admixed with metakaolin as a source of Al in geopolymer synthesis utilizing NaOH. The addition of appropriate metakaolin dosages enhanced compressive strength carrying capacity values due to the formation of additional gel phases, according to the obtained results (Jiao et al. 2011). The release of alumina and condensation was increased by the elevated temperature. At 60 °C and 30% metakaolin content, the maximum compressive strength carrying capacity values was around 55.7 MPa.

In another study, the mechanical activation of vanadium ore tailings with a planetary mill decreased particle size while increasing specific surface area. This resulted in a rapid setting time and a high compressive strength carrying capacity value of around 25 MPa (Wei et al. 2017). The compressive strength carrying capacity values of molybdenum ore tailings based geopolymers was 15 MPa, which was much higher than that of vanadium ore tailings and fly ash based geopolymers. In 3 days of curing at room temperature, the addition of 20% metakaolin and 35% Na_2SiO_3 resulted in a maximum compressive strength carrying capacity value of 46 MPa (Wang et al. 2019).

Ye et al. investigated a 6-year-old geopolymer made from calcined bauxite ore tailings and Na_2SiO_3 activated GGBS. In this study, compressive strength carrying capacity values increased from 50.0 MPa at 28 days to 75.0 MPa at 6 years. Progressive geopolymerization made the microstructure more compact and less porous, allowing C–A–S–H and N–A–S–H gels to coexist (Ye et al. 2017). Alkali-activating bauxite ore tailings at 1100°C with

K_2SiO_3 and curing at 60°C for 72 hours resulted in a thick structure with a compressive strength carrying capacity value of 40 MPa (Hertel et al. 2016).

2.9 CRITICAL REVIEW

The efficient usage of fly ash as well as wastes generated from mining and ore upgradation operations is very much critical in mitigating the various environmental issues. Upon conducting an extensive review of the relevant literature, it has been determined that the construction industry has the capacity to accommodate these enormous quantities of wastes if it is planned meticulously. Additionally, one of the greatest challenges for concrete and cement technologists is the development of methods to reduce the carbon footprints. This objective can solely be accomplished through the geopolymerization process. The literature suggests that geopolymerization has the greatest potential to entirely eliminate the need for cement in concrete.

Moreover, in light of the demands of the concrete manufacturing sector, it is evident that the extraction of aggregate, a critical component comprising approximately 70% of its volume, presents a significant challenge to the conservation of natural resources (Tajra et al. 2019). The mining of aggregates has been subjected to additional taxes imposed by the majority of regulatory authorities, and in certain areas, it is completely prohibited (Kiventerä et al. 2020; Qaidi et al. 2022). It was observed from the extensive literature that aggregates produced either by fly ash, bottom ash, rice husk ash etc. were mostly classified as lightweight aggregates as per EN 13055-1 based upon the obtained characteristics of these produced aggregates (Tajra et al. 2019). Some recent literature on the production of fly ash and slag-based aggregates with the inclusion of mine tailings discusses the characteristics of produced aggregates wherein it is stated that most of aggregates found to be satisfying the minimum gradation requirements, achieved the requisite strength characteristics, but were found to be still lightweight, highly water absorbent and porous (Asadizadeh et al. 2023a; b, 2024). As understood from the available literature, mine tailings are predominantly rich in alumina and silica and requires an efficient interaction with alkalis as well as other aluminosilicate materials (Kiventerä et al. 2016) which will impact the characteristics of final deliverables, that is pelletized aggregates. This incorporation of alkaline materials in conjunction with aluminosilicate rich binders helps in altering the physical and mechanical characteristics of mine tailings, facilitates the rise in concentration of aluminosilicates in the presence of alkaline activators resulting into an efficient occurrence of geopolymerization reaction (Kiventerä et al. 2016). Furthermore,

most of the mine tailings possess a higher specific gravity which can serve as an additional beneficial factor in the production of pelletized aggregates, thereby complying them to adhere BIS requirements.

The goal of this research work is to produce pelletized aggregates with the utilization of fly ash admixed with additive admixtures and mine tailings in conjunction with alkaline activators, cured under ambient temperature conditions, a well-designed experimental approach is crucial. This design of experiments methodology provides a structured and efficient way to study the effects of multiple factors (that is key factors of geopolymerization, additive admixtures and mine tailings) and their interactions that influences the characteristics of pelletized aggregates. This approach will bring more robustness in the production methodology of pelletized aggregates. Moreover, this experimental research also aims in solving the disposal problems of growing industrial byproducts as well as the environmental hazards in a more sustainable and cost-effective manner, so as to stick to the idea of sustainability which is the need of the hour.

2.10 OBJECTIVES OF THIS EXPERIMENTAL RESEARCH WORK

The objectives of this experimental research are

- To study, investigate and optimize the appropriate dosage levels of alkaline solutions with additive admixtures (bentonite, burnt lime and GGBS) on the production and engineering properties of pelletized aggregates.
- To identify the influence of optimized replacement level of the chief precursor (FA) with two types of mine tailings (iron ore and copper ore tailings) on the production of pelletized aggregates.
- To study and understand the influence of addition of ultrafine FA on the production and engineering properties of pelletized aggregates constituted with optimized dosage levels of partially replaced mine tailings and binding agents.
- To carry out advanced characterization studies such as SEM, TGA and FTIR analysis on all the different types of produced pelletized aggregates.

CHAPTER – 3

EXPERIMENTAL METHODOLOGY

3.1 GENERAL

This section discusses the numerous materials that were used and the tests conducted on those materials, and the corresponding results are shown. Additionally, the experimental mix design and methodology adopted in the production and testing of the engineering and microstructural properties of fly ash based pelletized aggregates are presented in this section.

3.2 SOURCE MATERIALS AND THEIR CORRESPONDING PROPERTIES

3.2.1 Fly ash

The fly ash (FA) utilized in the study was acquired from Udupi Power Corporation Limited, Udupi District, Karnataka. The physical characteristics and chemical composition of FA were determined, and the results are tabulated in Table 3.1. Based on the obtained chemical composition, it is classified as class F type according to IS 3812 (part-1) – 2013. The grain size distribution of FA utilized in this study is represented in Figure 3.1.

3.2.2 Bentonite

The bentonite (BT) utilized in the study was acquired from KIOCL Ltd., Mangalore, Dakshina Kannada District, Karnataka. The physical characteristics and chemical composition of BT were determined, and the results are tabulated in Table 3.1. The grain size distribution of BT is represented in Figure 3.1.

3.2.3 Burnt Lime

The burnt lime (BL) utilized in the study was acquired from KIOCL Ltd., Mangalore, Dakshina Kannada District, Karnataka. The physical characteristics and chemical composition of BL were determined, and the results are tabulated in Table 3.1. The grain size distribution of BL is represented in Figure 3.1.

3.2.4 Ground granulated blast furnace slag

The ground granulated blast furnace slag (GGBS) was acquired from Jindal Steels, Toranagallu, Bellary District, Karnataka. The physical characteristics and chemical

composition of GGBS were determined, and the results are tabulated in Table 3.1. The grain size distribution of GGBS is represented in Figure 3.1.

3.2.5 Iron ore tailings

The iron ore tailings (IOT) were acquired from a tailing dam located at Kudremukha, Chikmagalur District, Karnataka. The physical characteristics and chemical composition of IOT were determined, and the results are tabulated in Table 3.1. The grain size distribution of IOT is represented in Figure 3.1.

3.2.6 Copper ore tailings

The copper ore tailings (COT) were acquired from the Malanjkhand Copper Project, Hindustan Copper Ltd., Malanjkhand, Balaghat district, Madhya Pradesh. The physical characteristics and chemical composition of COT were determined, and the results are tabulated in Table 3.1. The grain size distribution of COT is represented in Figure 3.1.

3.2.7 Ultrafine fly ash

The ultrafine fly ash (UFA) was acquired from a local vendor in Nashik District, Maharashtra, India. The physical characteristics and chemical composition of UFA were determined, and the results are tabulated in Table 3.1. The grain size distribution of UFA is represented in Figure 3.1.

Table 3.1: Physical characteristics and chemical compositions of FA, BT, BL, GGBS, IOT, COT and UFA

Physical characteristics							
Property	**FA**	**BT**	**BL**	**GGBS**	**IOT**	**COT**	**UFA**
Blaine fineness (m^2/kg)	260	-	-	350	-	-	670
Specific gravity	2.2	2.3	2.3	2.8	3.3	2.4	2.2
Chemical compositions (%)							
Oxide	**FA**	**BT**	**BL**	**GGBS**	**IOT**	**COT**	**UFA**
Silicon dioxide + Aluminium oxide + Ferric oxide	84.2	81.2	9.3	46.0	97.3	83.4	95.4
Calcium oxide	6.3	1.8	75.8	44.8	0.6	3.6	1.3
Magnesium oxide	1.2	2.9	4.4	4.4	1.1	2.0	1.4
Sulfur trioxide	0.57	-	-	2.26	0.1	4.3	1.0
Loss on ignition	1.7	8.1	2.0	1.3			

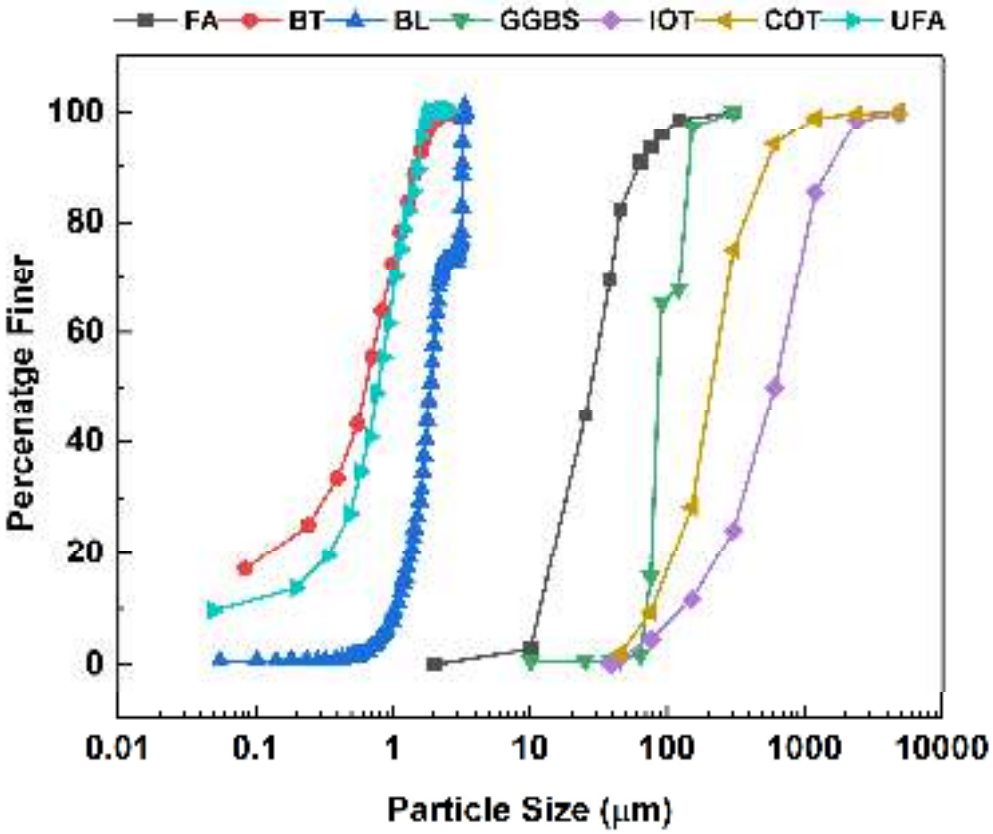

Figure 3.1: Grain size distribution of the materials utilized in this experimental research

3.2.8 Alkaline solution

The alkaline solution was prepared using laboratory-grade NaOH pellets and Na_2SiO_3 (7.5 to 8.5% Na_2O; 25–28% SiO_2; 65.5% H_2O by mass). To prepare a NaOH solution, NaOH pellets were dissolved in distilled water. Subsequently, the NaOH solution that had been prepared was combined with Na_2SiO_3 in order to obtain the alkaline solution. This alkaline solution is left to cool at room temperature for 24 hours before being used in the production of fly ash based pelletized aggregates.

3.3 SEQUENTIAL STEPS FOLLOWED IN THE PRODUCTION OF BINARY AND MULTI-BLENDED PELLETIZED AGGREGATES

This experimental research focuses on the production of binary blended pelletized aggregates like FA-BT, FA-BL, FA-GGBS, FA-IOT, FA-COT, and multi-blended blended pelletized aggregates like FA-UFA-BL-IOT/COT and FA-UFA-GGBS-IOT/COT, which involves pelletization of FA and UFA with aforementioned additive admixtures such as

BT, BL, and GGBS and mine tailings like IOT and COT by means of a laboratory-typed disc pelletizer having a disc diameter of 500 mm and a depth of 125 mm, as shown in Figure 3.2.

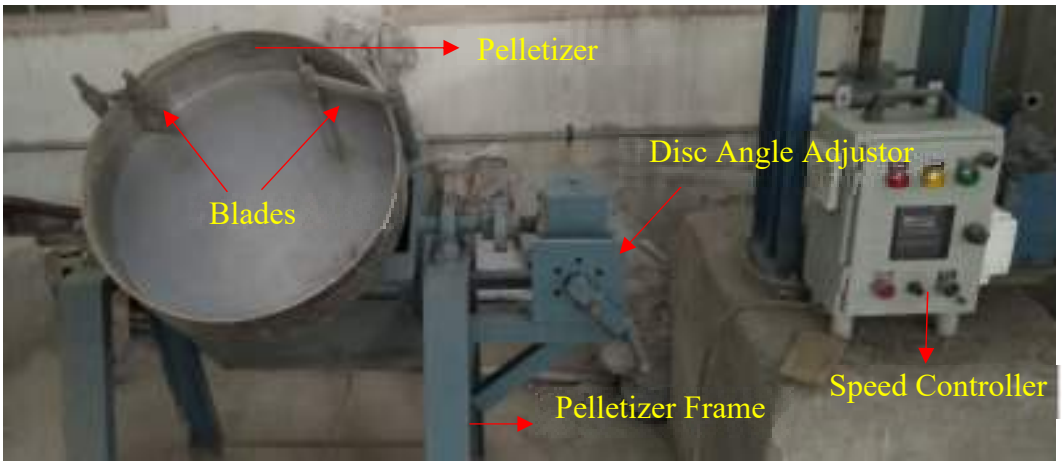

Figure 3.2: Laboratory-scale disc pelletizer with components (Sharath et al. 2023a)

The sequential steps followed in the pelletization process consists of (Sharath and Das 2021):

1. Thorough mixing of lump free materials is carried out which needs to be pelletized i.e., FA, BT, BL, GGBS, IOT, COT (pulverized) and UFA for producing FA-BT, FA-BL, FA-GGBS, FA-IOT, FA-COT, FA-UFA-BL-IOT/COT and FA-UFA-GGBS-IOT/COT aggregates, respectively.
2. The different types of mixtures are fed into the disc pelletizer by presetting the required adjustments in it like maintaining a constant degree of inclination as 45°, constant duration of pelletization as 15 min and a constant revolutionary speed of 45 RPM during the dure course of production of pelletized aggregates.
3. Spraying of the prepared alkali solution over the different types of mixtures within 3 min of the pelletization process. The produced FA-BT, FA-BL, FA-GGBS, FA-IOT, FA-COT, FA-UFA-BL-IOT/COT and FA-UFA-GGBS-IOT/COT were cured at ambient temperature conditions (28°C ± 2°C) for a curing period of 14, 28 and 100 days.

3.4 FACTORS OF GOVERNANCE IN THE PRODUCTION OF BINARY BLENEDED PELLETIZED AGGREGATES

3.4.1 Governing factors in the production of pelletized aggregates with admixture additions (BT, BL and GGBS)

As understood from the available literature, two factors that are connected to the strength and efficiency of geopolymerization are Na_2O and water content (Harikrishnan and Ramamurthy 2006; Ramamurthy and Harikrishnan 2006; Shivaprasad and Das 2018). Along with these two factors, an additional factor was the addition of varied dosages of admixtures, i.e., BT, BL, and GGBS (Sharath et al. 2023b). Hence, dosages of Na_2O, water, and mineral admixtures collectively serve as governing factors as well as experimental parameters for designing the production methodology for producing pelletized aggregates such as FA-BT, FA-BL, and FA-GGBS aggregates (Sharath et al. 2023b).

Preliminary trial studies were carried out to determine the combination of suitable ranges for Na_2O dosage (3%, 4%, 5%, and 6%), water content dosage (19%, 20%, 21%, and 22%), and additive admixtures (5%, 10%, 15%, and 20% by weight of fly ash) for producing pelletized FA-BT, FA-BL, and FA-GGBS aggregates (Sharath et al. 2023b). A solution with high Na_2O content was found to have a high strength in the resulting geopolymers (Fernández-Jiménez and Palomo 2005). Moreover, as the concentration of Na_2O in the alkaline solution increased, it became too cohesive and difficult for its use in the production of pelletized FA-BT, FA-BL, and FA-GGBS aggregates. Also, a high dosage of water and additive admixtures resulted in the formation of large, unevenly shaped agglomerates (Sharath et al. 2023b). Hence, the dosage of Na_2O content in the production of FA-BT and FA-GGBS aggregates was within the range of 3-5% of the combined mass of the precursor material and 4-6% of the combined mass of the precursor material for producing FA-BL aggregates (Sharath et al. 2023b). The water content was varied in the range of 19–21%, and the same was maintained for the production of pelletized FA-BT, FA-BL, and FA-GGBS aggregates (Sharath et al. 2023b). The ratio of SiO_2/Na_2O was maintained constant thought-out the production process of pelletized FA-BT, FA-BL and FA-GGBS aggregates.

3.4.2 Governing factors in the production of pelletized aggregates with mine tailings addition (IOT and COT)

As discussed in Section 3.4.1, apart from the dosage contents of Na_2O and water, the ratio of SiO_2/Na_2O was also found to be equally influential for imparting strength and efficiency

to the resultant geopolymers (Shivaprasad and Das 2018). In addition, the incorporation of various types of mine tailings was found to be influential for producing sustainable value-added products (here fly ash based pelletized aggregates) has attracted attention in recent times by various researchers (Kuranchie et al. 2016; Sharath et al. 2023a; Sharath and Das 2021; Thejas and Hossiney 2022; Zhang et al. 2013).

Preliminary trial studies stated that dosage levels and fineness of IOT and COT were found to alter the dosage contents of Na_2O and water in the production of binary blended pelletized FA-IOT and FA-COT aggregates as mine tailings are coarser in nature (Sharath and Das 2021). With the obtained observations, the dosage levels of Na_2O and water contents varied by 3–6% and 13%–15%, respectively, in the production of pelletized FA-IOT and FA-COT aggregates.

By analyzing the available literature focused on the physical and mechanical properties of the produced aggregates, such as particle size, particle density, and water absorption, it is evident that these properties varied in ranges of 4–20 mm, 0.88–2.12 g/cm^3, and 2.5–77% (Gesoğlu et al. 2012; Gomathi and Sivakumar 2014a; Kockal and Ozturan 2011; Tajra et al. 2018; Thomas and Harilal 2015). However, most of the produced aggregates possessed lesser particle density, thereby classifying them as lightweight aggregates (Sharath et al. 2023a). The high specific gravity of mine tailings (IOT and COT) would help in producing artificial coarse aggregates of equivalent or similar density to that of natural aggregates (Sharath et al. 2023a). Hence, the dosage levels of IOT and COT were selected as 50–90% (as a replacement for FA) in the production of pelletized FA-IOT and FA-COT aggregates. The variation ranges in the SiO_2/Na_2O ratio were fixed at 0.23–0.3 based on the preliminary trial investigations, as discussed above.

3.5 EXPERIENTAL DESIGN FOR THE PRODUCTION OF BINARY AND MULTI-BLENDED PELLETIZED AGGREGATES

In order to evaluate the interaction among the governing factors of geopolymerization and integration of additive admixtures as well as mine tailings (as discussed in Sections 3.4.1 and 3.4.2), the concept of the design of experiments was used. Among the various available experimental design methodologies, Taguchi's orthogonal arrays facilitates this assessment of various governing factors involved in the production of pelletized aggregates. By using Taguchi's experimental design methodology, numerous factors in a particular experiment can be studied by performing a minimum number of experiments by means of orthogonal

arrays (Sharath et al. 2023a). The sequential steps involved in Taguchi's experimental design method are listed as follows:

a) Selection of governing factors along with their corresponding levels.
b) Suitable orthogonal array selection by means of Taguchi experimental design followed by appropriate arrangement of factors of governance along with their corresponding levels.
c) Performing the production of binary blended pelletized aggregates which were FA-BT, FA-BL, FA-GGBS, FA IOT and FA-COT as per the mixes designed using Taguchi's experimental design methodology.
d) Evaluating the engineering properties of the produced aggregates (presented in subsequent sections) by carrying out a series of tests on the produced aggregates (FA-BT, FA-BL, FA-GGBS, FA-IOT and FA-COT).
e) Calculation of response indices for the obtained results of the produced aggregates (FA-BT, FA-BL, FA-GGBS, FA-IOT and FA-COT) with the help of statistical software that is MINITAB software version 20.2.
f) Adopting grey relational analysis method for analyzing the obtained results together and identifying the most influential experimental parameter among the selected ones.

3.5.1 Mix proportioning design for producing binary blended pelletized aggregates

In the production of binary blended pelletized aggregates, that is, FA-BT, FA-BL, FA-GGBS, FA-IOT, and FA-COT aggregates, the varying levels of geopolymerization factors (Na_2O and water content, ratio of SiO_2/Na_2O) and dosage levels of BT, BL, GGBS, IOT, and COT are depicted in Tables 3.2 and 3.3, respectively.

Table 3.2: Levels of governing factors in the production of pelletized FA-BT, FA-BL and FA-GGBS aggregates

Governing Factors	Level 1			Level 2			Level 3		
	FA-BT	FA-BL	FA-GGBS	FA-BT	FA-BL	FA-GGBS	FA-BT	FA-BL	FA-GGBS
I: Na_2O content (%)	3	4	3	4	5	4	5	6	5
II: Water content (%)	19	19	19	20	20	20	21	21	21
III: Admixture content (%)	5	5	5	10	10	10	15	15	15

Table 3.3: Levels of governing factors in the production of pelletized FA-IOT and FA-COT aggregates

Governing Factors	Variation levels			
	Level 1	**Level 2**	**Level 3**	**Level 4**
I: Na_2O dosage (%)	3	4	5	6
II: Water dosage (%)	13.5	14	14.5	15
III: FA: IOT and COT ratio	50:50	60:40	70:30	80:20
IV: SiO_2/Na_2O ratio	0.23	0.25	0.27	0.3

In the production of pelletized FA-BT, FA-BL, FA-GGBS, FA-IOT, and FA-COT aggregates, three and four levels of variation were considered, respectively (as shown in Tables 3.2 and 3.3, respectively). According to the full factorial design methodology, a total of 27 (that is, 3^3) experimental combinations are needed for evaluating the influence of every governing factor considered for producing pelletized FA-BT, FA-BL, and FA-GGBS (Sharath et al. 2023b). However, for producing pelletized FA-IOT and FA-COT aggregates, a total of 256 (that is, 4^4) experimental combinations need to be evaluated for understanding those governing factors considered in their production (Sharath et al. 2023a). In both scenarios, the whole production methodology could potentially become tedious and uneconomical. For this reason, Taguchi's experimental design methodology was adopted for evaluating the influence of different levels of governing factors on the properties of the produced binary blended pelletized aggregates with the help of a smaller number of experiments (Sharath et al. 2023b). Orthogonal arrays L_9 (3^3) (in pelletized FA-BT, FA-BL, and FA-GGBS aggregate scenarios) and L_{16} (4^4) (in pelletized FA-IOT and FA-COT aggregate scenarios) developed by Taguchi (Montgomery 2017) are presented in Tables 3.4 and 3.5 respectively was used in order to represent a full factorial experiment. The component variables in set of mixes for producing binary blended pelletized aggregates is listed in Tables 3.6 and 3.7.

Table 3.4: General Taguchi's L_9 (3^3) orthogonal array for producing pelletized FA-BT, FA-BL and FA-GGBS aggregates

Trial Run No.	Factor A	Factor B	Factor C
TRN 1	1	1	1
TRN 2	1	2	2
TRN 3	1	3	3
TRN 4	2	1	2
TRN 5	2	2	3
TRN 6	2	3	1
TRN 7	3	1	3
TRN 8	3	2	1
TRN 9	3	3	2

Table 3.5: General Taguchi's L_{16} (4^4) orthogonal array for producing pelletized FA-IOT and FA-COT aggregates

Trial Run Number (TRN)	Factor A	Factor B	Factor C	Factor D
TRN 1	1	1	1	1
TRN 2	1	2	2	2
TRN 3	1	3	3	3
TRN 4	1	4	4	4
TRN 5	2	1	2	3
TRN 6	2	2	1	4
TRN 7	2	3	4	1
TRN 8	2	4	3	2
TRN 9	3	1	3	4
TRN 10	3	2	4	3
TRN 11	3	3	1	2
TRN 12	3	4	2	1
TRN 13	4	1	4	2
TRN 14	4	2	3	1
TRN 15	4	3	2	4
TRN 16	4	4	1	3

Table 3.6: Experimental set of trial mixes as per L_9 orthogonal array for producing pelletized FA-BT, FA-BL and FA-GGBS aggregates

Na_2O content (%)			Water content (%)			Admixture content (%)		
FA-BT	FA-BL	FA-GGBS	FA-BT	FA-BL	FA-GGBS	FA-BT	FA-BL	FA-GGBS
3.0	4.0	3.0	19.0	19.0	19.0	5.0	5.0	5.0
3.0	4.0	3.0	20.0	20.0	20.0	10.0	10.0	10.0
3.0	4.0	3.0	21.0	21.0	21.0	15.0	15.0	15.0
4.0	5.0	4.0	19.0	19.0	19.0	10.0	10.0	10.0
4.0	5.0	4.0	20.0	20.0	20.0	15.0	15.0	15.0
4.0	5.0	4.0	21.0	21.0	21.0	5.0	5.0	5.0
5.0	6.0	5.0	19.0	19.0	19.0	15.0	15.0	15.0
5.0	6.0	5.0	20.0	20.0	20.0	5.0	5.0	5.0
5.0	6.0	5.0	21.0	21.0	21.0	10.0	10.0	10.0

Table 3.7: Experimental set of trial mixes as per L_{16} orthogonal array for producing pelletized FA-IOT and FA-COT aggregates

Experimental run No.	Na_2O dosage (%)	Water dosage (%)	FA: IOT/COT ratio	SiO_2/Na_2O ratio
FAIOT/COT 1	3	13.5	50:50	0.23
FAIOT/COT 2	3	14	40:60	0.25
FAIOT/COT 3	3	14.5	30:70	0.27
FAIOT/COT 4	3	15	20:80	0.3
FAIOT/COT 5	4	13.5	40:60	0.27
FAIOT/COT 6	4	14	50:50	0.3
FAIOT/COT 7	4	14.5	20:80	0.23
FAIOT/COT 8	4	15	30:70	0.25
FAIOT/COT 9	5	13.5	30:70	0.3
FAIOT/COT 10	5	14	20:80	0.27
FAIOT/COT 11	5	14.5	50:50	0.25
FAIOT/COT 12	5	15	60:40	0.23
FAIOT/COT 13	6	13.5	80:20	0.25
FAIOT/COT 14	6	14	70:30	0.23
FAIOT/COT 15	6	14.5	60:40	0.3
FAIOT/COT 16	6	15	50:50	0.27

All the produced binary blended pelletized aggregates, as presented in Tables 3.6 and 3.7, were produced and evaluated for their engineering properties, such as specific gravity, particle size distribution, aggregate impact value (AIV), aggregate crushing value (ACV), water absorption (WA), and individual crushing strength of the pellets and aggregates (IPS), for a curing period of 14, 28, and 100 days. The response index for each factor considered in the production of binary blended pelletized aggregates was assessed with the help of statistical software.

Subsequently, Grey relational analysis was carried out to analyze the obtained results for the engineering properties of binary blended pelletized aggregates. This method will help in obtaining an unbiased analysis for determining the order of influence of the selected governing factors in the produced binary blended pelletized aggregates (Sahoo et al. 2017). Firstly, the results of various tests as mentioned previously for binary blended pelletized aggregates were are transformed into a normalised value using the following equations (Sharath et al. 2022).

For smaller-is-better, the formula to transform $x_i(j)$ to $x_i^*(j)$ is,

$$x_i^*(j) = \frac{\max_j x_i(j) - x_i(j)}{\max_j x_i(j) - \min_j x_i(j)} \quad \text{(Eqn. 3.1)}$$

For larger-is-better transformation, $x_i(j)$ can be transformed to $x_i^*(j)$, the formula is,

$$x_i^*(j) = \frac{x_i(j) - \min_j x_i(j)}{\max_j x_i(j) - \min_j x_i(j)} \quad \text{(Eqn. 3.2)}$$

It is to be noted that properties like AIV, ACV and WA are principally, the lower the obtained value is, the better as per IS 2386 (part 4)-1963 (Bureau of Indian Standards (BIS) 1963). However, for individual crushing strength of pellets, the higher is the better.

Second, the grey relational coefficient, $\xi_i(k)$ from the normalised values is calculated by using the following formula (Sharath et al. 2022).

$$\xi i(k) = \frac{\Delta_{min} + \xi\Delta_{max}}{\Delta_{0i}(k) + \xi\Delta_{max}} \quad \text{(Eqn. 3.3)}$$

where, Δ_{0i} is the is the deviation sequence of the reference sequence and the comparability sequence and $\Delta_{0i} = \| x_0(k) - x_i(k) \|$

where, where x_0 (k) implies the reference sequence and xi (k) termed as comparability sequence. Δ_{min} and Δ_{max} are the minimum and maximum values of the absolute differences (Δ_{0i}) of all comparing sequences. ξ is a distinguishing coefficient ($0 \leq \xi \leq 1$) and in the present study, $\xi = 0.5$ is taken (Sahoo et al. 2017).

Finally, the grey relational grade (GRG) is calculated by summing up the weighted grey relational coefficients corresponding to the responses.

$$\gamma_i = \frac{1}{n}\sum_{k=1}^{n} \xi i(k) \qquad \text{(Eqn. 3.4)}$$

where, n = number of process responses considered in this study.

It is to be noted that a higher grey relational grade indicates a stronger relational degree between the ideal sequence and the given sequence (Sahoo et al. 2017). The sequential steps followed in Taguchi's experimental design methodology and grey relational analysis are represented in the form of the flowchart depicted in Figure 3.3.

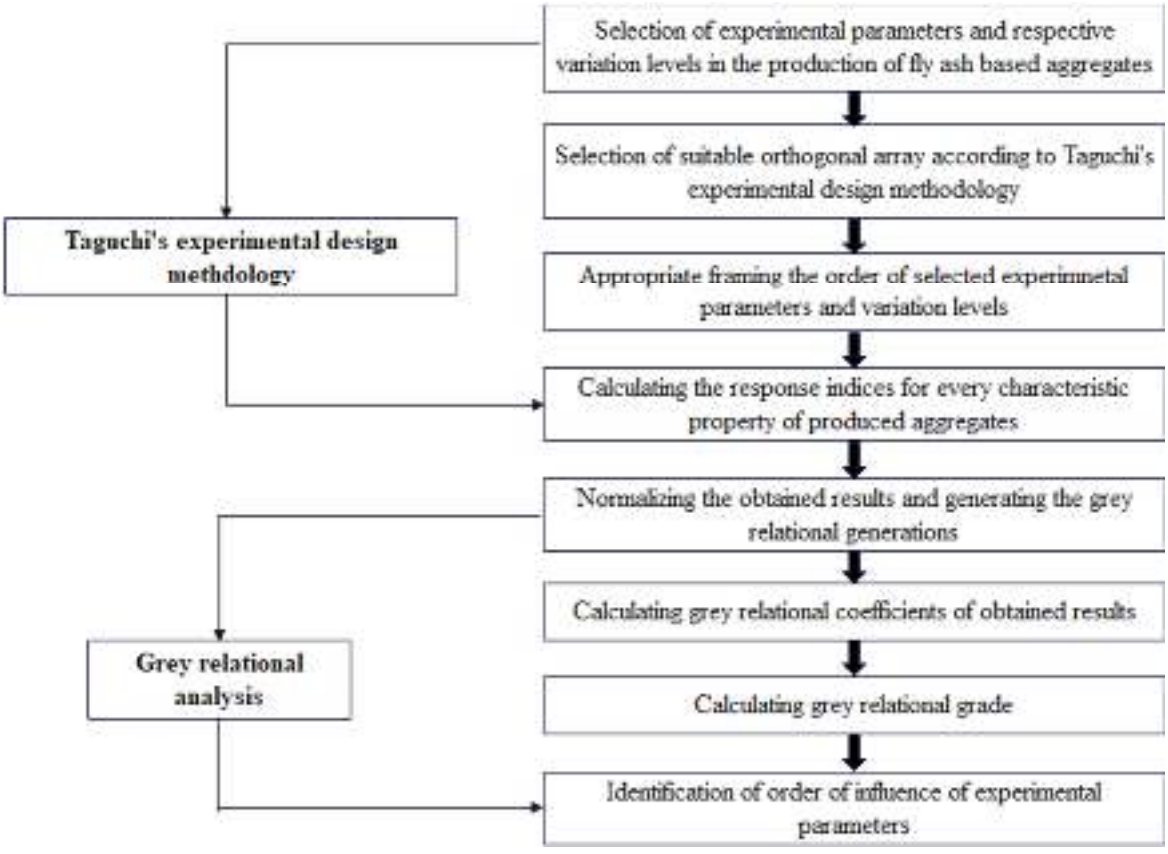

Figure 3.3: Flowchart representing the steps in Taguchi's experimental design methodology and Grey relational analysis

3.5.2 Mix proportioning design for producing multi-blended pelletized aggregates

The optimized binary blended pelletized aggregate mixes based upon their obtained engineering properties were used for producing aggregates with still more superior characteristics. These multi-blended composites involve the addition of UFA with FA, BL and IOT and COT. The aggregate mixes for producing multi-blended pelletized aggregates are presented in Table 3.8.

Table 3.8: Aggregate mixes for producing multi-blended pelletized aggregates

Trial No.	*Optimized BL	Mixes with UFA addition (FA:UFA:IOT/COT)	Trial No.	*Optimized GGBS	Mixes with UFA addition (FA:UFA:IOT/COT)
MMIOT/COTBL** 1	15% BL	50:5:45	MMIOT/COTGGBS 1	15% GGBS	50:5:45
MMIOT/COTBL 2		40:5:55	MMIOT/COTGGBS 2		40:5:55
MMIOT/COTBL 3		30:5:65	MMIOT/COTGGBS 3		30:5:65
MMIOT/COTBL 4		20:5:75	MMIOT/COTGGBS 4		20:5:75
MMIOT/COTBL 5		10:5:85	MMIOT/COTGGBS 5		10:5:85

* The BL and GGBS dosage here is considered based upon the optimizational study carried out on FA-BL and FA-GGBS aggregates

** "MMIOT/MMCOT": Nomenclature used for representing multi-blended pelletized aggregates admixed with IOT and COT; BL and GGBS

All the ambiently cured multi-blended pelletized aggregates were tested for their engineering properties for a curing period of 14, 28 and 100 days.

3.6 TESTS ON BINARY AND MULTI-BLENDED PELLETIZED AGGREGATES

Table 3.9 describes the testing methods adopted for binary and multi-blended pelletized aggregates.

Table 3.9: Testing methods applicable for all the produced binary and multi-blended pelletized aggregates

Tests	In accordance with/ Formula	Remarks
Aggregate impact value (AIV)	IS 2386:1963 (Part 4)	• Using AIV setup • Measured at 14, 28 and 100 for binary and multi-blended pelletized aggregates
Aggregate crushing value (ACV)		• Using compression testing machine • Measured at 14, 28 and 100 days for binary and multi-blended pelletized aggregates
Water absorption (WA)	IS 2386:1963 (Part 3)	Measured at 14, 28 and 100 days for binary and multi-blended pelletized aggregates
Specific gravity	IS 2386:1963 (Part 3)	-
Individual crushing strength of pellets (IPS) (σ)	$\sigma = \frac{2.8 \times P}{\pi \times x^2}$ P - fracture load x - size of the aggregate samples	• Using California bearing ratio setup • Measured at 14, 28 and 100 days for binary and multi-blended pelletized aggregates
Scanning electron microscopy-Energy dispersive spectroscopy (SEM-EDS)		• Using scanning electron microscope from JEOL (JSM-638OLA) associated by an EDS analyzer
Thermogravimetric analysis (TGA)		• Using TG/DTA analyzer from Rigaku TG-DTA 8122
Fourier transform infrared spectroscopy (FTIR)		• Using Bruker (Alpha II) instrument

3.6.1 Evaluation of grain size distribution

The particle size distribution of produced aggregates was determined by employing a standardized set of sieves in line with the Bureau of Indian Standards - IS 383: 2016.

3.6.2 Aggregate impact value, aggregate crushing value, water absorption and specific gravity

Aggregate impact value, aggregate crushing value, water absorption and specific gravity of produced aggregates were determined following the guidelines set by the Bureau of Indian Standards - IS 2386:1963 part and IS 2386:1963 part 3 respectively.

3.6.3 Individual crushing strength of pellets/aggregates

The individual crushing strength of produced pellets/aggregates were determined by evaluating the crushing load of every single aggregate by placing them diametrically. Every single aggregate was loaded between two parallel plates under a diametrically applied load as per Figure 3.4.

Figure 3.4: IPS test arrangement

The individual pellet strength (σ) was calculated when a spherical-shaped particle undergoes compression between two diametrically opposed plates or points, using the following equation (Sivakumar and Gomathi 2012)

$$\sigma = \frac{2.8 \times P}{\pi \times x^2} \qquad (Eqn. 5)$$

Where, x is the distance between the two loading points or the size of the aggregate samples selected for the test, and P is fracture load for the sample.

3.6.4 Scanning electron microscopy coupled with energy dispersive spectroscopy (SEM-EDS)

The spherical-shaped pellets of produced aggregates that got broken into two halves obtained from the individual pellet strength test were gold sputtered for morphological characterization with the help of a scanning electron microscope. Morphological images were taken through a scanning electron microscope (JEOL, JSM-638OLA, Peabody, Massachusetts) in secondary electron mode. Additionally, elemental analysis was performed using an EDS analyzer (only for multi-blended pelletized aggregates) to determine the variations in the chemical composition inside the image boundary.

3.6.5 Thermogravimetric analysis (TGA)

TGA was performed by using a TG/DTA analyzer from Rigaku TG-DTA 8122. Produced aggregate samples were crushed, followed by sieving the crushed samples through 75-µm IS sieve and heating within the temperature boundaries of 25°C–850°C, at a heating rate of 10°C/min in nitrogen purge environment (purge rate 20 mL/min).

3.6.6 Fourier transform infrared spectroscopy (FTIR) analysis

FTIR analysis was performed on the produced aggregates using Bruker (Alpha II) instrument at wavenumber range of 4,000 to 500 cm^{-1} with of resolution of 2 cm^{-1}. The test samples from the produced aggregates were crushed and sieved through a 75-µm IS sieve for obtaining a very fine type sample for minimizing the scattering in the FTIR instrument.

CHAPTER – 4

RESULTS AND DISCUSSION ON BINARY BLENDED PELLETIZED AGGREGATES

4.1 GENERAL

The section discusses the results obtained from the various tests performed on binary blended pelletized aggregates cured at room temperature. Additionally, the influence of the governing factors on the engineering properties of binary blended pelletized aggregates is also discussed in this section. Important observations obtained from advanced characterization techniques like SEM, TGA, and FTIR are presented in this section. Grey relational analysis on the binary blended pelletized aggregate is also presented in this section.

4.2 ENGINEERING PROPERTIES OF BINARY BLENDED PELLETIZED AGGREGATES

4.2.1 Grain size distribution

The grain size distribution results obtained for binary blended pelletized aggregates (FA-BT, FA-BL, FA-GGBS, FA-IOT, and FA-COT) as per the trial mixes specified in Tables 3.6 and 3.7 are presented in Figures 4.1 (a-c), 4.2 (a-d), and 4.3 (a-d), respectively. In order to check the suitability of the produced aggregates, the lower and higher limits for coarse aggregates as stated in the IS 383-2016 specification are plotted in all these figures.

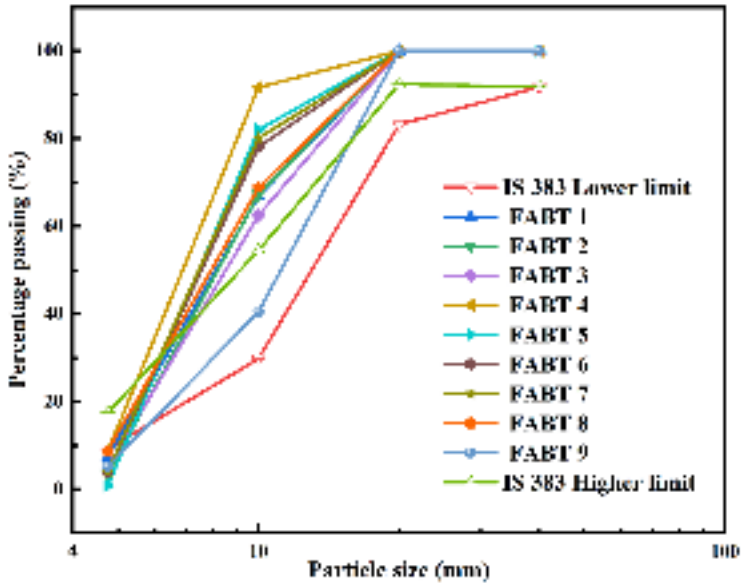
Percentage passing (%)
Particle size (mm)
IS 383 Lower limit
FABT 1
FABT 2
FABT 3
FABT 4
FABT 5
FABT 6
FABT 7
FABT 8
FABT 9
IS 383 Higher limit

(a)

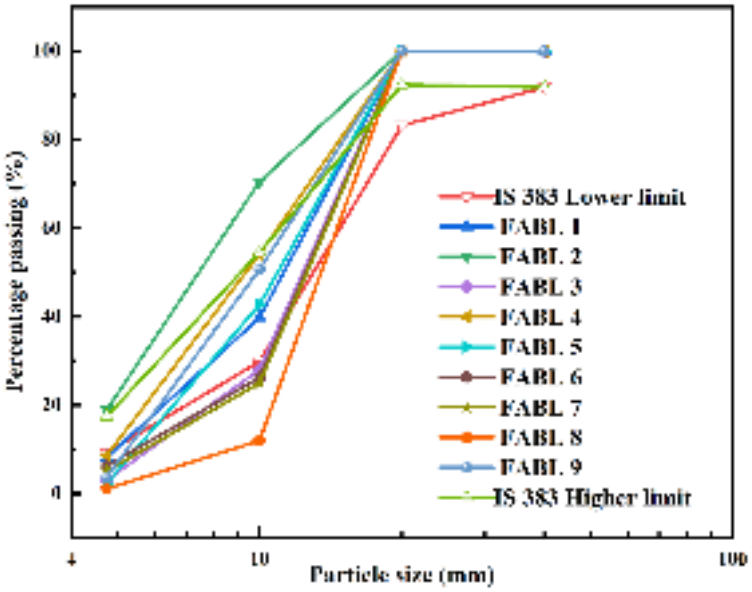
Percentage passing (%)
Particle size (mm)
IS 383 Lower limit
FABL 1
FABL 2
FABL 3
FABL 4
FABL 5
FABL 6
FABL 7
FABL 8
FABL 9
IS 383 Higher limit

(b)

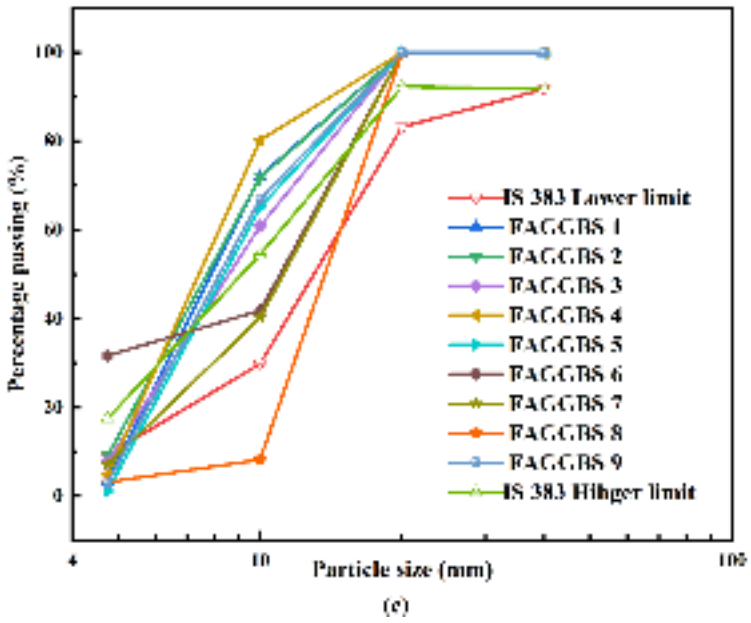

Figure 4.1: Grain size distribution of pelletized (a) FA-BT (b) FA-BL and (c) FA-GGBS aggregates

From Figure 4.1, it can be understood that apart from the mixes FABT 9, FABL 5, and FAGGBS 7, the other mixes in the FA-BT, FA-BL, and FA-GGBS groups were not fully satisfying the required limits specified by IS 383-2016. This can be attributed to the inadequate dosage levels of Na_2O, water, and mineral admixtures in their production. Hence, it can be understood that selected governing factors in the production of pelletized FA-BT, FA-BL, and FA-GGBS aggregates have influenced the gradation of aggregates produced (Sharath et al. 2022).

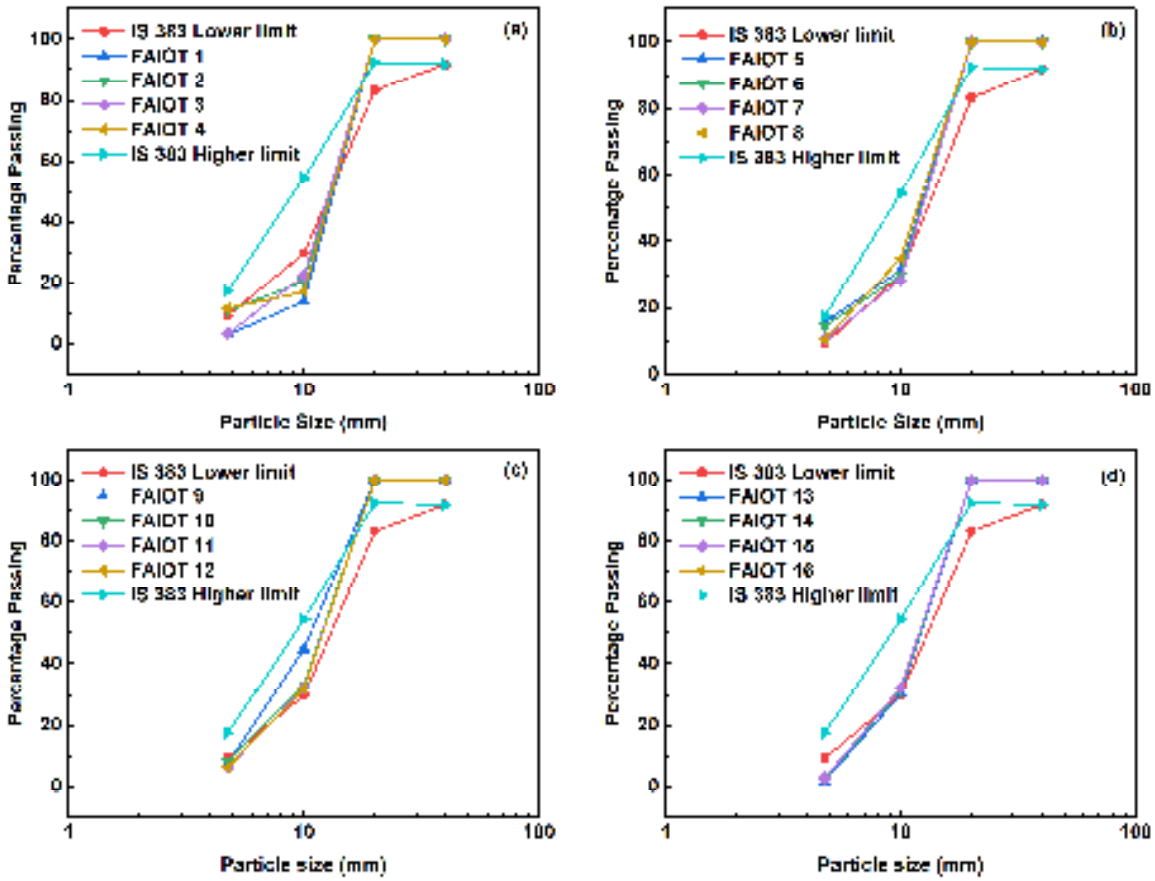

Figure 4.2: Grain size distribution for pelletized (a) FAIOT 1-FAIOT 4 (b) FAIOT 5-FAIOT 8 (c) FAIOT 9-FAIOT 12 (d) FAIOT 13-FAIOT 16 aggregates

It can be concluded from the test results shown in Figure 4.2 that the size of the pelletized FA-IOT aggregates that were produced increased depending upon the amount of Na_2O, and water content, the amount of FA:IOT used and the SiO_2/Na_2O ratio. Figure 4.2a shows that when different amounts of water and FA:IOT were used (from FAIOT 1 to FAIOT 4), a constant 3% Na_2O dosage was insufficient for the production of pelletized FA-IOT aggregates. This is also clear from the gradation curves of the four mixes that were shown. All four curves are falling outside of IS 383's higher and upper limits. Whereas, from Figure 4.2b, it can be noticed that with a constant 4% Na_2O content and varying dosages of water and FA:IOT (FAIOT 5–FAIOT 8), a slight variation in the four gradation curves can be witnessed. This can be attributed to Na_2O dosage content that has influenced slightly the gradation curves, and only FAIOT 8 is falling between IS 383's lower and higher limits (Sharath et al. 2023a).

However, in the case of Figure 4.2c, a constant Na_2O dosage of 5% was found to be suitable for producing aggregates for varied dosages of water and FA:IOT (FAIOT 9-FAIOT 12).

Aggregates produced under mix FAIOT 9 fell exactly between IS 383's lower and higher limits, which could be attributed to optimum dosages of Na_2O, water, and FA:IOT (Sharath et al. 2023a).

But 5% dosage of Na_2O content was also found to be fulfilling in the production of aggregates under aggregate production mixes FAIOT 10–FAIOT 12, as their respective gradation curves have moved upwards from IS 383's lower limits, whereas 6% Na_2O dosage significantly influenced the production of aggregates under mixes FAIOT 13–FAIOT 16. From Figure 4.2d, it can be understood that even though all the produced aggregates are of an appropriate size between 10 and 4.75 mm, they do not fall within the grading limits. By summing up the obtained results, it can be generalized that the gradation of the aggregates was susceptible to the dosages of Na_2O, water, and FA:IOT (Sharath et al. 2023a).

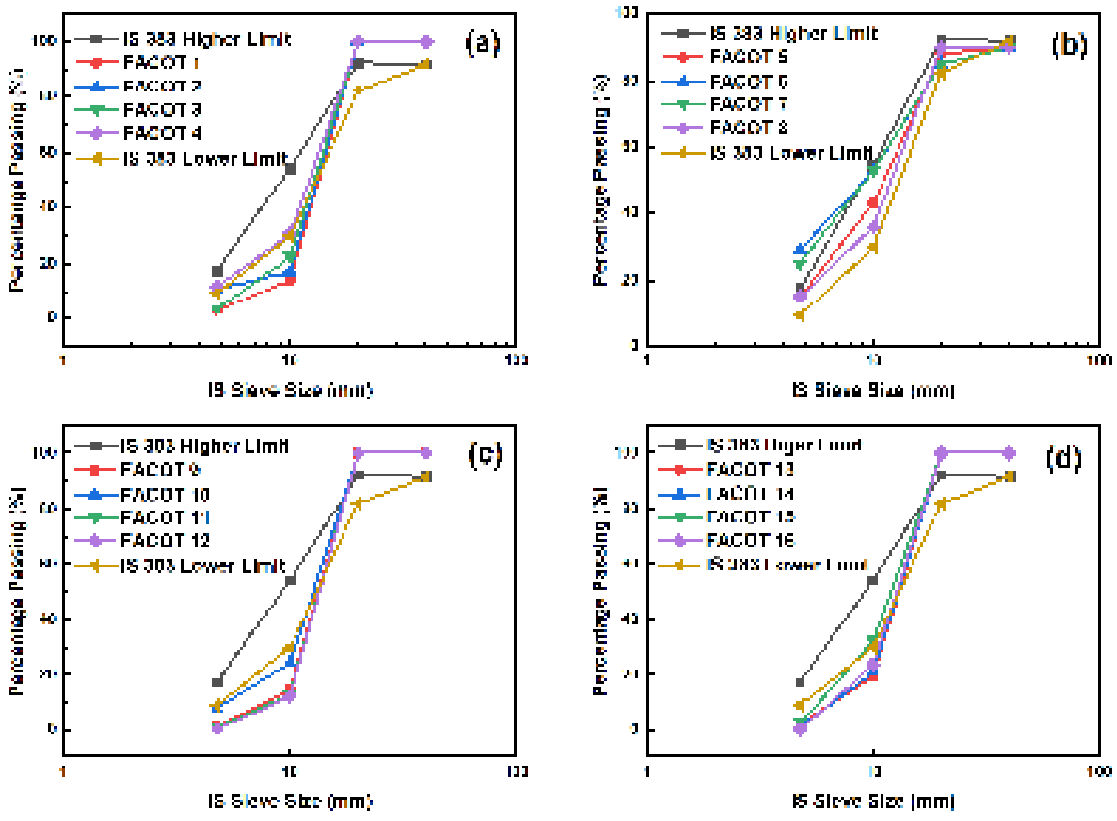

Figure 4.3: Grain size distribution for pelletized (a) FACOT 1-FACOT 4 (b) FACOT 5-FACOT 8 (c) FACOT 9-FACOT 12 (d) FACOT 13-FACOT 16 aggregates

From Figure 4.3a, it can be noticed that the varying FA:COT dosages (FACOT 1-FACOT 4), water content, and a fixed 3% Na_2O dosage were found to be inadequate in the

production of aggregates. The gradation curves of the aggregates produced under FACOT 1-FACOT 4 were found to in adherent to IS 383 upper and lower limits. Whereas in the case of Figure 4.3b, a fixed dosage of 4% was found to be adequate for producing aggregates with varied dosages of water and FA:COT (under FACOT 5-FACOT 8 aggregate mixes). The aggregates produced under the FACOT 5 mix only are perfectly adhering to the IS 383 standard upper and lower limits, which could be attributed towards to optimum dosages of Na_2O, water, and FA:COT. However, from Figure 4.3b, it can also be understood that 4% Na_2O dosage was also found to be influential in the production of aggregates under FACOT 6-FACOT 8 aggregate mixes, as their respective gradation curves are slightly adhering to the IS 383 upper and lower limits.

From Figures 4.3c and 4.3d, it can be stated that 5 and 6% Na_2O dosages have remarkably influenced the production of aggregates under mixes FACOT 9-FACOT 12 (5% Na_2O group) and FACOT 13-FACOT 16 (6% Na_2O group). Upon observing the gradation curves of FACOT 9-FACOT 12 and FACOT 13-FACOT 16 aggregate mixes, it can be deduced that they are falling out of IS 383's upper and higher limits. However, the produced aggregates were sized between 10 and 4.75 mm, which makes them in adherent to IS 383 gradation limits.

4.2.2 Influence of governing factors on aggregate impact value and aggregate crushing value of binary blended pelletized aggregates

4.2.2.1 Pelletized FA-BT, FA-BL and FA-GGBS aggregates

Figures 4.4(a-c) and 4.5(a-c) show the test results for the aggregate impact value and aggregate crushing value of pelletized FA-BT, FA-BL, and FA-GGBS aggregates, respectively.

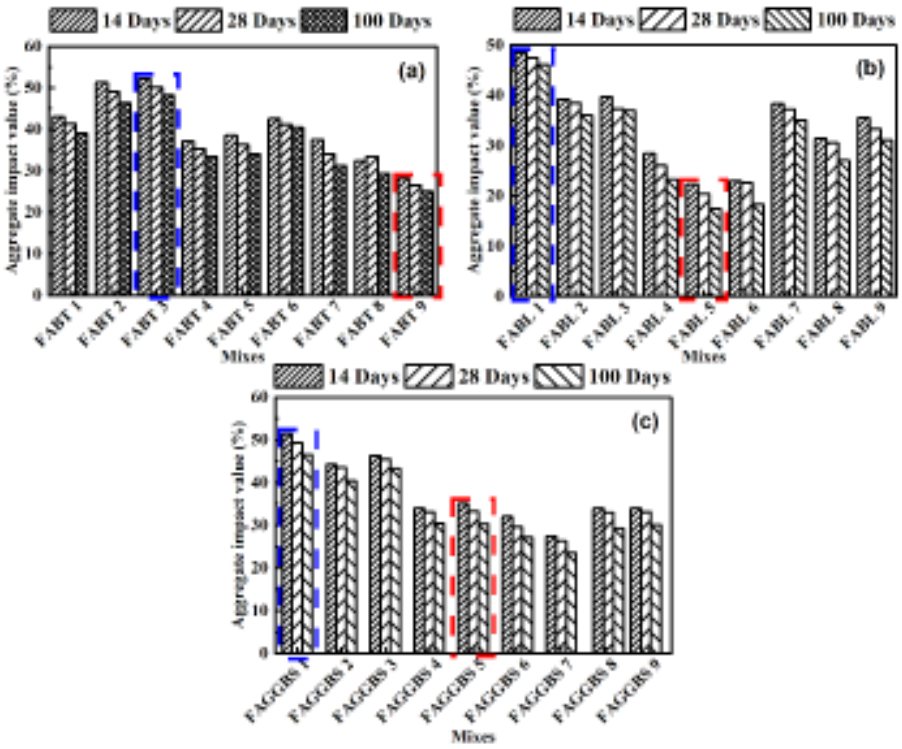

Figure 4.4: Obtained experimental results for aggregate impact value of pelletized (a) FA-BT (b) FA-BL and (c) FA-GGBS aggregates

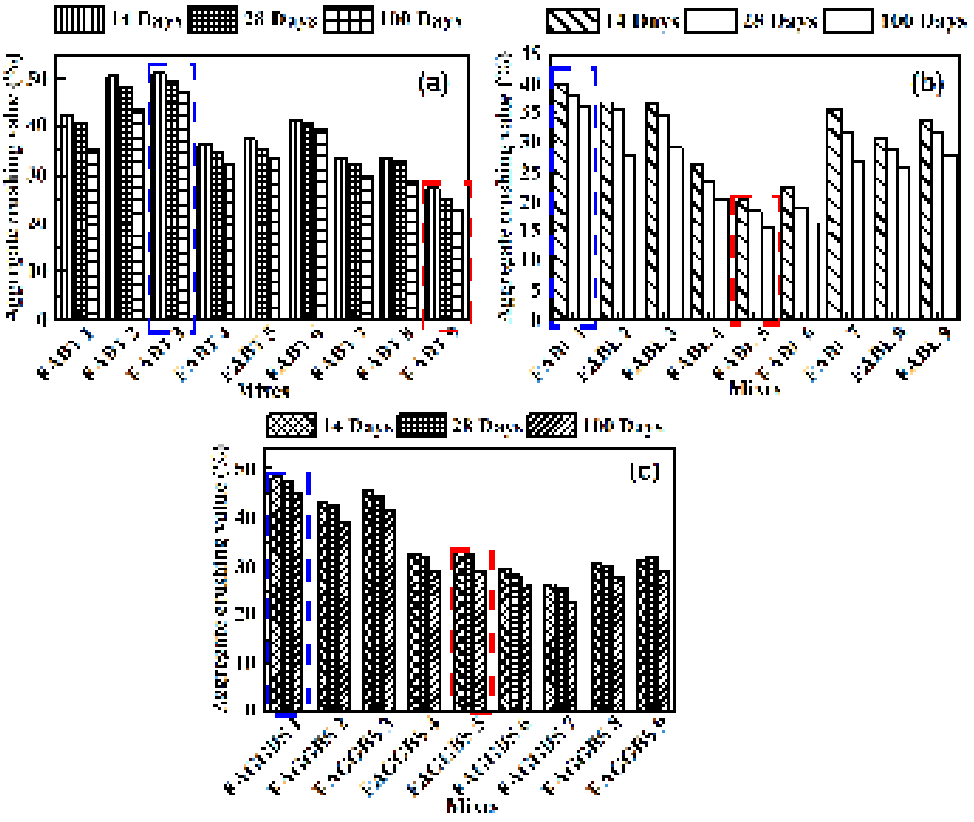

Figure 4.5: Obtained experimental results for aggregate crushing value of pelletized (a) FA-BT (b) FA-BL and (c) FA-GGBS aggregates

Figures 4.4(a) and 4.5(a) show that mix FABT 9 (shown in red) had the best aggregate impact value and aggregate crushing value out of all the FA-BT aggregates tested. This can be attributed to the highest dosage of Na_2O content, i.e., 5% present in the mix proportion and BT content of 10% (Sharath et al. 2022). However, FABT 3 (marked in blue) fared the poorest of all. It is important to note that FABT 3 consists of the lowest dosage of Na_2O content, i.e., 3%, and the highest dosage of BT content, i.e., 15% (Sharath et al. 2022).

Figures 4.4(b) and 4.5(b) show that mix FABL 5 (marked in red) has the best aggregate impact value and aggregate crushing value out of all the FA-BL aggregates tested. This can be associated to highest dosage of Na_2O content, i.e., 5% present in the mix proportion and water content of 20%. However, FABL 1 (marked in blue) performed poorest among all, which consists of the lowest dosages of Na_2O and water content, i.e., 4% and 19%, respectively (Sharath et al. 2022).

By observing the presented Figures 4.4(c) and 4.5(c) for the aggregate impact value and aggregate crushing value of FA-GGBS aggregates, the mix FAGGBS 5 (marked in red) has performed best in comparison with all other FAGGBS aggregates, which is attributed to the highest dosages of Na_2O and GGBS content, i.e., 5% and 15%, respectively. The mix FAGGBS 1 (marked in blue) has performed the lowest of all. This mix is associated with the lowest dosages of Na_2O and GGBS content, i.e., 3% and 5%, respectively.

For aggregate impact value and aggregate crushing value the response indices of all governing factors associated with pelletized FA-BT, FA-BL, and FA-GGBS aggregates were determined and plotted in Figures 4.6(a-b), 4.7(a-b) and 4.8(a-c), respectively.

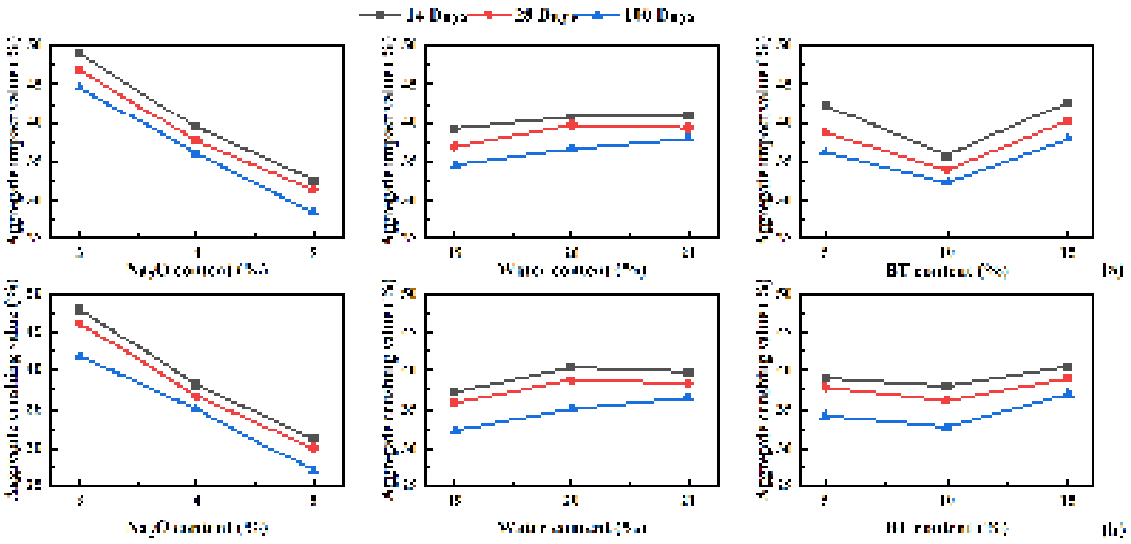

Figure 4.6: Relationship between response indices of governing factors and (a) aggregate impact value and (b) aggregate crushing value for FA-BT aggregates

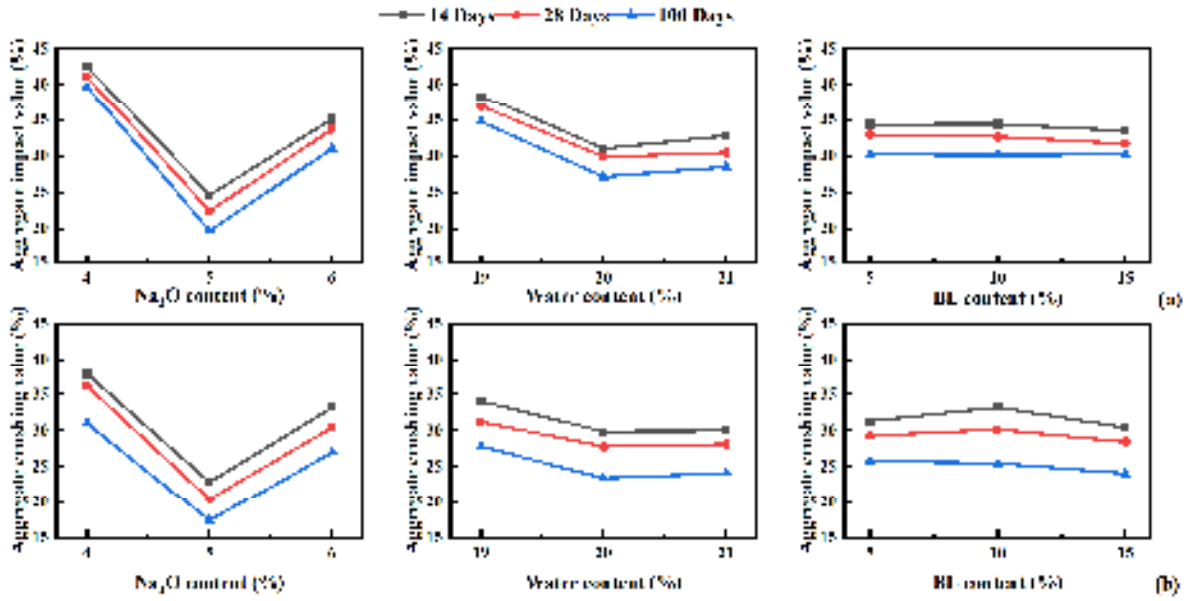

Figure 4.7: Relationship between response indices of governing factors and (a) aggregate impact value and (b) aggregate crushing value for FA-BL aggregates

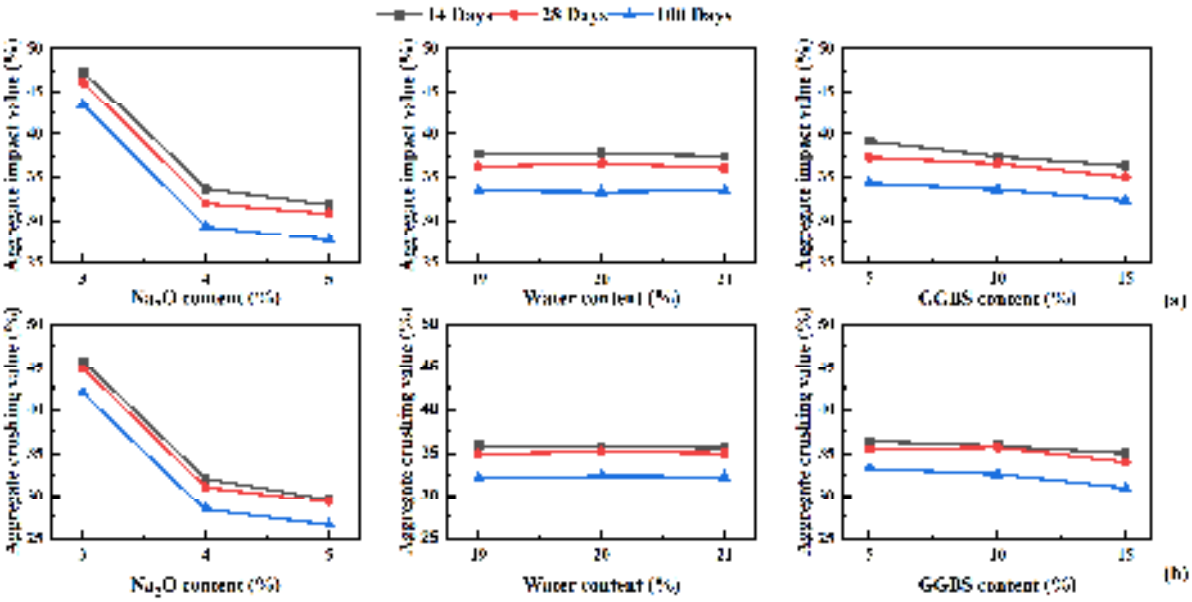

Figure 4.8: Relationship between response indices of governing factors and (a) aggregate impact value and (b) aggregate crushing value for FA-GGBS aggregates

It can be noticed from the figures that, among the three governing factors, water content dosage was found to have the least effect on aggregate impact and crushing value of FA-BT and FA-GGBS aggregates. However, for FA-BL aggregates, it was found that the dosage of BL has the least effect on aggregate impact value and aggregate crushing value among the three governing factors for FA-BL aggregates. From the figures, it can be

understood that the dosage of Na_2O was found to be directly proportional to the aggregate impact and crushing value of FA-BT, FA-BL, and FA-GGBS aggregates (Sharath et al. 2022). It can also be observed that 10% of BT and 15% of GGBS were found to be optimal for both aggregate impact value and aggregate crushing value of FA-BT and FA-GGBS aggregates, whereas, 20% of water content was found to be optimal for FA-BL aggregates (Sharath et al. 2022).

As per the prescribed limits specified by Indian standards IS 383-2016 (IS:383-2016) and 2386:1963-part 4 (IS 2386:1963-part 4), the aggregate impact value and aggregate crushing values for produced aggregates should not exceed 45 and 30%, respectively, provided they are used for concreting purposes. The aggregate impact and crushing values obtained for the produced FA-BT (FABT 9: 5% Na_2O content; 21% water content; 10% BT content), FA-BL (FABL 5: 5% Na_2O content: 20% water content; 15% BL content) and FA-GGBS (FAGGBS 7: 5% Na_2O content; 19% water content; 15% GGBS content) aggregates were hence found to be adhering to the prescribed limits as per Indian standards (Sharath et al. 2022).

4.2.2.2 Pelletized FA-IOT and FA-COT aggregates

Figures 4.9 (a–b) and 4.10 (a–b) show the test results for the aggregate impact value and the aggregate crushing value of pelletized FA-IOT and FA-COT aggregates, respectively.

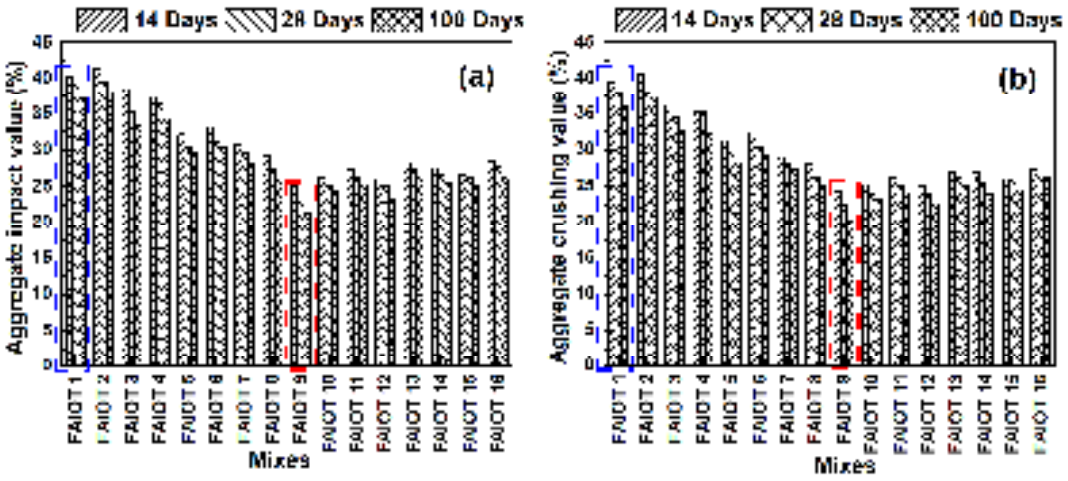

Figure 4.9: Obtained experimental results for (a) aggregate impact value and (b) aggregate crushing value of pelletized FA-IOT aggregates

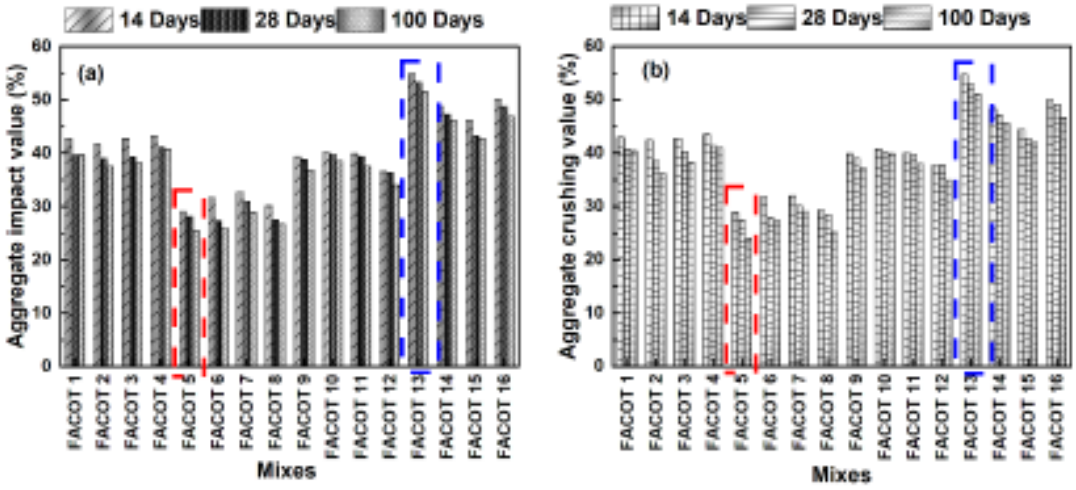

Figure 4.10: Obtained experimental results for (a) aggregate impact value and (b) aggregate crushing value of pelletized FA-COT aggregates

According to the obtained results for aggregate impact value and aggregate crushing value of pelletized FA-IOT aggregates presented in Figure 4.9(a-b), the lowest aggregate impact value and aggregate crushing value for curing ages of 14, 28, and, 100 days were, 25.1%, 23% and 21.2%; 24.4%, 22.3%, and 20.3%, respectively for trial mix FAIOT 9. However, the trial mix FAIOT 1 (marked in blue) showed the highest aggregate impact value as 40.2%, 39.3% and 37.2%; 39.4%, 38.1% and 36.1% for curing ages of 14, 28, and 100 days, respectively (Sharath et al. 2023a) (Note: for aggregate impact and crushing values, as per IS 2386:1963, part-IV, the obtained value should be less than 30% for aggregates that are going to be embedded in concrete).

From Figure 4.10(a-b), among all the pelletized FA-COT aggregate mixes, the mix FACOT 5 (marked in red) showed the lowest values for aggregate impact value at 14, 28, and 100 days, which were 29.1, 28.1, and 25.6% respectively. Similarly, for aggregate crushing value, the values obtained were 28.9, 27.3, and 24.1% for 14, 28, and 100 days, respectively. Whereas, the aggregate mix FACOT 13 (marked in blue) exhibited the highest values for aggregate impact value (54.9, 53.3, and 51.4% at all three curing ages, respectively). Similarly, the highest values for aggregate crushing value were also obtained, which were 54.8, 53, and 51.1% for 14, 28, and 100 days, respectively. (Note: for aggregate impact value and aggregate crushing value, as per IS 2386:1963, part-IV, the values should be less than 30% for aggregates that are going to be embedded in concrete.)

For aggregate impact value and aggregate crushing value, the response indices of all governing factors associated with pelletized FA-IOT were determined and plotted in

Figures 4.11(a-d) and 4.12(a-d), respectively. Similarly, for aggregate impact value and aggregate crushing value of FA-COT aggregates, they were represented in Figures 4.13(a-d) and 4.14(a-d) respectively.

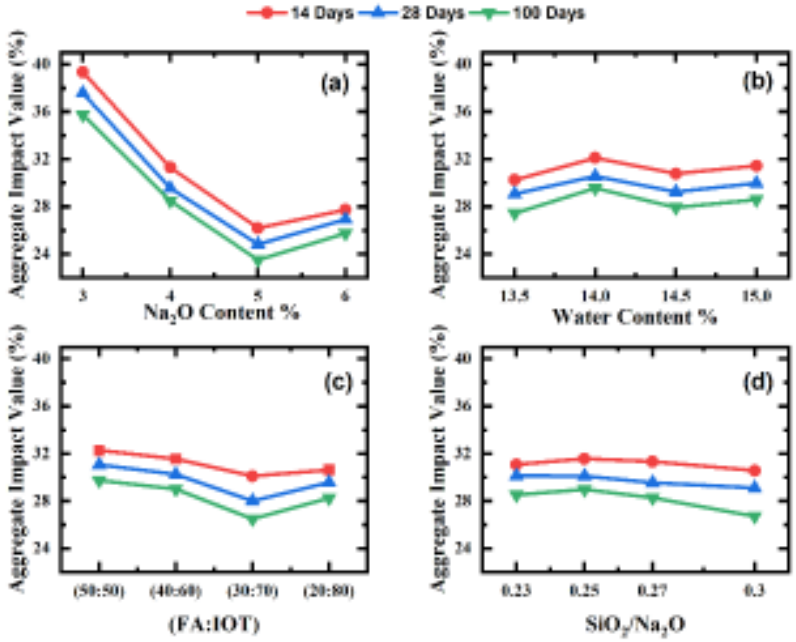

Figure 4.11: Relationship between response indices of governing factors (a) dosage of Na_2O (b) dosage of water content (c) dosage of FA:IOT (d) ratio of SiO_2 and Na_2O and aggregate impact value of pelletized FA-IOT aggregates

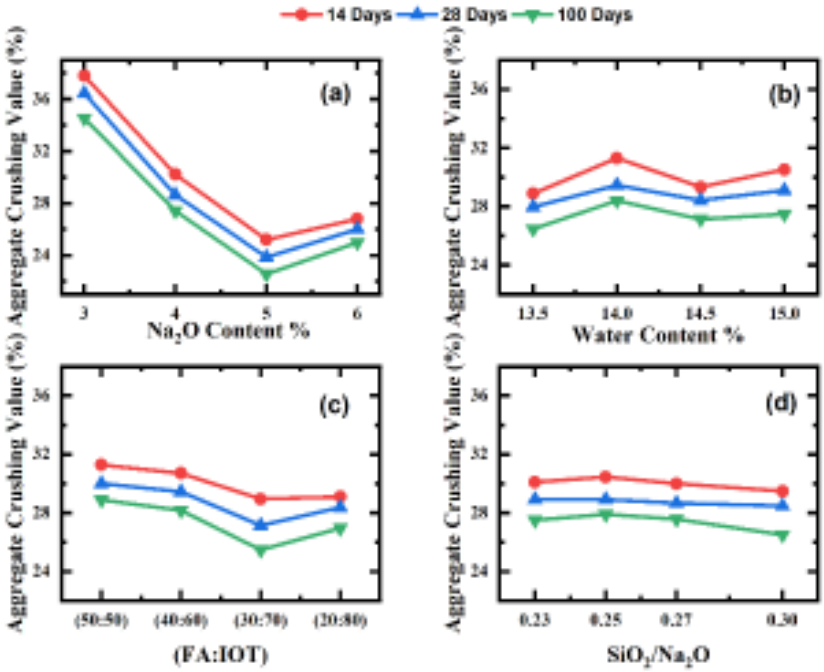

Figure 4.12: Relationship between response indices of governing factors (a) dosage of Na_2O (b) dosage of water content (c) dosage of FA:IOT (d) ratio of SiO_2 and Na_2O and aggregate crushing value of pelletized FA-IOT aggregates

Four different dosage contents of Na_2O were used in the production of pelletized FA-IOT aggregates: 3, 4, 5, and 6%, out of which the lowest aggregate impact value and aggregate crushing value from governing factor 1 (dosage of Na_2O), were exhibited by 5% of Na_2O, as observed from Figures 4.11a and 4.12a, respectively, for all the three curing ages. However, a decreasing trend for aggregate impact value and aggregate crushing value was observed with increasing dosages of Na_2O% from 3 to 5% gradually from 14 to 28 days (Sharath et al. 2023a). But this trend escalated with a dosage of Na_2O as 6 %. This implies that, in this case of aggregate impact value and aggregate crushing value, higher dosages of Na_2O can be related to achieving lower aggregate impact value and aggregate crushing value. However, when the dosage of Na_2O was increased of 6%, slightly higher values were obtained for aggregate impact and crushing property (Sharath et al. 2023a). This could be attributed to the high concentration of NaOH in the solution, which resulted in the quick and early precipitation of aluminosilicate gel along with quick hardening, which in turn suppressed the formation of other geopolymer- based precursors in the solution (Obenaus-Emler et al. 2020).

The influence of the water content dosages on the aggregate impact and aggregate crushing value of the produced FA-IOT aggregates can be noticed in Figures 4.11b and 4.12b, respectively. For this experimental parameter, the lowest aggregate impact value and aggregate crushing value were exhibited by 13.5% dosage of water content for curing ages of 14, 28, and 100 days. The influence of 13.5 to 14% dosage of water content showed an increasing trend for both properties, which decremented further with an increase in the dosage of water content. However, a 14% dosage of water content exhibited the highest value for aggregate impact value and aggregate crushing value (Sharath et al. 2023a).

Figures 4.11c and 4.12c explain the influence of the dosage of FA:IOT on the aggregate impact and crushing value of the produced FA-IOT aggregates. It can be observed from Figures 4.11c and 4.12c that the lowest aggregate impact value and aggregate crushing value were exhibited with a FA:IOT ratio of 30:70 at all three curing ages. The values for both properties were higher with FA:IOT ratios of 50:50, 40:60 and 20:80 (Sharath et al. 2023a). This could possibly be attributed to ground IOT (in this experimental study, the IOT was pulverized for better binding), which exhibits adhesive gelling properties in the alkaline environment created (Yao et al. 2020).

Figures 4.11d and 4.12d exhibit the influence of the SiO_2/Na_2O ratio on the aggregate impact value and aggregate crushing value of the produced FA-IOT aggregates. It can be observed from both figures that the lowest values for aggregate impact value and aggregate

crushing value were obtained with a SiO_2/Na_2O ratio of 0.3 for curing ages of 14, 28, and 100 days. There is a slight variation in the properties of the produced FA-IOT aggregates when the ratio of SiO_2/Na_2O is increased from 0.23 to 0.3 (Sharath et al. 2023a). An earlier study reported that a suitable range of SiO_2/Na_2O should be selected in the production of aggregates as it is an influential factor in strength gain, but only up to some extent (Shivaprasad and Das 2017). In general, a rise in the ratio of SiO_2/Na_2O results in an increase in the amount of sodium in the mixture, which is essential for the formation of polymers, but only up to some extent (Yao et al. 2020).

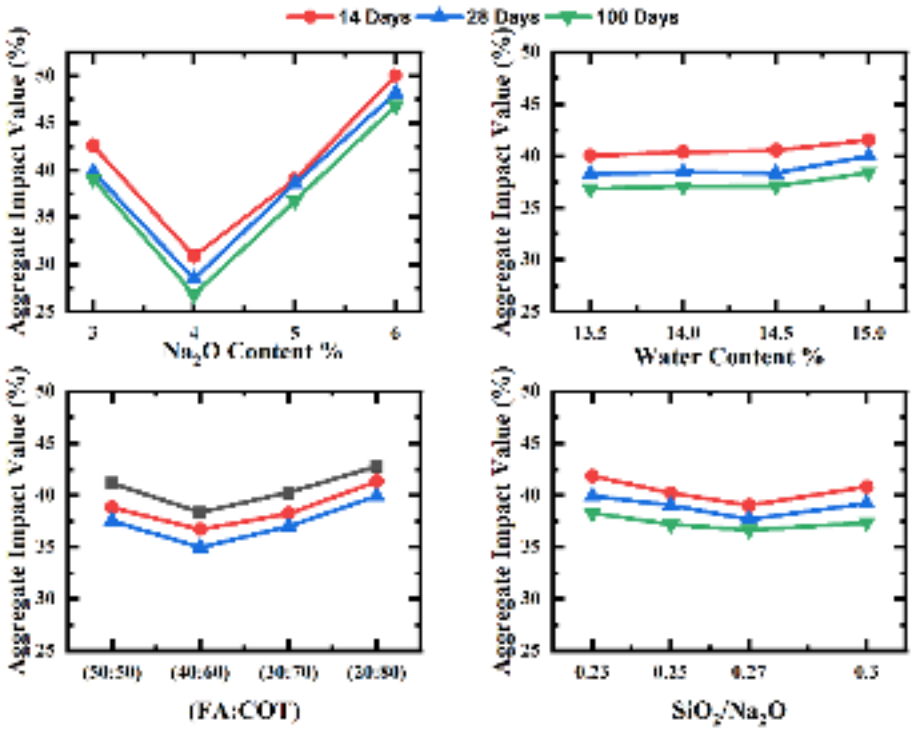

Figure 4.13: Relationship between response indices of governing factors (a) dosage of Na_2O (b) dosage of water content (c) dosage of FA:COT (d) ratio of SiO_2 and Na_2O and aggregate impact value of pelletized FA-COT aggregates

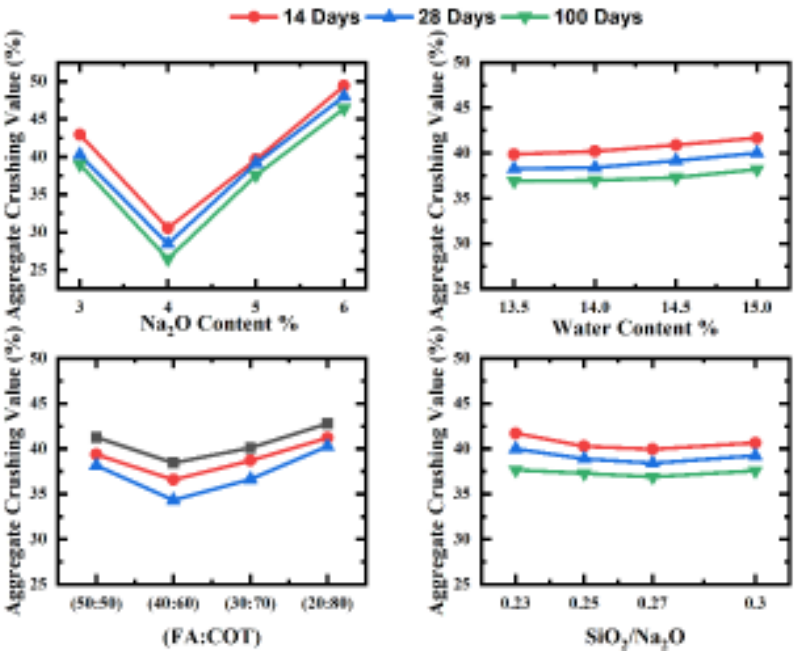

Figure 4.14: Relationship between response indices of governing factors (a) dosage of Na_2O (b) dosage of water content (c) dosage of FA:COT (d) ratio of SiO_2 and Na_2O and aggregate crushing value of pelletized FA-COT aggregates

By considering the varying dosage contents of Na_2O selected in the production of pelletized FA-COT aggregates (3, 4, 5, and 6%), the lowest aggregate impact value and aggregate crushing value obtained were for 4% Na_2O content, as noticed from Figures 4.13a and 4.14a, respectively, for all three curing ages. From the figures, it can be noticed that the trend for both the properties of the produced FA-COT aggregates decreased initially from 3 to 4% Na_2O content dosage, which was found to increase thereafter with the increasing Na_2O dosages (5 and 6%). This kind of behaviour can be related to the influence of Na_2O content on the dissolution of silica and alumina entities and the polycondensation process, as stated by various researchers (Khale and Chaudhary 2007; Panagiotopoulou et al. 2007; Rattanasak et al. 2011). For instance, Panagiotopoulou et al. (Panagiotopoulou et al. 2007) investigated the dissolution of silica and alumina from different industrial minerals as well as by products using varying Na_2O concentrations, and it was observed that the amount of silica in dissolved form increases with respect to the alkalinity of the solution, but only up to certain level and decreases there afterwards.

By taking into account the different dosage contents of water and blending ratios of FA with COT (FA:COT) in the production of pelletized FA:COT aggregates (13.5, 14, 14.5, and 15%) and (50:50, 40:60, 30:70, and 20:80), respectively, the lowest values for

aggregate impact value and aggregate crushing value were obtained for 13.5% water content and 40:60 as FA:COT ratio, as observed from Figures 4.13c and 4.14c, respectively, for 14, 28, and 100 days curing of produced FA-COT aggregates. From the exhibited figures, it can be observed that the trend for aggregate impact value and aggregate crushing value started increasing gradually with an increase in water content dosages (14-15%), whereas, in the case of the FA:COT ratio, it was found to be completely opposite. The aggregate impact value and aggregate crushing value decreased initially with the increasing FA:COT ratio (from 50:50 to 40:60), but were found to be increase gradually with increasing blending ratios of FA with COT (30:70 to 20:80). The behaviour of water content as well as the blending ratio of FA with COT can be combinedly related to the observations obtained during the production stage of aggregates, where it was noticed that an increment in both the experimental parameters (water content dosage and FA:COT ratio's) resulted in the formation of uneven and bigger-sized agglomerates, hence higher values for aggregate impact value and aggregate crushing value of produced FA-COT aggregates. A water content of 13.5% for a 40:60 blend ratio indicates an appropriate combination for producing pelletized FA-COT aggregates, wherein an increase in either water content or blend ratio affects the aggregate impact value and aggregate crushing value. Moreover, it can also be attributed to the gradation characteristics of COT, which is a coarser fraction compared to FA, for which an appropriate dosage of water content is necessary in order to obtain right-sized aggregates that can attain permissible values for aggregate impact value and aggregate crushing value.

From the SiO_2/Na_2O ratios selected for producing pelletized FA-COT aggregates (0.23, 0.25, 0.27, and 0.3), the lowest aggregate impact value and aggregate crushing value were obtained for 0.27, as represented in Figures 4.13d and 4.14d, respectively, for all three curing ages. The behaviour of aggregate impact value and aggregate crushing value with respect to the addition of SiO_2/Na_2O can be observed in the exhibited figures. The attained values of AIV and ACV were decreased gradually with increasing ratios and were found to be marginally increased with a 0.3 SiO_2/Na_2O ratio. This kind of observation can be due to the fact that the addition of Na_2SiO_3 to NaOH tends to improve the strength of the binder since it provides additional silica (Ahmari et al. 2012). However, this improvement is limited only up to certain level that tends to increase afterwards, as too much addition of silicate suppresses the evaporation of water, making the produced aggregates remain in a moist state themselves, hence attaining higher values for both aggregate impact value and aggregate crushing value even after 100 days.

By overlooking the behaviour of the four governing factors which are dosages of Na_2O, followed by water, FA:COT proportion and SiO_2/Na_2O ratio from the exhibited figure (Fig. 4.14), it can be deduced that the among all these governing factors, the dosages of Na_2O as well as FA:COT proportion majorly influenced the aggregate impact value and aggregate crushing value of the produced FA-COT aggregates. However, it can also be stated that 4% of Na_2O was found to be adequate to dissolve 60% of COT combined with 40% of FA, of course combined with lesser impactful factors was found to impart the requisite strength, hence leading to the attainment of lesser values of aggregates impact value and aggregate crushing value of produced FA-COT aggregates.

By summarizing the influence of governing factors like dosage levels of Na_2O, water and admixture contents (BT, BL and GGBS) on the aggregate impact value and aggregate crushing value of produced FA-BT, FA-BL and FA-GGBS aggregates, firstly, it can be stated that in all these three types of aggregates, Na_2O dosage of 5% has led in attainment of good values for aggregate impact value and aggregate crushing value. Secondly, for FA-BT and FA-BL aggregates, the aggregate impact value and aggregate crushing value is majorly influenced by 20% dosage of water content whereas it is 19% for FA-GGBS aggregates. Thirdly, an admixture content of 15% as BL and 15% of GGBS aided in achieving good values for aggregate impact value and aggregates crushing value for FA-BL and FA-GGBS aggregates. However, it stood as 5% of BT in FA-BT aggregates.

In light with the four governing factors (dosage levels of Na_2O, water, proportion of FA and IOT/COT (FA:IOT/FA:COT) and SiO_2/Na_2O ratio) on the aggregate impact value and aggregate crushing value of produced FA-IOT and FA-COT aggregates, firstly, it can be formulated that Na_2O dosage of 5% led in attaining good values for aggregate impact value and aggregate crushing value for FA-IOT aggregates whereas it is 4% for FA-COT aggregates. Secondly, a water content dosage of 13.5% majorly influenced the aggregate impact value and aggregate crushing value of both FA-IOT and FA-COT aggregates. Thirdly, the proportion of FA:IOT and FA:COT as 30:70 and 40:60, respectively led in achieving the desired values for aggregate impact value and aggregates crushing value for these two types of aggregates. Fourthly, an SiO_2/Na_2O ratio of 0.3 for FA:IOT aggregates and 0.27 for FA:COT aggregates served in achieving good values for aggregate impact value and aggregate crushing value.

4.2.3 Influence of governing factors on water absorption of binary blended pelletized aggregates

4.2.3.1 Pelletized FA-BT, FA-BL and FA-GGBS aggregates

Figure 4.15(a-c) shows the test results for the water absorption of pelletized FA-BT, FA-BL and FA-GGBS aggregates, respectively.

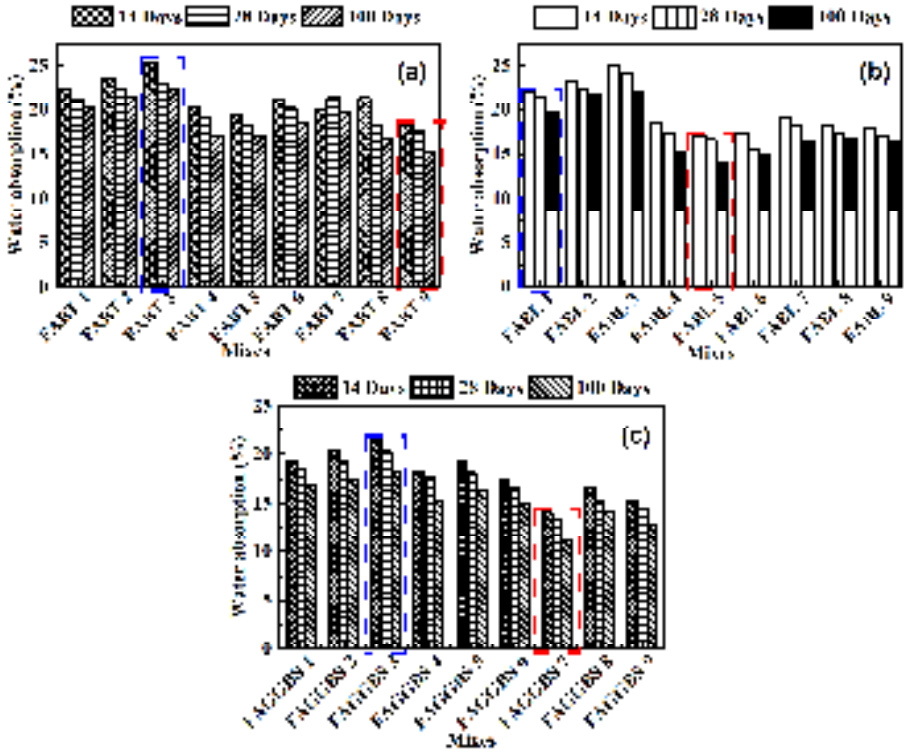

Figure 4.15: Obtained experimental results for water absorption of pelletized (a) FA-BT (b) FA-BL and (c) FA-GGBS aggregates

According to the results obtained on water absorption for produced FA-BT, FA-BL, and FA-GGBS aggregates [Figure 4.15a-c, respectively], FABT 9, FABL 5, and FAGGBS 7 (marked in red) had the lowest water absorption values, i.e., 15.3%, 14.1%, and 11.3%, respectively, at the curing age of 100 days (Sharath et al. 2022).

For water absorption, the response indices of all governing factors associated with pelletized FA-BT, FA-BL, and FA-GGBS aggregates were determined and plotted in Figure 4.16(a-c), respectively.

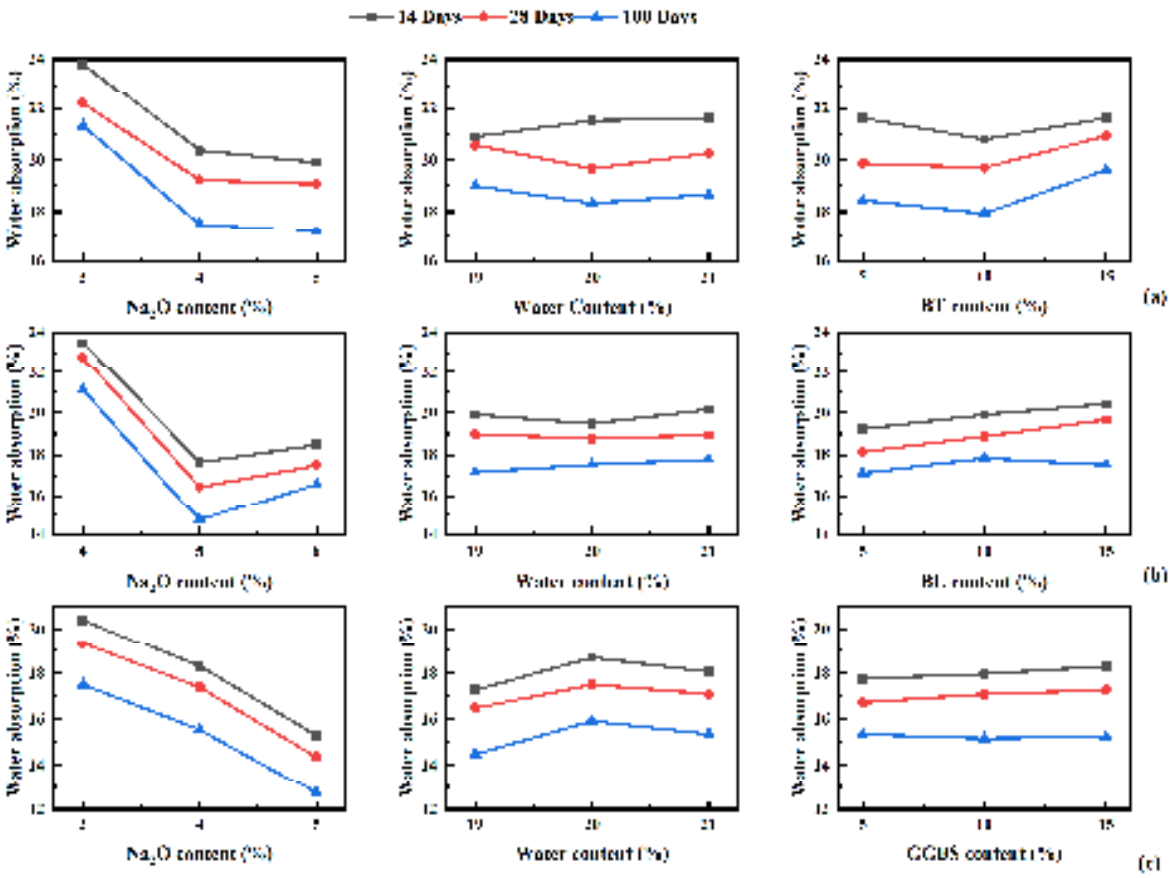

Figure 4.16: Relationship between response indices of governing factors and water absorption for pelletized (a) FA-BT (b) FA-BL and (c) FA-GGBS aggregates

According to the plotted relationship between calculated response indices and governing factors for produced FA-BT, FA-BL, and FA-GGBS aggregates (Figure 4.16(a-c)), the governing factor Na_2O content had the greatest influence on the water absorption of FA-BT, FA-BL, and FA-GGBS aggregates. It is reported that artificially produced aggregates of structural grade were found to absorb 5-25% by weight of dry aggregates (Holm and Ries 2006).

4.2.3.2 Pelletized FA-IOT and FA-COT aggregates

Figure 4.17(a-b) shows the test results for the water absorption of pelletized FA-IOT and FA-COT aggregates, respectively.

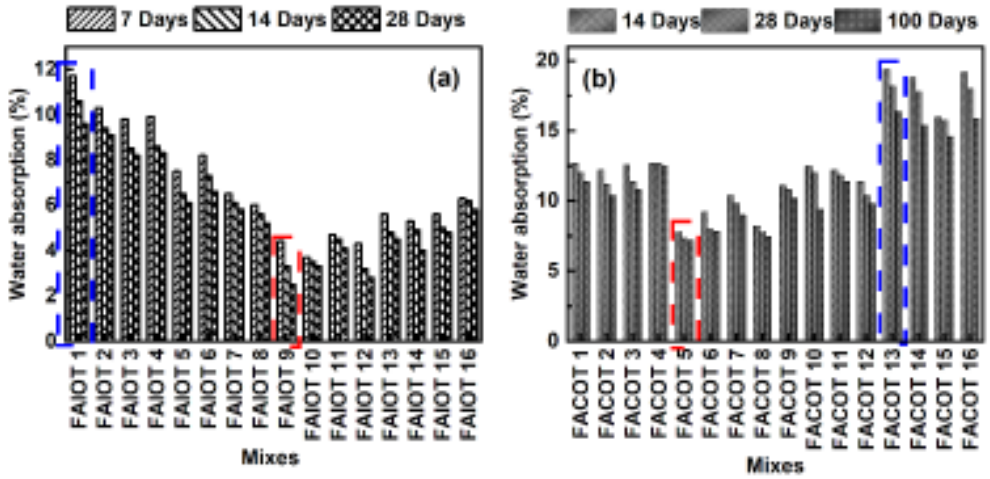

Figure 4.17: Obtained experimental results for water absorption of pelletized (a) FA-IOT and (b) FA-COT aggregates

According to the obtained results for water absorption of pelletized FA-IOT aggregates presented in Figure 4.17a, the lowest water absorption for all three curing periods was 4.4, 3.3, and 2.5%, respectively, which was observed in trial mix FAIOT 9 (marked in red), whereas FAIOT 1 (marked in blue) showed the highest water absorption of 11.7, 10.6, and 9.6% for curing periods of 14, 28 and 100 days (Sharath et al. 2023a), respectively.

From Figure 4.17b, among all the pelletized FA-COT aggregate mixes, the aggregate mix FACOT 5 (marked in red) obtained the lowest values for water absorption at 14, 28, and 100 days, which were 7.8%, 7.3%, and 7.2%, respectively. Whereas, the aggregate mix FACOT 13 (marked in blue) obtained higher values for water absorption (19.4, 18.2, and 16.4%) at all three curing ages, respectively.

For water absorption, the response indices of all governing factors associated with pelletized FA-IOT and FA-COT aggregates were determined and plotted in Figures 4.18(a-d) and 4.19 (a-d), respectively.

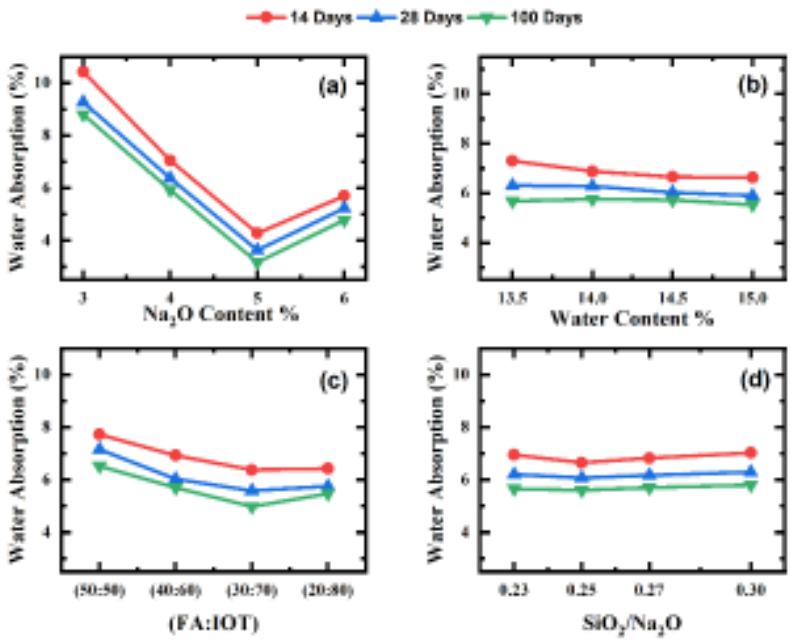

Figure 4.18: Relationship between response indices of governing factors (a) dosage ofNa2O (b) dosage of water content (c) dosage of FA:IOT (d) ratio of SiO2 and Na2O and water absorption of pelletized FA-IOT aggregates

From Figure 4.18a, it can be understood that a 5% dosage of Na_2O presented lower values in the produced FA-IOT aggregates at curing ages 14, 28, and 100 days. A decreasing trend for water absorption was noticed with increasing Na_2O dosages from 3 to 5%, which incremented further when the dosage content reached 6%. By reviewing this behavior, it can be specified that lower water absorption was associated with higher dosages of Na_2O in the production of pelletized FA-IOT aggregates (Sharath et al. 2023a). However, the impact of dosages of FA:IOT on the water absorption of the produced FA-IOT aggregates is represented in Figure 4.18c. The lowest water absorption is depicted by 70% of IOT to 30% FA for all three curing ages. Water absorption of produced FA-IOT aggregates decreased gradually with the increase in IOT dosage, which increased further (in a few amounts, viz., 4.9 to 5.4%) for the 20:80 ratio of FA:IOT, at curing ages 14, 28, and 100 days. This could be attributed to the that the finer IOT used in this experimental study behaves as a microaggregate filling agent, which diffuses in the geopolymer and fills up the internal space by bridging the gap inside the microstructure of the produced FA-IOT aggregates (Jang et al. 2014).

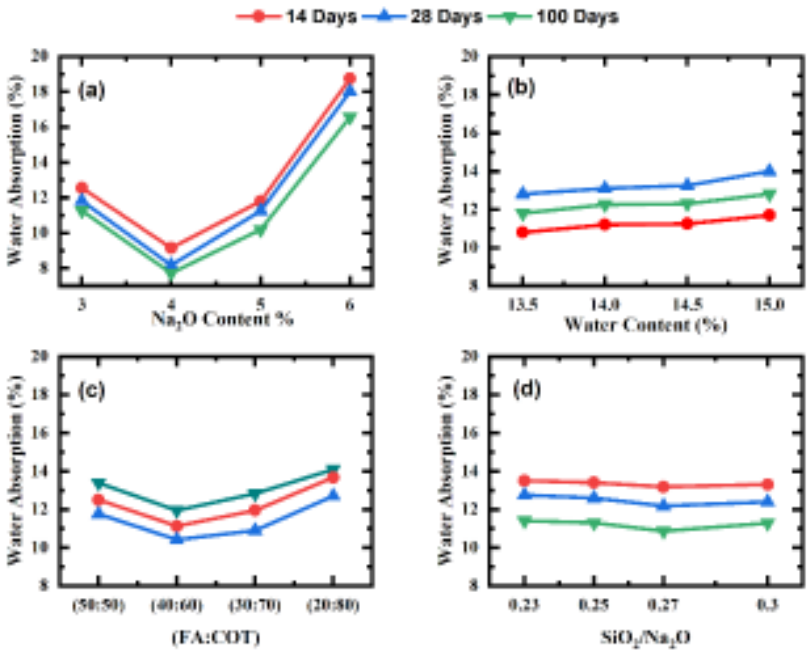

Figure 4.19: Relationship between response indices of governing factors (a) dosage of Na_2O (b) dosage of water content (c) dosage of FA:COT (d) ratio of SiO_2 and Na_2O and water absorption of pelletized FA-COT aggregates

As per the obtained response indices for water absorption of the produced FA-COT aggregates presented in Figure 4.19(a-d), it can be observed that the governing factors, such as the varying dosage contents of Na_2O, water, FA:COT, and SiO_2/Na_2O, are having a significant influence on the water absorption of the produced FA-COT aggregates. By taking the variation in dosage contents of Na_2O into account (3, 4, 5, and 6%), the lowest water absorption value was obtained for 4% Na_2O content, as noticed from Figure 4.19a for all three curing ages, respectively. From the figure, it can be observed that the values for water absorption of the produced FA:COT aggregates decreased initially as the Na_2O dosage changed from 3 to 4% and started increasing thereafter with the increasing Na_2O dosages (5 and 6%). This could be related to the filling up of voids by NaOH as well as the lubrication provided by NaOH, as stated by some researchers (Kang et al. 2015; Osinubi et al. 2015).

By considering the variation in water content dosages (13.5, 14, 14.5, and 15%), the lowest water absorption value of produced FA-COT aggregates was obtained for 13.5% water content, as observed from Figure 4.19b, for 14, 28, and 100 days of curing of the produced FA-COT aggregates. From the figure, it can be noticed that the water absorption values for the produced FA-COT aggregates kept on increasing with the increase in the water content

dosages for the production of pelletized FA-COT aggregates, which aims to prove the general fact that water content dosages act like a medium for the geopolymeric reaction. It is very much necessary that sufficient amount of water be available for the geopolymeric binder formation that links the unreacted and partially reacted particles (Ahmari et al. 2012). The presence of excess water leads to the formation of large pores, weakens the produced aggregate samples, and hence attains greater values of water absorption for the produced FA-COT aggregates.

By considering the variation in blend ratio of FA and COT (FA:COT – 50:50, 40:60, 30:70, and 20:80), the lowest value for water absorption of the produced FA-COT aggregates was attained for 60:40, as observed from Figure 4.19d, for all three curing ages. From the figure, it can be observed that water absorption values for the produced FA-COT aggregates decreased as the FA:COT ratio changed from 50:50 to 40:60 and increased marginally thereafter as the ratio changed from 30:70 to 20:80. This behaviour can be related to the general fact that an increase in the content of COT from 50 to 60% has led to the formation of right-sized and compact agglomerates by the complete consumption of the fed materials in the pelleting disc during the production of the aggregates. A further increase in the proportion of copper had led to weak and uneven-shaped agglomerates, which explains the attainment of higher values for water absorption. Hence, it can be stated in a generalized manner that an appropriate blend ratio of FA with COT is necessary, as it aids in filling up the pores and voids in the produced FA-COT aggregates.

Summarizing the influence of governing factors like Na_2O dosage, water, and admixture contents (BT, BL, and GGBS) on the water absorption of FA-BT, FA-BL, and FA-GGBS aggregates, firstly, 5% Na_2O dosage has aided in achieving lesser values of water absorption for all the three types of aggregates. Secondly, a dosage of 20% as water content helped in attaining lesser values of water absorption for FA-BT and FA-BL aggregates, whereas it stood at 19% for FA-GGBS aggregates. Thirdly, 15% BL and 15% GGBS admixture dosages aided FA-BL and FA-GGBS aggregates achieve good values for water absorption. For FA-BT aggregates, it is achieved with 5% dosage of BT.

In light of the four governing factors (dosage levels of Na_2O, water, proportion of FA and IOT/COT (FA:IOT/FA:COT) and SiO_2/Na_2O ratio) on the water absorption of produced FA-IOT and FA-COT aggregates, a 5% Na_2O dosage led to attain lesser water absorption for FA-IOT aggregates and 4% for FA-COT aggregates. Secondly, 13.5% as water content dosage greatly affected the water absorption of both FA-IOT and FA-COT aggregates. Thirdly, FA:IOT and FA:COT ratios of 30:70 and 40:60 achieved the necessary water

absorption values for these two kinds of aggregates. Fourthly, SiO_2/Na_2O ratio of 0.3 for FA:IOT aggregates and 0.27 for FA:COT aggregates improved water absorption values.

4.2.4 Influence of governing factors on individual crushing strength of pellets of binary blended pelletized aggregates

4.2.4.1 Pelletized FA-BT, FA-BL and FA-GGBS aggregates

Figure 4.20(a-c) shows the test results for the individual crushing strength of pellets of pelletized FA-BT, FA-BL and FA-GGBS aggregates, respectively.

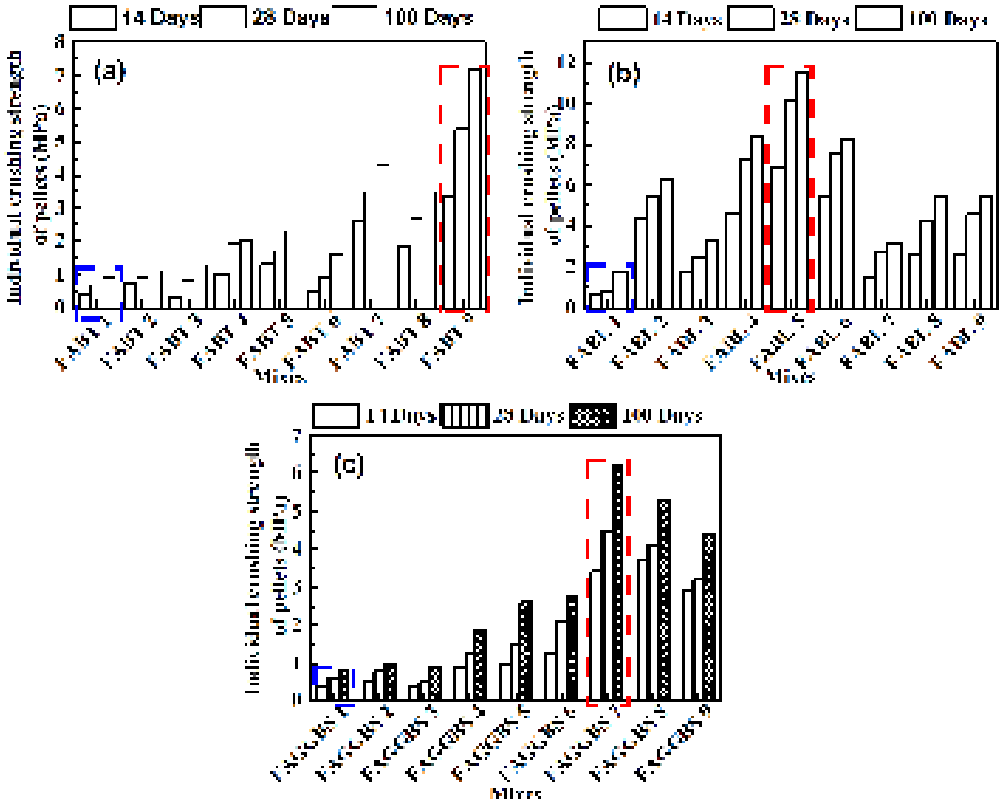

Figure 4.20: Obtained experimental results for individual crushing strength of pellets of pelletized (a) FA-BT (b) FA-BL and (c) FA-GGBS aggregates

As per the data presented in Figure 4.20a, the individual crushing strength of pellets measured for aggregate mix FABT 9 was found to be to 7.2 MPa at 100 days of curing. This mix consists of the highest dosage contents of Na_2O and water, i.e., 5% and 21%, respectively, with a BT content of 10%. Aggregate mix FABT 1 was found to have the lowest crushing strength of pellets at 0.9 MPa at the curing age of 100 days (Sharath et al. 2022). This is attributed to the lowest dosage content of Na_2O, water, and BT content in the aggregate mix, i.e., 3%, 19%, and 5%, respectively. Previous research has reported that fly

ash–based pelletized aggregates produced by admixing clay minerals as an admixture have an individual crushing strength of 1.0–8.2 MPa (Gomathi and Sivakumar 2014b).

Based on the measured values of the crushing strengths of the FA-BL aggregates (Figure 4.20b), the FABL 5 aggregate mix had the highest crushing strength, at 11.6 MPa after 100 days of curing. Whereas the lowest crushing strength value was obtained for the FABL 1 aggregate mix, i.e., 1.8 MPa at the curing age of 100 days. The variations in the dosage contents of Na_2O, water, and BL caused the resulting difference in individual crushing strength between

these two mixes. Increased crushing strength for aggregate mix FABL 5 corresponds to dosage contents of Na_2O (5%) and water (20%) with the highest BL content (15%). For FABL 1, the aggregate mix, which possessed lower crushing strength, consisted of a combination of lower dosage contents of Na2O (4%), water (19%), and BL (5%) (Sharath et al. 2022). However, it is understood from past research that fly ash–based aggregates produced using lime as an additive admixture have reported an individual pellet strength of 2.6 MPa (Sivakumar and Gomathi 2012).

According to the results obtained on the individual crushing strength of pellets of FA-GGBS aggregates [Figure 4.20c], the mix FAGGBS 7 demonstrated the highest individual crushing strength of 6.2 MPa at 100 days of curing age. This increase in crushing strength of the aforementioned mix corresponds to the high dosage contents of Na_2O (5%), water (19%), and GGBS (15%) (Sharath et al. 2022). The aggregate mix FAGGBS 1 exhibited the lowest individual crushing strength of 0.8 MPa at 100 days of curing age, which corresponds to low-dosage contents of Na_2O (3%), water (19%), and GGBS (5%).

For individual crushing strength of pellets, the response indices of all governing factors associated with pelletized FA-BT, FA-BL, and FA-GGBS aggregates were determined and plotted in Figure 4.21(a-c), respectively.

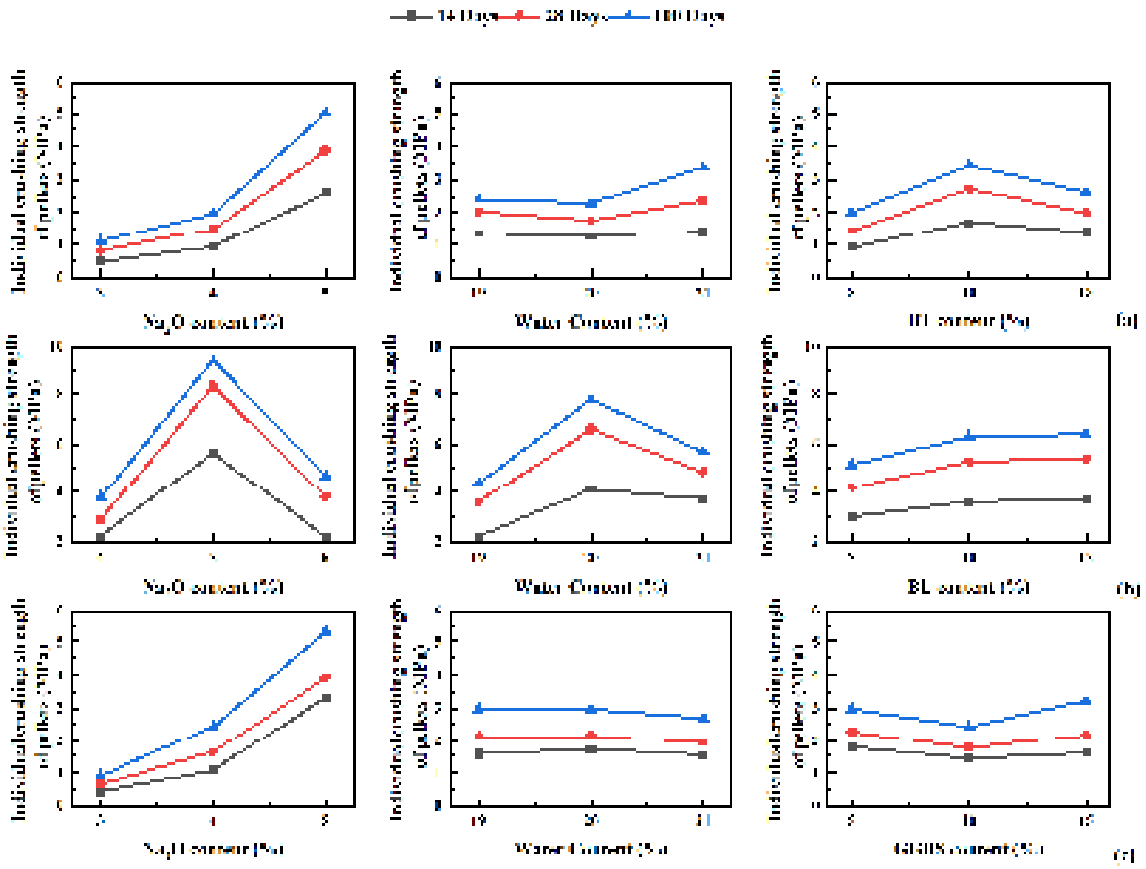

Figure 4.21: Relationship between response indices of governing factors and individual crushing of pellets for pelletized (a) FA-BT (b) FA-BL and (c) FA-GGBS aggregates

The plotted relationship between the calculated response indices and governing factors in pelletized FA-BT aggregates presented in Figure 4.21a suggests that the individual crushing strength of FA-BT aggregates is directly proportional to Na_2O and water content dosages. In addition to this, dosages of BT content up to a certain percentage (i.e., 10%) showed an increment in individual crushing strength only. Further, with the increase in curing age, a relative superiority in crushing strength for FA-BT aggregates can be witnessed (Sharath et al. 2022).

The plotted relationship between the calculated response indices and governing factors in pelletized FA-BL aggregates presented in Figure 4.21b suggests the individual crushing strength values increase up to a certain dosage level of Na_2O (5%) and water content (20%), after which the individual crushing strength decreases. But, in the case of the governing factor, BL content, an increase in individual crushing strength values was found to be proportional to BL content (Sharath et al. 2022).

The relationship between calculated response indices and governing factors in FA-GGBS aggregates is depicted in Figure 4.21c. From the figure, the following interpretations can be drawn: (1) with the increase in dosage contents of Na_2O, the individual crushing strength increased; (2) marginal changes in individual crushing strength values were observed for different dosage contents of water; and (3) as the GGBS dosage content increased (up to 10%), individual crushing strength decreased, which again increased with an increment in GGBS dosage contents (Sharath et al. 2022).

4.2.4.2 Pelletized FA-IOT and FA-COT aggregates

Figure 4.22(a-b) shows the test results of individual crushing strength of pellets of pelletized FA-IOT and FA-COT aggregates, respectively.

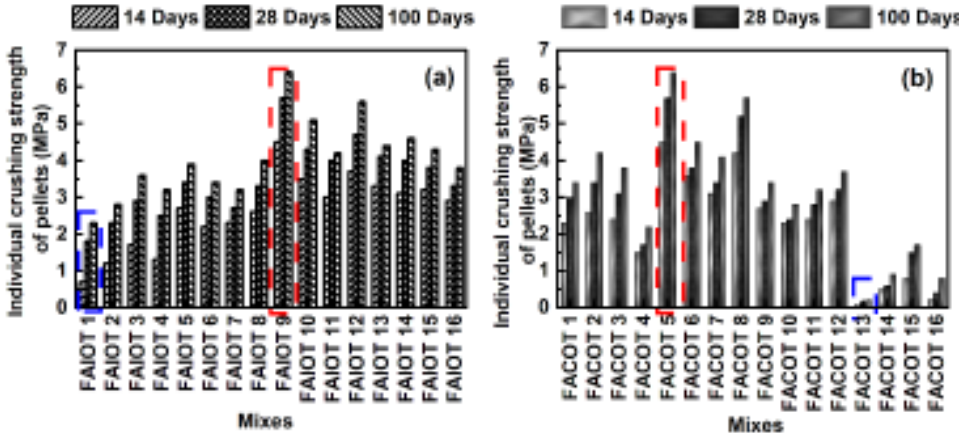

Figure 4.22: Obtained experimental results for individual crushing strength of pellets of pelletized (a) FA-IOT and (b) FA-COT aggregates

Figure 4.22a shows the results for the individual crushing strength of pellets of pelletized FA-IOT aggregates. For curing periods of 14, 28, and 100 days, the highest individual crushing strength of pellets was 4.5, 5.7, and 6.4 MPa in trial mix FAIOT 9 (marked in red), while FAIOT 1 (marked in blue) had the lowest individual crushing strength of pellets at 0.7, 1.8, and 2.3 MPa for curing periods of 14, 28, and 100 days (Sharath et al. 2023a). From Figure 4.22b, among all the pelletized FA-COT aggregate mixes, the aggregate mix FACOT 5 (marked in red) attained the highest values for individual crushing strength of pellets at 14, 28, and 100 days, which are 4.5, 5.7, and 6.4 MPa, respectively. While the aggregate mix FACOT 13 attained lower values for individual crushing strength of pellets (0.08, 0.15, and 0.2 MPa) at all three curing ages.

For individual crushing strength of pellets, the response indices of all governing factors associated with pelletized FA-IOT and FA-COT aggregates were determined and plotted in Figures 4.23(a-d) and 4.24(a-d), respectively.

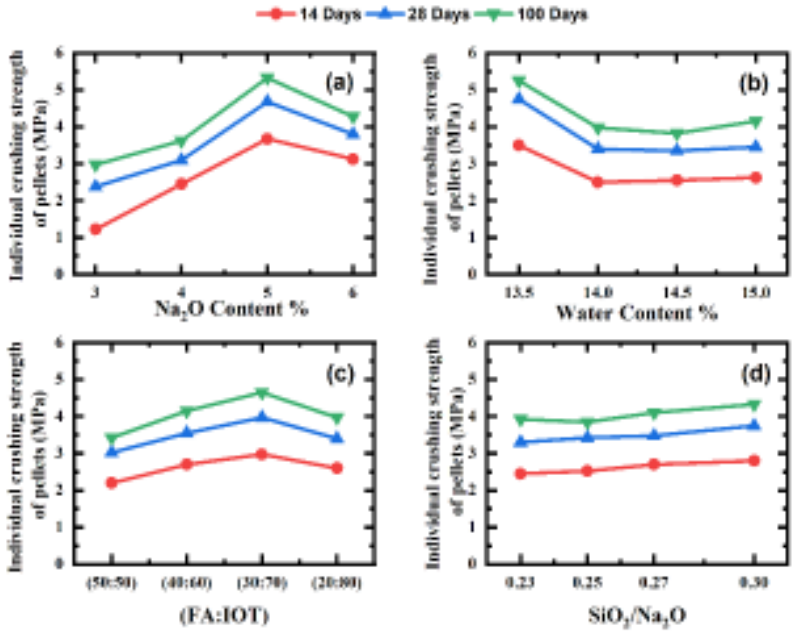

Figure 4.23: Relationship between response indices of governing factors (a) dosage of Na_2O (b) dosage of water content (c) dosage of FA:IOT (d) ratio of SiO_2 and Na_2O and individual crushing strength of pellets of pelletized FA-IOT aggregates

The impact of Na_2O dosage content on the individual crushing strength of pellets of produced FA-IOT aggregates is depicted in Figure 4.23a. Four dissimilar dosage contents of Na_2O were considered in this study: 3, 4, 5, and 6%. The 5% dosage of Na_2O content showed the highest individual crushing strength of pellets in the produced FA-IOT aggregates at all three curing ages. An incrementing trend of individual crushing strength of pellets was observed with an increase in Na_2O dosages from 3 to 5%, which decreased when it reached to 6%. From this observation, it can be indicated that greater individual crushing strength of pellet values was related to higher amounts of Na_2O in the production of aggregates (Sharath et al. 2023a). Furthermore, the influence of dosages of FA:IOT can be combined with the behavior of Na_2O amounts in production, represented in Figure 4.23c. In the case of the dosage of FA:IOT the highest individual crushing strength of pellets was depicted by 70% of IOT for curing ages of 14, 28, and 100 days. The individual crushing strength of pellets increased gradually with an increase in FA:IOT, which decremented further for the 20:80 ratio of FA:IOT at all three curing ages (Sharath et al. 2023a). In the

production of pelletized FA:IOT aggregates, the procured raw IOT was pulverized to a fine powder, which has aided in the individual crushing strength of pellet development in the produced FA-IOT aggregates. It has been reported that a variation in grain size distribution during the binding phase significantly impacts the strength properties and also enhances the physical properties (dos Santos et al. 2019). An additional fact (which has been reported in previous findings) is that usage of IOT as an additive in geopolymers has a strong relationship between dosage of IOT content and formation of C-S-H, which leads to improvements in strength properties (Duan et al. 2016b). More amounts of IOT suppress its reactivity compared with FA, which decelerates the individual crushing strength of the pellets of the produced FA-IOT aggregates.

Figure 4.23d represents the impact of the SiO_2/Na_2O ratio on the individual crushing strength of the produced FA-IOT aggregates. Out of the four governing factors considered, SiO_2/Na_2O ratio seems to be the one with the lowest level of impact on individual crushing strength. Although this observation is not simple, as there are other variations in experimental factors apart from SiO_2/Na_2O, the obtained results clearly depict that an increment in the SiO_2/Na_2O ratio produces a very gradual increase in the individual crushing strength of the produced FA-IOT aggregates.

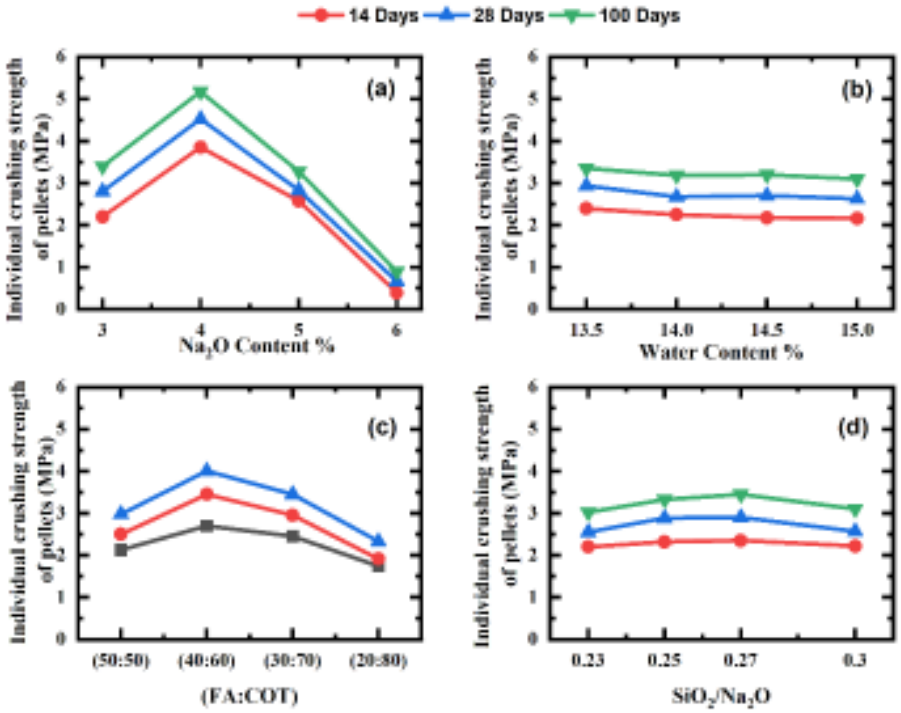

Figure 4.24: Relationship between response indices of governing factors (a) dosage of Na_2O (b) dosage of water content (c) dosage of FA:COT (d) ratio of SiO_2 and Na_2O and individual crushing strength of pellets of pelletized FA-COT aggregates

By examining the variability in dosage contents of Na_2O (3, 4, 5, and 6%) in the production of pelletized FA-COT aggregates, the highest individual crushing strength of pellets was obtained for 4% Na_2O, as depicted in Figure 4.24a for 14, 28, and 100 days of curing of produced FA-COT aggregates. From the represented figure, a subsequently increasing trend in the individual crushing strength of pellets can be observed with respect to Na_2O dosages that is between 3 and 4%, which decreased sharply when the Na_2O dosages changed from 5 to 6% (the lowest values are observed for 6% Na_2O). This kind of behaviour clearly explains the underlying effect of Na_2O dosages on the characteristic property, but only up to some extent. The presence of Na_2O dosages or concentration of NaOH dissolves silica and alumina in the incorporated aluminosilicates during the production of FA-COT aggregates, which leads to the formation of thicker geopolymeric-based binder (Ahmari and Zhang 2012). The geopolymer-based binder assists in developing a link between partially reacted particles and contributes directly to the strength development of the geopolymer materials. The refinement of alkalinity in the geopolymerization process is stated by a number of researchers (Khale and Chaudhary 2007; Rattanasak and Chindaprasirt 2009; Somna et al. 2011; Wang et al. 2005).

By evaluating the variability in water content dosages (13.5, 14, 14.5, and 15%), the highest individual crushing strength of pellets was attained for 13.5% water, as shown in Figure 4.24b, for 14, 28 and 100 days curing of produced FA-COT aggregates. From the figure, a decrease in the individual crushing strength of pellets can be clearly observed with increasing water content dosages, where the lowest individual crushing strength of pellets was obtained for a 15% water content dosage. At higher water content dosages, the existing sodium cations could get diffused without any contribution in the process of geopolymerization, which hence affects the strength parameter (individual crushing strength of pellets) of the produced FA-COT aggregates (Sadat et al. 2016).

By considering the variation in blending ratio of FA:COT (FA:COT – 50:50, 40:60, 30:70, and 20:80) in the production of pelletized FA-COT aggregates, the highest individual crushing strength of pellets was obtained for 40:60 FA:COT ratio, as shown in Figure 4.24c, for all the three curing ages of the produced FA-COT aggregates. The individual crushing strength of pellets increased with the increasing blend ratio from 50:50 to 40:60, which was found to be decrease thereafter as the blend ratio increased further (from 30:70 to 20:80). This can be attributed to the filling up of voids in the produced FA-COT aggregates, which makes the aggregates partially denser with the addition of COT, as it possesses a higher specific gravity compared to FA. Moreover, the incorporation of pulverized COT in the

production of FA-COT aggregates also helps in promoting the alkali-activation process, and it enhances the strength characteristics of the produced geopolymer-based materials (Singh and Singh 2019).

From the SiO_2/Na_2O ratios selected for this experimental investigation (0.23, 0.25, 0.27, and 0.3), the highest individual crushing strength of pellets was obtained for 0.27, as depicted in Figure 4.24d, for 14, 28, and 100 days of curing of produced FA-COT aggregates. The behaviour of individual crushing strength of pellets with respect to the variation of SiO_2/Na_2O can be observed in the exhibited figure, where the individual crushing strength of pellets increased gradually with the increasing ratio and were found to decrease thereafter. This kind of observation can be related to the stated fact that adding Na_2SiO_3 to NaOH refines the strength characteristics of the binding agent as more silica is made available in the geopolymer system (Ahmari et al. 2012). It is commonly known that the alumina component in the aluminosilicate raw material gets dissolved with ease compared to silica in the early stages. Since in this case, the dissolved alumina content requires more amounts of silica for the geopolymerization reaction and hence the addition of Na_2SiO_3 fulfils the need of extra silica. But the improvement in the strength characteristics (in this case, the individual crushing strength of pellets) because of Na_2SiO_3 addition is limited only up to a certain level (Bernal et al. 2012) (in this case, the 0.27 SiO_2/Na_2O ratio). This could be due to the presence of excess Na_2SiO_3 that delays water evaporation by making the produced FA-COT aggregates exist in the moist condition itself, hence the low individual crushing strength of the pellets of the produced FA-COT aggregates.

To summarize the effect of governing parameters such as Na_2O dose, water, and admixture contents (BT, BL, and GGBS) on individual crushing strength of FA-BT, FA-BL, and FA-GGBS aggregates, firstly, a 5% Na_2O dosage helped to attain greater values for individual crushing strength for all three types of aggregates. Secondly, using 20% water content resulted in achieving good individual crushing strength values for FA-BT and FA-BL aggregates, whereas it stood at 19% for FA-GGBS aggregates. Thirdly, admixture dosages of 15% BL and 15% GGBS helped FA-BL and FA-GGBS aggregates reach good individual crushing strength values, wherein it was possible with a 5% BT dosage for FA-BT aggregates.

In light of the four governing factors (Na_2O, water, FA:IOT/FA:COT, and SiO_2/Na_2O ratio) on the individual crushing strength characteristics of produced FA-IOT and FA-COT aggregates, firstly, a 5% and 4% Na_2O dosage resulted in greater individual crushing

strength values for FA-IOT and FA-COT aggregates, respectively. Secondly, 13.5% water content dose had a significant impact on the individual crushing strength of both FA-IOT and FA-COT aggregates. Thirdly, FA:IOT and FA:COT ratios of 30:70 and 40:60 respectively helped in attaining good values for individual crushing strength for these two types of aggregates. Fourthly, a SiO_2/Na_2O ratio of 0.3 for FA:IOT aggregates and 0.27 for FA:COT aggregates resulted in higher individual crushing strength values.

4.2.5 Specific gravity

The average specific gravity measured for FA-BT, FA-BL, and FA-GGBS aggregates was found to be within the range of 2.0–2.2 (Sharath et al. 2022). However, for FA-IOT and FA-COT aggregates, it was found to be within the range of 2.4–2.6. As IOT and COT were denser than FA, their dosage influenced the specific gravity of the produced FA-IOT and FA-COT aggregates (Sharath et al. 2023a). A detailed table showing the obtained values for the specific gravity of pelletized FA-BT, FA-BL, FA-GGBS, FA-IOT, and FA-COT aggregates is presented in Figure 4.25.

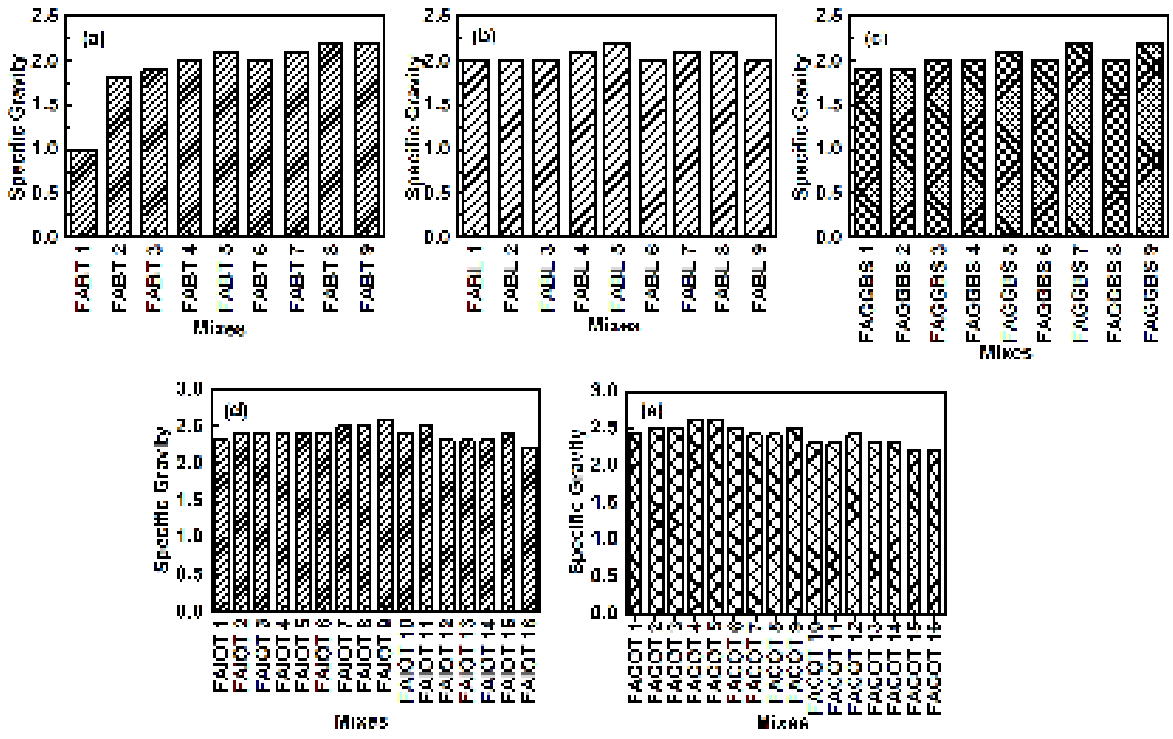

Figure 4.25: Specific gravity of pelletized (a) FABT (b) FABL (c) FAGGBS (d) FAIOT and (d) FACOT aggregates

4.3 ADVANCED CHARACTERIZATION STUDIES ON BINARY BLENDED PELLETIZED AGGREGATES

The advanced characterization studies like SEM, TGA and FTIR was performed on the best-performing binary blended pelletized aggregate mixes (FABT 9, FABL 5, FAGGBS 7, FAIOT 9, and FACOT 5: all the aggregate samples cured at 100 days) which were identified based on the obtained engineering properties and the relationship between the governing factors and engineering properties of these binary blended pelletized aggregates.

4.3.1 Morphology of the best performing binary blended pelletized aggregate mixes (SEM)

The microphotographs of best performing binary blended pelletized aggregates are presented in Figure 4.26.

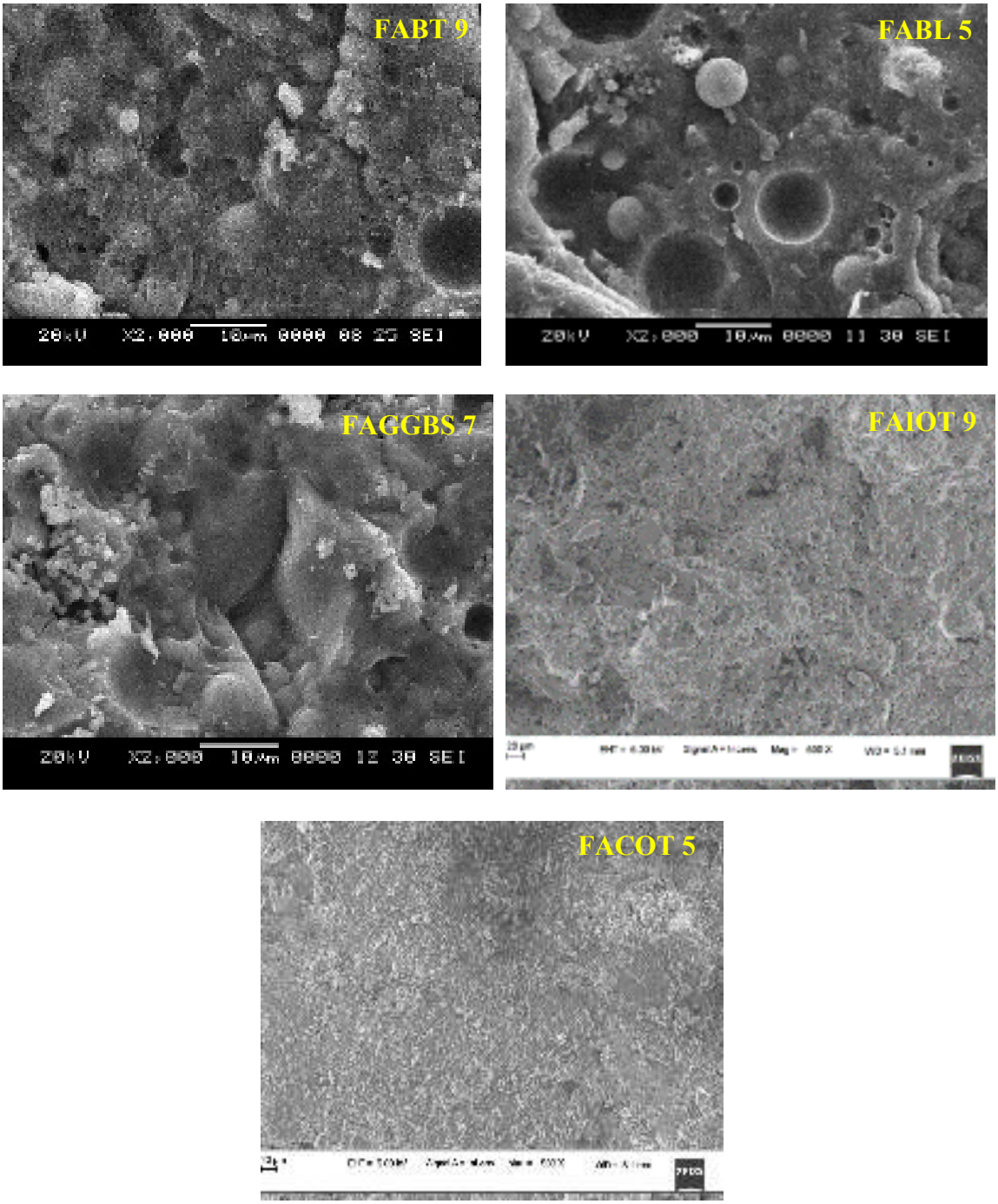

Figure 4.26: Microphotographs of binary blended pelletized aggregates

From Figure 4.26, it can be noticed that FABT 9, FABL 5, and FAGGBS 7 mixes showed large traces of unreacted spherical fly-ash particles. The FABT 9 mix depicted reduced traces of spherical and plate-like structures (plate-like structures of BT) which indicates the involvement of FA and BT particles in the process of polymerization. Further, the image displays a more compact and denser grey microstructure owing to the larger formation of hydration products [sodium aluminosilicate gel (N-A-S-H) or calcium-aluminosilicate gel (C-A-S-H)] (Sharath et al. 2022). From the depicted SEM images of FABL 5 and FAGGBS

7 mixes, it can be understood that mushy-like particles adhering over the surface of FA (in FABL 5) and granular particles of GGBS (in FAGGBS 7) were found to be minimized in the micrograph, which is a representation of improved microstructure with a denser and more homogeneous matrix of hydration products in these mixes (Sharath et al. 2022).

The SEM microphotograph of the FAIOT 9 mix, presented in Figure 4.26, shows reduced traces of spherical and trapezoidal-shaped structures (IOT has a trapezoidal shaped structure), which indicated two facts: one is the involvement of FA and IOT particles in the whole process of geopolymerization, and the second one is the increased dosage of Na_2O at 5% and FA:IOT at a 30:70 ratio. Additionally, the occurrence of a more compact, dense, and grayish microstructure is an indication of the attainment of higher values of individual crushing strength for pellets produced under this mix.

The SEM microphotograph of the FACOT 5 mix presented in Figure 4.26 mainly signifies the presence of two kinds of material phases, which are (1) unreacted COT (which can possibly identified by sharp irregular triangle structures) and FA (which can possibly be identified by round-shaped structures) and (2) geopolymeric binding gel (Manjarrez and Zhang 2018). Here, the geopolymeric gel serves as a binding agent between the incorporated materials like FA and COT and hence collectively contributes towards the strength development and resistance to absorption of water, which is the reason for the higher individual crushing strength of pellets and lower water absorption values of the produced FA-COT aggregates. Additionally, adequate Na_2O dosages help in the homogenous dissolution of a large amounts of alumina and silica from the incorporated aluminosilicate precursors, which serves a major role in the geopolymer gel formation kinetics (Fernández-Jiménez et al. 2006) and in turn necessitates the bond strength between the particles.

4.3.2 Thermogravimetric analysis (TGA) of best performing binary blended pelletized aggregate mixes

The TG-DTG plots of best performing binary blended pelletized aggregates (FABT 9, FABL 5, FAGGBS 7; FA-IOT and FA-COT) are presented in Figures 4.27 and 4.29, respectively. Commonly, in Figures 4.27 and 4.28, the TG curve represents the occurrence of thermogravimetric mass loss for binary blended pelletized aggregates during the process of heating from the temperature range of 25°C–825°C, whereas the DTG curve signifies the temperature boundaries for the decomposition of specific compounds that are discussed in the subsequent sections.

4.3.2.1 Pelletized FA-BT, FA-BL and FA-GGBS aggregates

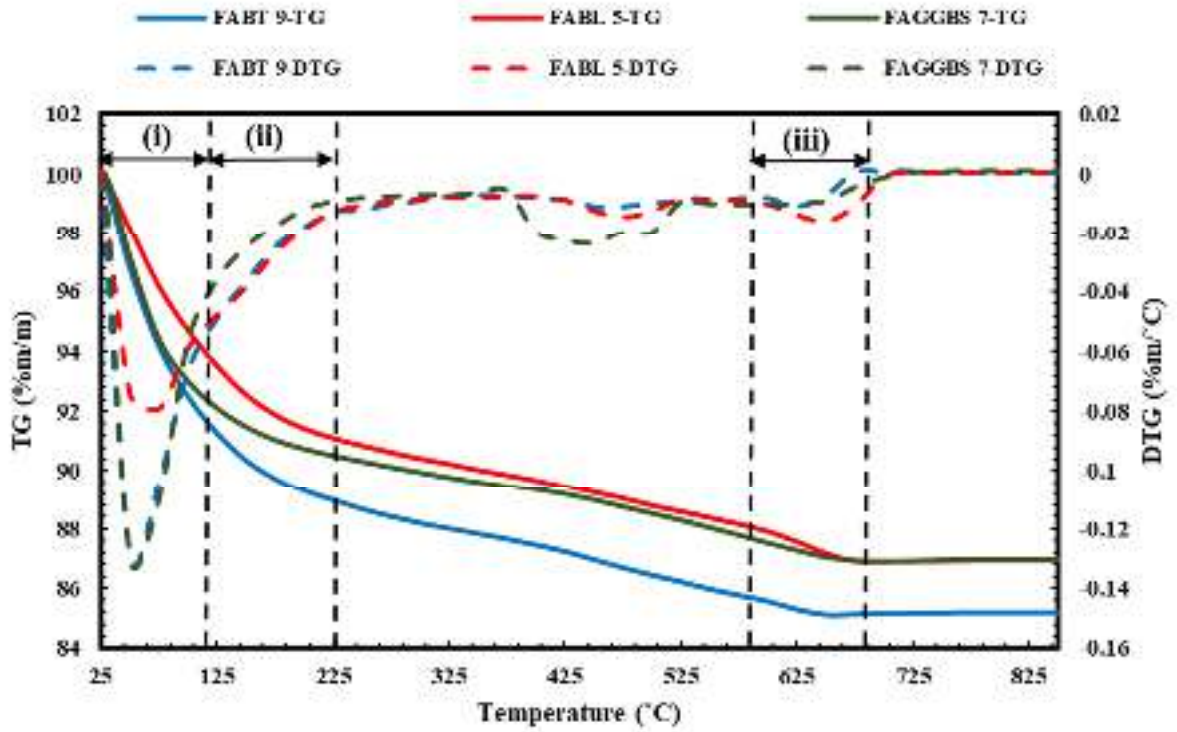

Figure 4.27: TG-DTG plot for FABT 9, FABL 5 and FAGGBS 7 aggregate mixes

From Figure 4.27, significant endothermic peaks at 25-120 °C in the pelletized FABT 9, FABL 5, and FAGGBS 7 aggregate mix indicate the loss of physically absorbed free water molecules on the pores and surfaces of the samples (Adriano et al. 2013; Longhi et al. 2019; Wuddivira et al. 2012). The next significant peaks were noticed in the temperature range of 120-225 °C in the aforementioned mixes and were associated with the thermal degradation of chemically bound water from sodium aluminosilicate gel (N-A-S-H) or calcium-aluminosilicate gel (C-A-S-H) (Adesanya et al. 2018; Ismail et al. 2014; Palomo et al. 2015). The endothermic peaks at the temperature boundaries of 600-700 °C in the aforementioned mixes indicate the associated decomposition of carbonates (C) (Abdullah et al. 2018; Cornejo et al. 2018; Everaert et al. 2017).

By adopting the mass loss from the TG-DTG, the following equation at certain boundaries of temperature is depicted below.

$$\Delta M_{N-A-S-H/C-A-S-H}\,\% = M_{120°C} - M_{225°C} \qquad \text{Eqn. 4.1(Sharath et al. 2022)}$$

where, $\Delta M_{N-A-S-H/C-A-S-H}$ is the change in mass loss percentage of N-A-S-H/C-A-S-H and $M_{120°C}$, $M_{225°C}$ is the mass loss at the temperatures of 120 and 225 °C.

The decomposition of N-A-S-H/C-A-S-H for the obtained TG-DTG curves for pelleted FABT 9, FABL 5, and FAGGBS 7 was quantified following the mathematical equation depicted above (Eqn. 4.1), and the same is presented in Figure 4.28.

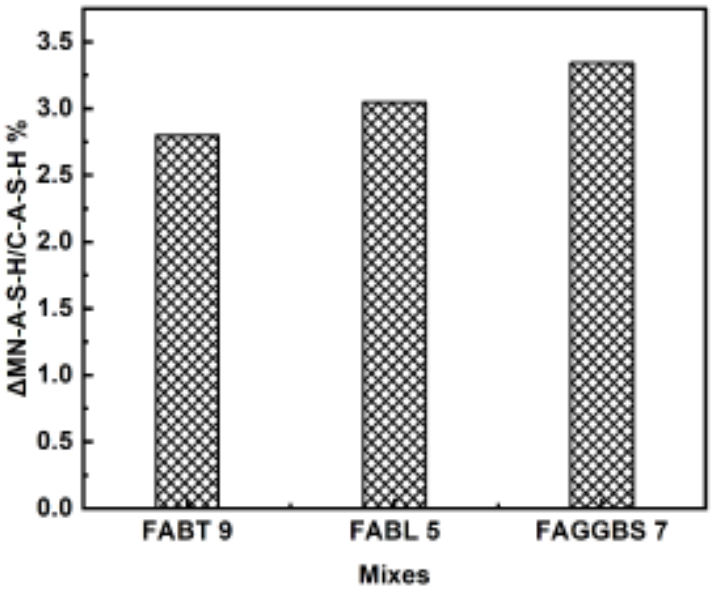

Figure 4.28: Quantification of N-A-S-H/C-A-S-H in pelletized FABT 9, FABL 5 and FAGGBS 7 aggregate mixes (Sharath et al. 2022)

It can be observed from Figure 4.28 that the quantified amount of the major reaction product, which is sodium aluminium silicate hydrate gel (N-A-S-H), is found to be intensified in proportion to Na_2O dosages, irrespective of the best performing mixes (that is, FABT 9, FABL 5, and FAGGBS 7), discussed here. It is reported that the amount of N-A-S-H formed in the best-performing aggregate mixes indicates the extent of the geopolymerization reaction (Garg et al. 2019).

Figure 4.28 (pelletized FABL 5 and FAGGBS 7 aggregate mixes) shows that calcium-rich mixes have a higher percentage of mass loss at temperature boundaries of 120-225 °C, indicating the formation of reaction products related to both C-A-S-H and N-A-S-H (Rafeet et al. 2019). Mass loss associated with C-A-S-H/N-A-S-H was found to be increased with the increase in BT (15%) and GGBS (15%) content. Additionally, pelletized FABL 5 aggregate mix (5% Na_2O, 20% water, and 15% burnt lime content) and pelletized FAGGBS 7 aggregate mix (5% Na_2O, 19% water, and 15% GGBS content) also represented the highest amount of hydration products (i.e., C-A-S-H and N-A-S-H) formed in these best performing aggregate mixes (Sharath et al. 2022).

4.3.2.2 Pelletized FA-IOT and FA-COT aggregate mixes

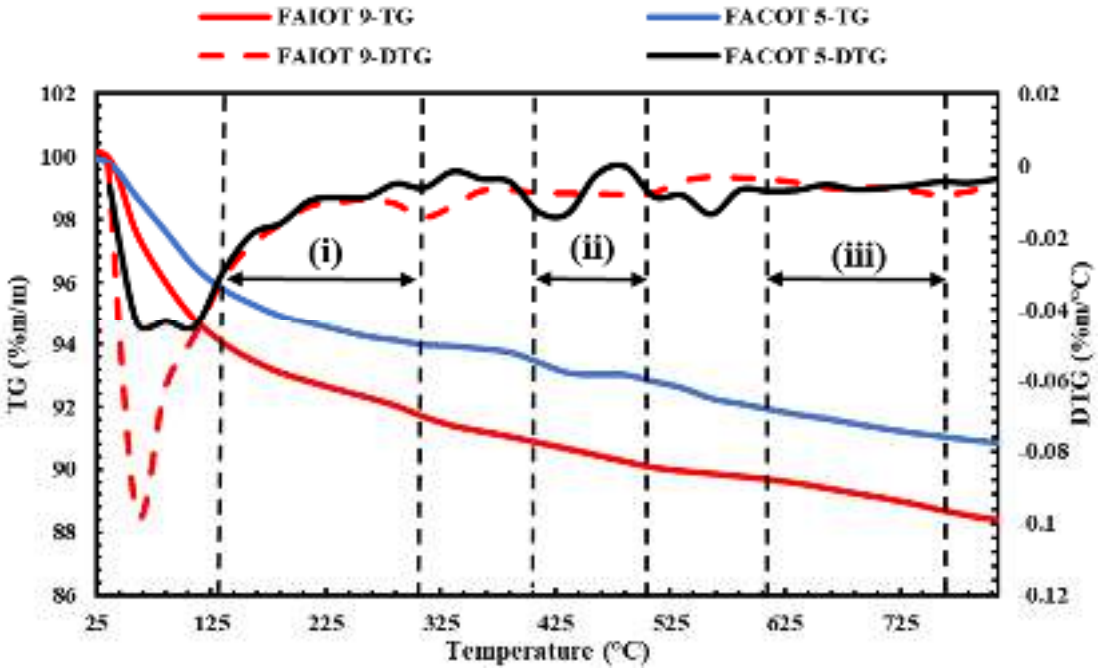

Figure 4.29: TG-DTG plots of pelletized FAIOT 9 and FACOT 5 aggregate mixes

From Figure 4.29, it can be observed that there is an existence of a series of endothermic peaks between the temperature range of 25 to 825°C. First, the major endothermic peak between the temperature boundaries 100-300°C in pelletized FAIOT 9 and FACOT 5 aggregate mixes exhibits the loss of physically absorbed free water molecules from the Na_2SiO_3 solution and calcium silicate hydrate, C-S-H (Obenaus-Emler et al. 2020; Sharath et al. 2023a; Snehal et al. 2022). Second, the next important peak was witnessed between the temperature boundaries 400-500°C in pelletized FAIOT 9 and FACOT 5 aggregate mixes, which is linked to the thermal degradation of chemically bound water from $Ca(OH)_2$ (CH) (Duan et al. 2016a; b; Sharath et al. 2023a; Singh et al. 2015; Snehal et al. 2022). Third, endothermic peaks between the temperature boundaries 610°C–825°C in pelletized FAIOT 9 and FACOT 5 aggregate mixes exhibit the associated decomposition of carbonates into CaO and CO_2 (Duan et al. 2016a; Obenaus-Emler et al. 2020).

From the aforementioned literature, it is to be noted that to determine the mass loss from TG DTG, the following equations at specific temperature boundaries are considered:

In pelletized FAIOT 9 and FACOT 5 aggregate mixes,

$\Delta M_{C-S-H}\% = M_{100°C} - M_{300°C}$ Eqn. 4.2 (Sharath et al. 2023a; Singh et al. 2015; Snehal et al. 2020),

where, ΔM_{C-S-H} is change in mass loss percentage of C-S-H and $M_{100°C}$, $M_{300°C}$ is the mass loss temperatures of 100 and 300 °C.

In pelletized FAIOT 9 and FACOT 5 aggregate mixes,

$\Delta M_{CH}\% = M_{400°C} - M_{500°C}$ Eqn. 4.4 (Sharath et al. 2023a; Singh et al. 2015; Snehal et al. 2020)

where, ΔM_{CH} is change in mass loss percentage of Ca $(OH)_2$ and $M_{400°C}$, $M_{500°C}$ is the mass loss temperatures of 400 and 500 °C.

The quantified mass loss percentages of C-S-H and CH in pelletized FAIOT 9 and FACOT 5 aggregate mix were calculated and same is presented in Figure 4.30, respectively.

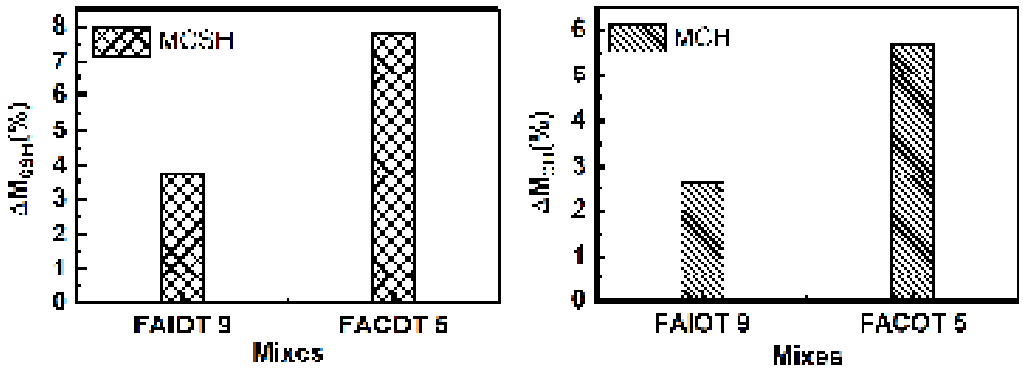

Figure 4.30: Quantification of C-S-H and C-H in FAIOT 9 and FACOT 5 pelletized aggregate mixes

The amounts of C-S-H and $Ca(OH)_2$ found in pelletized FAIOT 9 and FACOT 5 aggregate mixes are shown in Figure 4.30. It can be witnessed from the above figure that the amount of CH was found to be increased with the increasing percentage of FA:IOT and FA:COT as well as dosages of Na_2O in the pelletized FAIOT 9 and FACOT 5 aggregate mixes (Sharath et al. 2023a). The incorporation of incrementing dosages of IOT has led to the formation of calcium silicate hydrate with the simultaneous consumption of calcium hydroxide (Sharath et al. 2023a). Additionally, the emergence of CH with the simultaneous consumption of CSH tends to offer a positive effect on the produced FAIOT 9 and FACOT 5 aggregates, as it helps in achieving significant characteristic properties as the hydrated CH necessitates the formation process of CSH, which accelerates the dissolution of alumina and silica from the incorporated aluminosilicate precursors in the production process of aggregates (Zhao et al. 2019).

4.3.3 FTIR analysis on best performing binary blended pelletized aggregate mixes

FTIR spectra of best performing binary blended pelletized aggregate mixes (FABT 9, FABL 5, FAGGB 7, FAIOT 9 and FACOT 5) are presented in Figure 4.31, respectively.

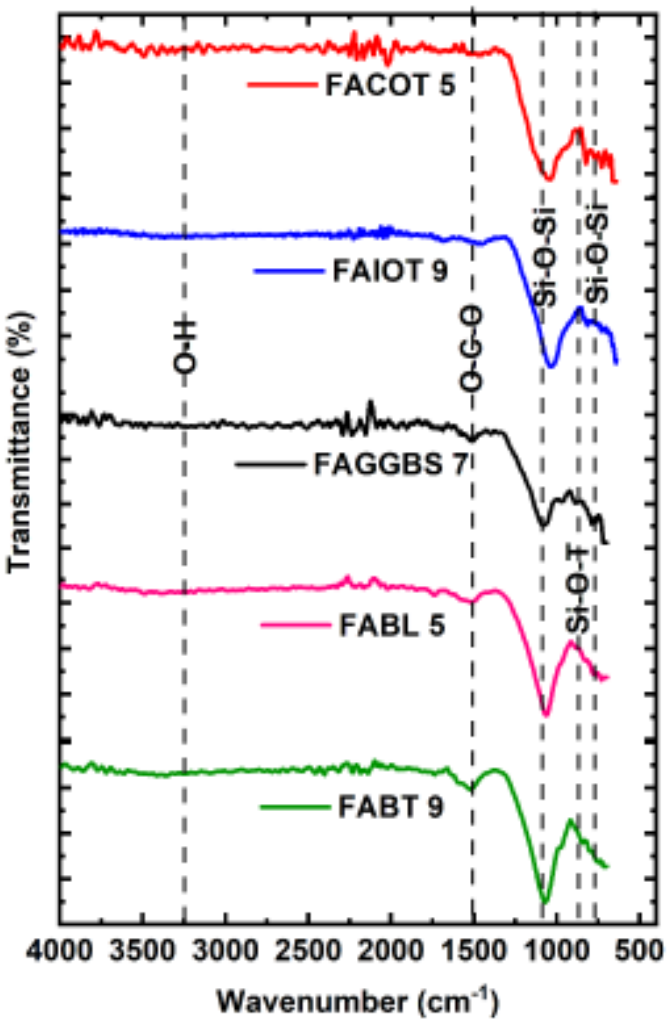

Figure 4.31: FTIR spectra of binary blended pelletized aggregates

From Figure 4.31, it can be observed that in all the FTIR spectra of binary blended pelletized aggregates, the existence of an O-H bond (marked at ~3300 cm^{-1} and ~1650 cm^{-1}) is due the presence of residual water present in the binary blended pelletized aggregates (Sharath et al. 2023 a,b). The existence or formation of carbonates in O-C-O region marked at (~1493 cm^{-1}) could be attributed to the reaction between Na and atmospheric CO_2, as these produced aggregates were cured under ambient temperature conditions. The peaks marked at ~1073.2, 1067.3, 1083.7, ~992.6, and 1001.2 cm^{-1} indicate the peaks of Si-O-Si in pelletized FABT 9, FABL 5, FAGGBS 7, FAIOT 9, and FACOT 5 aggregate mixes

(Ahmari et al. 2012; Azhar et al. 2020; Gao et al. 2015). The formation of Si-O-Si in these mixes can contribute to the strength achievement of the respective aggregate mixes or produced aggregates (Davidovits 2008). The emergence of peaks marked at ~888.7 in all the binary blended pelletized aggregates is an indication of the occurrence of more amounts of geopolymerization taking place in the due course of the reaction (Manjarrez et al. 2019; Rosas-Casarez et al. 2014). Furthermore, it is important to note the difference in emergence of the peaks of FABT 9; FABL 5; FAGGBS 7; FAIOT 9; FACOT 5 which could be an indicative of the difference in the characteristic properties of aggregates produced under these mixes.

4.4 GREY RELATIONAL ANALYSIS ON BINARY BLENDED PELLETIZED AGGREGATES

As explained in the previous sections, the characteristic properties of binary blended pelletized aggregates, which are FA-BT, FA-BL, FA-GGBS, FA-IOT, and FA-COT, are aggregate impact value and aggregate crushing value, individual crushing strength of pellets, and water absorption. In order to employ grey relational analysis for this experimental study, the responses yielded through the nine trial sets of Taguchi's L_9 orthogonal array (in pelletized FA-BT, FA-BL and FA-GGBS aggregates) and sixteen trial sets of Taguchi's L_{16} (in pelletized FA-IOT and FA-COT) presented in Tables 3.6 and 3.7, respectively, were used.

4.4.1 Normalizing the data and generating the grey relational generations

Experimentally obtained responses for Taguchi's L_9 (in pelletized FA-BT, FA-BL and FA-GGBS aggregates) and L_{16} (in pelletized FA-IOT, and FA-COT) orthogonal array design (Tables 3.6 and 3.7, respectively) presented in Figures 4.4(a-c), 4.5(a-c), 4.14(a-c), 4.20(a-c) [obtained results of pelletized FA-BT, FA-BL, and FA-GGBS aggregates] and Figures 4.9(a-b), 4.10 (a-b), 4.17(a-b), 4.22(a-b) [obtained results of pelletized FA-IOT and FA-COT aggregates] were used for obtaining an unbiased analysis for determining the order of influence of governing factors in the produced FA-BT, FA-BL, FA-GGBS, FA-IOT, and FA-COT aggregates (Sahoo et al. 2017).

Firstly, the obtained results for FA-BT, FA-BL, FA-GGBS, FA-IOT, and FA-COT aggregates were normalized, and grey relational generations were calculated. For pelletized FA-BT, FA-BL, FA-GGBS, FA-IOT, and FA-COT aggregates, the grey relational generations for properties like aggregate impact value, aggregate crushing value, and water

absorption at all three curings were calculated using Eqn. 3.1, respectively. However, for the individual pellet strength properties of pelletized FA-BT, FA-BL, FA-GGBS, FA-IOT, and FA-COT, the gray relational generations at 14, 28, and 100 days were calculated using Eqn. 3.2, respectively.

The grey relational generations for the obtained characteristic properties of the produced FA-BT, FA-BL, and FA-GGBS aggregates at 14, 28, and 100 days of curing are presented in Tables 4.1, 4.2, and 4.3, respectively. Similarly, the grey relational generations for the obtained characteristic properties of the produced FA-IOT and FA-COT aggregates at 14, 28, and 100 days of curing are presented in Tables 4.4 and 4.5, respectively.

Table 4.1: Grey relational generations for aggregate impact value (AIV) and aggregate crushing value (ACV), individual crushing strength (IPS) and water absorption of FA-BT aggregates for 14, 28 and 100 days of curing

Trial No.	Grey relational generations (14 Days)				Grey relational generations (28 Days)				Grey relational generations (100 Days)			
	AIV (%)	ACV (%)	IPS (MPa)	WA (%)	AIV (%)	ACV (%)	IPS (MPa)	WA (%)	AIV (%)	ACV (%)	IPS (MPa)	WA (%)
FABT 1	0.378	0.366	0.032	0.437	0.376	0.365	0.000	0.357	0.399	0.508	0.000	0.286
FABT 2	0.037	0.025	0.129	0.239	0.046	0.037	0.043	0.125	0.082	0.176	0.032	0.129
FABT 3	0.000	0.000	0.000	0.000	0.000	0.000	0.021	0.000	0.000	0.000	0.063	0.000
FABT 4	0.627	0.626	0.226	0.704	0.629	0.614	0.255	0.696	0.635	0.619	0.175	0.743
FABT 5	0.568	0.584	0.323	0.831	0.586	0.589	0.213	0.857	0.609	0.566	0.222	0.757
FABT 6	0.402	0.420	0.065	0.592	0.380	0.378	0.043	0.518	0.339	0.340	0.111	0.557
FABT 7	0.610	0.752	0.742	0.761	0.679	0.705	0.596	0.304	0.734	0.721	0.540	0.386
FABT 8	0.822	0.744	0.484	0.563	0.705	0.697	0.426	0.857	0.815	0.775	0.413	0.814
FABT 9	1.000	1.000	1.000	1.000	1.000	1.000	1.000	1.000	1.000	1.000	1.000	1.000

Table 4.2: Grey relational generations for aggregate impact value (AIV) and aggregate crushing value (ACV), individual crushing strength (IPS) and water absorption of FA-BL aggregates for 14, 28 and 100 days of curing

Trial No.	Grey relational generations (14 Days)				Grey relational generations (28 Days)				Grey relational generations (100 Days)			
	AIV (%)	ACV (%)	IPS (MPa)	WA (%)	AIV (%)	ACV (%)	IPS (MPa)	WA (%)	AIV (%)	ACV (%)	IPS (MPa)	WA (%)
FABL 1	0.000	0.000	0.000	0.370	0.000	0.000	0.000	0.307	0.000	0.000	0.000	0.291
FABL 2	0.355	0.177	0.603	0.222	0.330	0.146	0.505	0.216	0.350	0.390	0.459	0.038
FABL 3	0.336	0.192	0.175	0.000	0.374	0.196	0.172	0.000	0.315	0.341	0.153	0.000
FABL 4	0.767	0.690	0.635	0.815	0.793	0.744	0.699	0.807	0.797	0.756	0.663	0.848
FABL 5	1.000	0.882	0.762	1.000	1.000	0.955	1.000	0.875	0.969	0.961	1.000	1.000
FABL 6	0.973	1.000	1.000	0.951	0.993	1.000	0.731	1.000	1.000	1.000	0.653	0.911
FABL 7	0.389	0.236	0.143	0.728	0.378	0.347	0.204	0.705	0.385	0.439	0.133	0.709
FABL 8	0.653	0.483	0.302	0.852	0.626	0.492	0.366	0.795	0.664	0.488	0.378	0.658
FABL 9	0.496	0.330	0.317	0.877	0.522	0.352	0.409	0.830	0.524	0.390	0.378	0.696

Table 4.3: Grey relational generations for aggregate impact value (AIV) and aggregate crushing value (ACV), individual crushing strength (IPS) and water absorption of FA-GGBS aggregates for 14, 28 and 100 days of curing

Trial No.	Grey relational generations (14 Days)				Grey relational generations (28 Days)				Grey relational generations (100 Days)			
	AIV (%)	ACV (%)	IPS (MPa)	WA (%)	AIV (%)	ACV (%)	IPS (MPa)	WA (%)	AIV (%)	ACV (%)	IPS (MPa)	WA (%)
FAGGBS 1	0.000	0.000	0.000	0.284	0.000	0.000	0.025	0.261	0.000	0.000	0.000	0.188
FAGGBS 2	0.301	0.237	0.030	0.162	0.252	0.219	0.075	0.159	0.265	0.250	0.037	0.116
FAGGBS 3	0.213	0.128	0.000	0.000	0.165	0.143	0.000	0.000	0.139	0.167	0.019	0.000
FAGGBS 4	0.728	0.699	0.152	0.432	0.704	0.683	0.200	0.391	0.700	0.697	0.204	0.420
FAGGBS 5	0.682	0.689	0.182	0.297	0.696	0.665	0.250	0.319	0.704	0.684	0.333	0.275
FAGGBS 6	0.812	0.836	0.273	0.554	0.857	0.853	0.400	0.551	0.839	0.816	0.370	0.449
FAGGBS 7	1.000	1.000	0.909	1.000	1.000	1.000	1.000	1.000	1.000	1.000	1.000	1.000
FAGGBS 8	0.728	0.790	1.000	0.676	0.709	0.759	0.900	0.739	0.748	0.741	0.833	0.594
FAGGBS 9	0.728	0.767	0.758	0.838	0.704	0.679	0.675	0.841	0.713	0.697	0.667	0.783

Table 4.4: Grey relational generations for aggregate impact value (AIV) and aggregate crushing value (ACV), individual crushing strength (IPS) and water absorption of FA-IOT aggregates for 14, 28 and 100 days of curing

Trial No.	Grey relational generations (14 Days)				Grey relational generations (28 Days)				Grey relational generations (100 Days)			
	AIV (%)	ACV (%)	IPS (MPa)	WA (%)	AIV (%)	ACV (%)	IPS (MPa)	WA (%)	AIV (%)	ACV (%)	IPS (MPa)	WA (%)
FAIOT 1	0.074	0.068	0.000	0.000	0.018	0.000	0.000	0.000	0.347	0.350	0.333	0.333
FAIOT 2	0.000	0.000	0.132	0.175	0.000	0.006	0.128	0.162	0.333	0.333	0.363	0.350
FAIOT 3	0.178	0.267	0.263	0.238	0.271	0.228	0.282	0.284	0.413	0.409	0.423	0.384
FAIOT 4	0.252	0.335	0.158	0.225	0.199	0.184	0.179	0.270	0.394	0.419	0.390	0.380
FAIOT 5	0.571	0.571	0.526	0.525	0.560	0.525	0.410	0.554	0.506	0.515	0.451	0.497
FAIOT 6	0.503	0.503	0.395	0.438	0.518	0.487	0.308	0.446	0.483	0.491	0.406	0.464
FAIOT 7	0.663	0.714	0.421	0.650	0.602	0.633	0.231	0.608	0.552	0.548	0.390	0.518
FAIOT 8	0.742	0.764	0.500	0.713	0.741	0.747	0.385	0.676	0.639	0.644	0.461	0.568
FAIOT 9	1.000	1.000	1.000	0.913	1.000	1.000	1.000	0.986	1.000	1.000	1.000	1.000
FAIOT 10	0.926	0.944	0.737	1.000	0.873	0.892	0.641	0.959	0.739	0.746	0.612	0.816
FAIOT 11	0.865	0.894	0.605	0.875	0.807	0.823	0.564	0.824	0.675	0.691	0.482	0.689
FAIOT 12	0.945	0.963	0.789	0.925	0.880	0.892	0.744	1.000	0.802	0.787	0.719	0.922
FAIOT 13	0.804	0.839	0.684	0.763	0.741	0.753	0.590	0.784	0.620	0.634	0.506	0.640
FAIOT 14	0.853	0.839	0.632	0.800	0.783	0.804	0.564	0.770	0.664	0.697	0.532	0.703
FAIOT 15	0.902	0.901	0.658	0.763	0.813	0.766	0.513	0.757	0.691	0.669	0.494	0.607
FAIOT 16	0.798	0.826	0.579	0.675	0.717	0.741	0.385	0.595	0.634	0.590	0.441	0.518

Table 4.5: Grey relational generations for aggregate impact value (AIV) and aggregate crushing value (ACV), individual crushing strength (IPS) and water absorption of FA-COT aggregates for 14, 28 and 100 days of curing

Trial No.	Grey relational generations (14 Days)				Grey relational generations (28 Days)				Grey relational generations (100 Days)			
	AIV (%)	ACV (%)	IPS (MPa)	WA (%)	AIV (%)	ACV (%)	IPS (MPa)	WA (%)	AIV (%)	ACV (%)	IPS (MPa)	WA (%)
FACOT 1	0.469	0.456	0.502	0.578	0.523	0.479	0.514	0.559	0.457	0.396	0.516	0.543
FACOT 2	0.516	0.475	0.570	0.621	0.550	0.560	0.586	0.631	0.539	0.552	0.645	0.652
FACOT 3	0.473	0.463	0.525	0.586	0.538	0.494	0.532	0.613	0.512	0.470	0.581	0.609
FACOT 4	0.450	0.436	0.321	0.578	0.465	0.451	0.279	0.496	0.411	0.374	0.323	0.424
FACOT 5	1.000	1.000	1.000	0.966	0.969	1.000	1.000	1.000	1.000	1.000	1.000	0.971
FACOT 6	0.903	0.884	0.796	0.879	1.000	0.981	0.658	0.920	0.984	0.878	0.694	0.930
FACOT 7	0.860	0.880	0.683	0.776	0.858	0.887	0.586	0.757	0.872	0.815	0.629	0.804
FACOT 8	0.961	0.981	0.932	1.000	0.992	0.953	0.910	0.938	0.957	0.959	0.887	1.000
FACOT 9	0.601	0.575	0.593	0.716	0.558	0.545	0.495	0.667	0.562	0.515	0.516	0.674
FACOT 10	0.570	0.541	0.502	0.595	0.519	0.498	0.405	0.559	0.496	0.415	0.419	0.761
FACOT 11	0.581	0.568	0.525	0.621	0.535	0.514	0.477	0.577	0.539	0.481	0.484	0.543
FACOT 12	0.713	0.656	0.638	0.690	0.650	0.599	0.550	0.703	0.674	0.596	0.565	0.717
FACOT 13	0.000	0.000	0.000	0.017	0.000	0.000	0.000	0.018	0.000	0.000	0.000	0.054
FACOT 14	0.236	0.251	0.095	0.052	0.231	0.233	0.081	0.036	0.202	0.200	0.113	0.109
FACOT 15	0.337	0.398	0.163	0.293	0.385	0.397	0.243	0.216	0.333	0.337	0.242	0.196
FAIOT 16	0.182	0.181	0.027	0.000	0.173	0.148	0.045	0.000	0.174	0.163	0.097	0.000

4.4.2 Assessment of grey relational coefficients

The deviation sequences Δ_{0i} and grey relational coefficients ξ_i (k) for pelletized FA-BT, FA-BL, FA-GGBS, FA-IOT and FA-COT aggregates at all the three curing ages were computed by using Eqn. 3.3. For pelletized FA-BT, FA-BL and FA-GGBS aggregates, the values for deviation sequence and grey relational coefficients for 14, 28, and 100 days of curing are presented in Tables 4.6-4.8, 4.9-4.11, and 4.12-4.14, respectively. Similarly, for pelletized FA-IOT and FA-COT aggregates, values for deviation sequence and grey relational coefficients for the three curing periods is presented in Tables 4.15-4.17 and 4.18-4.20, respectively.

Table 4.6: Δ_{0i} and grey relation coefficients for 14 days of curing with respect to governing factors in FA-BT aggregates

Trial No	Δ_{0i}				Grey relational coefficients			
	AIV (%)	ACV (%)	IPS (MPa)	WA (%)	AIV (%)	ACV (%)	IPS (MPa)	WA (%)
FABT 1	0.622	0.634	0.968	0.563	0.445	0.441	0.341	0.470
FABT 2	0.963	0.975	0.871	0.761	0.342	0.339	0.365	0.397
FABT 3	1.000	1.000	1.000	1.000	0.333	0.333	0.333	0.333
FABT 4	0.373	0.374	0.774	0.296	0.572	0.572	0.392	0.628
FABT 5	0.432	0.416	0.677	0.169	0.537	0.546	0.425	0.747
FABT 6	0.598	0.580	0.935	0.408	0.456	0.463	0.348	0.550
FABT 7	0.390	0.248	0.258	0.239	0.562	0.669	0.660	0.676
FABT 8	0.178	0.256	0.516	0.437	0.737	0.661	0.492	0.534
FABT 9	0.000	0.000	0.000	0.000	1.000	1.000	1.000	1.000

Table 4.7: Δ_{0i} and grey relation coefficients for 28 days of curing with respect to governing factors in FA-BT aggregates

Trial No	Δ_{0i}				Grey relational coefficients			
	AIV (%)	ACV (%)	IPS (MPa)	WA (%)	AIV (%)	ACV (%)	IPS (MPa)	WA (%)
FABT 1	0.624	0.635	1.000	0.643	0.445	0.441	0.333	0.438
FABT 2	0.954	0.963	0.957	0.875	0.344	0.342	0.343	0.364
FABT 3	1.000	1.000	0.979	1.000	0.333	0.333	0.338	0.333

FABT 4	0.371	0.386	0.745	0.304	0.574	0.564	0.402	0.622
FABT 5	0.414	0.411	0.787	0.143	0.547	0.549	0.388	0.778
FABT 6	0.620	0.622	0.957	0.482	0.446	0.445	0.343	0.509
FABT 7	0.321	0.295	0.404	0.696	0.609	0.629	0.553	0.418
FABT 8	0.295	0.303	0.574	0.143	0.629	0.623	0.465	0.778
FABT 9	0.000	0.000	0.000	0.000	1.000	1.000	1.000	1.000

Table 4.8: Δ_{0i} and grey relation coefficients for 100 days of curing with respect to governing factors in FA-BT aggregates

Trial No	Δ_{0i}				Grey relational coefficients			
	AIV (%)	ACV (%)	IPS (MPa)	WA (%)	AIV (%)	ACV (%)	IPS (MPa)	WA (%)
FABT 1	0.601	0.492	1.000	0.714	0.454	0.504	0.333	0.412
FABT 2	0.918	0.824	0.968	0.871	0.352	0.378	0.341	0.365
FABT 3	1.000	1.000	0.937	1.000	0.333	0.333	0.348	0.333
FABT 4	0.365	0.381	0.825	0.257	0.578	0.567	0.377	0.660
FABT 5	0.391	0.434	0.778	0.243	0.561	0.535	0.391	0.673
FABT 6	0.661	0.660	0.889	0.443	0.431	0.431	0.360	0.530
FABT 7	0.266	0.279	0.460	0.614	0.653	0.642	0.521	0.449
FABT 8	0.185	0.225	0.587	0.186	0.730	0.689	0.460	0.729
FABT 9	0.000	0.000	0.000	0.000	1.000	1.000	1.000	1.000

Table 4.9: Δ_{0i} and grey relation coefficients for 14 days of curing with respect to governing factors in FA-BL aggregates

Trial No	Δ_{0i}				Grey relational coefficients			
	AIV (%)	ACV (%)	IPS (MPa)	WA (%)	AIV (%)	ACV (%)	IPS (MPa)	WA (%)
FABL 1	1.000	1.000	1.000	0.630	0.333	0.333	0.333	0.443
FABL 2	0.645	0.823	0.397	0.778	0.437	0.378	0.558	0.391
FABL 3	0.664	0.808	0.825	1.000	0.430	0.382	0.377	0.333
FABL 4	0.233	0.310	0.365	0.185	0.682	0.617	0.578	0.730
FABL 5	0.000	0.118	0.238	0.000	1.000	0.809	0.677	1.000
FABL 6	0.027	0.000	0.000	0.049	0.949	1.000	1.000	0.910

FABL 7	0.611	0.764	0.857	0.272	0.450	0.396	0.368	0.648
FABL 8	0.347	0.517	0.698	0.148	0.590	0.492	0.417	0.771
FABL 9	0.504	0.670	0.683	0.123	0.498	0.427	0.423	0.802

Table 4.10: Δ_{0i} and grey relation coefficients for 28 days of curing with respect to governing factors in FA-BL aggregates

Trial No	Δ_{0i}				Grey relational coefficients			
	AIV (%)	ACV (%)	IPS (MPa)	WA (%)	AIV (%)	ACV (%)	IPS (MPa)	WA (%)
FABL 1	1.000	1.000	1.000	0.693	0.333	0.333	0.333	0.419
FABL 2	0.670	0.854	0.495	0.784	0.427	0.369	0.503	0.389
FABL 3	0.626	0.804	0.828	1.000	0.444	0.383	0.377	0.333
FABL 4	0.207	0.256	0.301	0.193	0.707	0.661	0.624	0.721
FABL 5	0.000	0.045	0.000	0.125	1.000	0.917	1.000	0.800
FABL 6	0.007	0.000	0.269	0.000	0.985	1.000	0.650	1.000
FABL 7	0.622	0.653	0.796	0.295	0.446	0.434	0.386	0.629
FABL 8	0.374	0.508	0.634	0.205	0.572	0.496	0.441	0.710
FABL 9	0.478	0.648	0.591	0.170	0.511	0.435	0.458	0.746

Table 4.11: Δ_{0i} and grey relation coefficients for 100 days of curing with respect to governing factors in FA-BL aggregates

Trial No	Δ_{0i}				Grey relational coefficients			
	AIV (%)	ACV (%)	IPS (MPa)	WA (%)	AIV (%)	ACV (%)	IPS (MPa)	WA (%)
FABL 1	1.000	1.000	1.000	0.709	0.333	0.333	0.333	0.414
FABL 2	0.650	0.610	0.541	0.962	0.435	0.451	0.480	0.342
FABL 3	0.685	0.659	0.847	1.000	0.422	0.432	0.371	0.333
FABL 4	0.203	0.244	0.337	0.152	0.711	0.672	0.598	0.767
FABL 5	0.031	0.039	0.000	0.000	0.941	0.928	1.000	1.000
FABL 6	0.000`	0.000	0.347	0.089	1.000	1.000	0.590	0.849
FABL 7	0.615	0.561	0.867	0.291	0.448	0.471	0.366	0.632
FABL 8	0.336	0.512	0.622	0.342	0.598	0.494	0.445	0.594
FABL 9	0.476	0.610	0.622	0.304	0.513	0.451	0.445	0.622

Table 4.12: Δ_{0i} and grey relation coefficients for 14 days of curing with respect to governing factors in FA-GGBS aggregates

Trial No	Δ_{0i}				Grey relational coefficients			
	AIV (%)	ACV (%)	IPS (MPa)	WA (%)	AIV (%)	ACV (%)	IPS (MPa)	WA (%)
FAGGBS 1	1.000	1.000	1.000	0.716	0.500	0.333	0.333	0.411
FAGGBS 2	0.699	0.763	0.970	0.838	0.589	0.396	0.340	0.374
FAGGBS 3	0.787	0.872	1.000	1.000	0.560	0.364	0.333	0.333
FAGGBS 4	0.272	0.301	0.848	0.568	0.786	0.624	0.371	0.468
FAGGBS 5	0.318	0.311	0.818	0.703	0.759	0.617	0.379	0.416
FAGGBS 6	0.188	0.164	0.727	0.446	0.842	0.753	0.407	0.529
FAGGBS 7	0.000	0.000	0.091	0.000	1.000	1.000	0.846	1.000
FAGGBS 8	0.272	0.210	0.000	0.324	0.786	0.704	1.000	0.607
FAGGBS 9	0.272	0.233	0.242	0.162	0.786	0.682	0.673	0.755

Table 4.13: Δ_{0i} and grey relation coefficients for 28 days of curing with respect to governing factors in FA-GGBS aggregates

Trial No	Δ_{0i}				Grey relational coefficients			
	AIV (%)	ACV (%)	IPS (MPa)	WA (%)	AIV (%)	ACV (%)	IPS (MPa)	WA (%)
FAGGBS 1	1.000	1.000	0.975	0.739	0.500	0.333	0.339	0.404
FAGGBS 2	0.748	0.781	0.925	0.841	0.572	0.390	0.351	0.373
FAGGBS 3	0.835	0.857	1.000	1.000	0.545	0.368	0.333	0.333
FAGGBS 4	0.296	0.317	0.800	0.609	0.772	0.612	0.385	0.451
FAGGBS 5	0.304	0.335	0.750	0.681	0.767	0.599	0.400	0.423
FAGGBS 6	0.143	0.147	0.600	0.449	0.875	0.772	0.455	0.527
FAGGBS 7	0.000	0.000	0.000	0.000	1.000	1.000	1.000	1.000
FAGGBS 8	0.291	0.241	0.100	0.261	0.774	0.675	0.833	0.657
FAGGBS 9	0.296	0.321	0.325	0.159	0.772	0.609	0.606	0.758

Table 4.14: Δ_{0i} and grey relation coefficients for 100 days of curing with respect to governing factors in FA-GGBS aggregates

Trial No	Δ_{0i}				Grey relational coefficients			
	AIV (%)	ACV (%)	IPS (MPa)	WA (%)	AIV (%)	ACV (%)	IPS (MPa)	WA (%)
FAGGBS 1	1.000	1.000	1.000	0.812	0.333	0.333	0.333	0.381
FAGGBS 2	0.735	0.750	0.963	0.884	0.405	0.400	0.342	0.361
FAGGBS 3	0.861	0.833	0.981	1.000	0.367	0.375	0.338	0.333
FAGGBS 4	0.300	0.303	0.796	0.580	0.625	0.623	0.386	0.463
FAGGBS 5	0.296	0.316	0.667	0.725	0.628	0.613	0.429	0.408
FAGGBS 6	0.161	0.184	0.630	0.551	0.757	0.731	0.443	0.476
FAGGBS 7	0.000	0.000	0.000	0.000	1.000	1.000	1.000	1.000
FAGGBS 8	0.252	0.259	0.167	0.406	0.665	0.659	0.750	0.552
FAGGBS 9	0.287	0.303	0.333	0.217	0.635	0.623	0.600	0.697

Table 4.15: Δ_{0i} and grey relation coefficients for 14 days of curing with respect to governing factors in FA-IOT aggregates

Trial No	Δ_{0i}				Grey relational coefficients			
	AIV (%)	ACV (%)	IPS (MPa)	WA (%)	AIV (%)	ACV (%)	IPS (MPa)	WA (%)
FAIOT 1	0.926	0.932	1.000	1.000	0.351	0.349	0.333	0.333
FAIOT 2	1.000	1.000	0.868	0.825	0.333	0.333	0.365	0.377
FAIOT 3	0.822	0.733	0.737	0.763	0.378	0.406	0.404	0.396
FAIOT 4	0.748	0.665	0.842	0.775	0.400	0.429	0.373	0.392
FAIOT 5	0.429	0.429	0.474	0.475	0.538	0.538	0.514	0.513
FAIOT 6	0.497	0.497	0.605	0.563	0.502	0.502	0.452	0.471
FAIOT 7	0.337	0.286	0.579	0.350	0.597	0.636	0.463	0.588
FAIOT 8	0.258	0.236	0.500	0.288	0.660	0.679	0.500	0.635
FAIOT 9	0.000	0.000	0.000	0.088	1.000	1.000	1.000	0.851
FAIOT 10	0.074	0.056	0.263	0.000	0.872	0.899	0.655	1.000
FAIOT 11	0.135	0.106	0.395	0.125	0.787	0.826	0.559	0.800
FAIOT 12	0.055	0.037	0.211	0.075	0.901	0.931	0.704	0.870

FAIOT 13	0.196	0.161	0.316	0.238	0.718	0.756	0.613	0.678
FAIOT 14	0.147	0.161	0.368	0.200	0.773	0.756	0.576	0.714
FAIOT 15	0.098	0.099	0.342	0.238	0.836	0.834	0.594	0.678
FAIOT 16	0.202	0.174	0.421	0.325	0.712	0.742	0.543	0.606

Table 4.16: Δ_{0i} and grey relation coefficients for 28 days of curing with respect to governing factors in FA-IOT aggregates

Trial No	Δ_{0i}				Grey relational coefficients			
	AIV (%)	ACV (%)	IPS (MPa)	WA (%)	AIV (%)	ACV (%)	IPS (MPa)	WA (%)
FAIOT 1	0.982	1.000	1.000	1.000	0.337	0.333	0.333	0.333
FAIOT 2	1.000	0.994	0.872	0.838	0.333	0.335	0.364	0.374
FAIOT 3	0.729	0.772	0.718	0.716	0.407	0.393	0.411	0.411
FAIOT 4	0.801	0.816	0.821	0.730	0.384	0.380	0.379	0.407
FAIOT 5	0.440	0.475	0.590	0.446	0.532	0.513	0.459	0.529
FAIOT 6	0.482	0.513	0.692	0.554	0.509	0.494	0.419	0.474
FAIOT 7	0.398	0.367	0.769	0.392	0.557	0.577	0.394	0.561
FAIOT 8	0.259	0.253	0.615	0.324	0.659	0.664	0.448	0.607
FAIOT 9	0.000	0.000	0.000	0.014	1.000	1.000	1.000	0.974
FAIOT 10	0.127	0.108	0.359	0.041	0.798	0.823	0.582	0.925
FAIOT 11	0.193	0.177	0.436	0.176	0.722	0.738	0.534	0.740
FAIOT 12	0.120	0.108	0.256	0.000	0.806	0.823	0.661	1.000
FAIOT 13	0.259	0.247	0.410	0.216	0.659	0.669	0.549	0.698
FAIOT 14	0.217	0.196	0.436	0.230	0.697	0.718	0.534	0.685
FAIOT 15	0.187	0.234	0.487	0.243	0.728	0.681	0.506	0.673
FAIOT 16	0.283	0.259	0.615	0.405	0.638	0.658	0.448	0.552

Table 4.17: Δ_{0i} and grey relation coefficients for 100 days of curing with respect to governing factors in FA-IOT aggregates

Trial No	Δ_{0i}				Grey relational coefficients			
	AIV (%)	ACV (%)	IPS (MPa)	WA (%)	AIV (%)	ACV (%)	IPS (MPa)	WA (%)
FAIOT 1	0.347	0.350	0.333	0.333	0.347	0.350	0.333	0.333
FAIOT 2	0.333	0.333	0.363	0.350	0.333	0.333	0.363	0.350
FAIOT 3	0.413	0.409	0.423	0.384	0.413	0.409	0.423	0.384
FAIOT 4	0.394	0.419	0.390	0.380	0.394	0.419	0.390	0.380
FAIOT 5	0.506	0.515	0.451	0.497	0.506	0.515	0.451	0.497
FAIOT 6	0.483	0.491	0.406	0.464	0.483	0.491	0.406	0.464
FAIOT 7	0.552	0.548	0.390	0.518	0.552	0.548	0.390	0.518
FAIOT 8	0.639	0.644	0.461	0.568	0.639	0.644	0.461	0.568
FAIOT 9	1.000	1.000	1.000	1.000	1.000	1.000	1.000	1.000
FAIOT 10	0.739	0.746	0.612	0.816	0.739	0.746	0.612	0.816
FAIOT 11	0.675	0.691	0.482	0.689	0.675	0.691	0.482	0.689
FAIOT 12	0.802	0.787	0.719	0.922	0.802	0.787	0.719	0.922
FAIOT 13	0.620	0.634	0.506	0.640	0.620	0.634	0.506	0.640
FAIOT 14	0.664	0.697	0.532	0.703	0.664	0.697	0.532	0.703
FAIOT 15	0.691	0.669	0.494	0.607	0.691	0.669	0.494	0.607
FAIOT 16	0.634	0.590	0.441	0.518	0.634	0.590	0.441	0.518

Table 4.18: **Δ_{0i} and grey relation coefficients for 14 days of curing with respect to governing factors in FA-COT aggregates**

Trial No	Δ_{0i}				Grey relational coefficients			
	AIV (%)	ACV (%)	IPS (MPa)	WA (%)	AIV (%)	ACV (%)	IPS (MPa)	WA (%)
FACOT 1	0.477	0.521	0.486	0.441	0.485	0.479	0.501	0.542
FACOT 2	0.450	0.440	0.414	0.369	0.508	0.488	0.538	0.569
FACOT 3	0.462	0.506	0.468	0.387	0.487	0.482	0.513	0.547
FACOT 4	0.535	0.549	0.721	0.504	0.476	0.470	0.424	0.542
FACOT 5	0.031	0.000	0.000	0.000	1.000	1.000	1.000	0.935

FACOT 6	0.000	0.019	0.342	0.080	0.838	0.812	0.711	0.806
FACOT 7	0.142	0.113	0.414	0.243	0.782	0.807	0.612	0.690
FACOT 8	0.008	0.047	0.090	0.062	0.928	0.963	0.880	1.000
FACOT 9	0.442	0.455	0.505	0.333	0.556	0.541	0.551	0.637
FACOT 10	0.481	0.502	0.595	0.441	0.538	0.521	0.501	0.552
FACOT 11	0.465	0.486	0.523	0.423	0.544	0.536	0.513	0.569
FACOT 12	0.350	0.401	0.450	0.297	0.635	0.593	0.580	0.617
FACOT 13	1.000	1.000	1.000	0.982	0.333	0.333	0.333	0.337
FACOT 14	0.769	0.767	0.919	0.964	0.396	0.400	0.356	0.345
FACOT 15	0.615	0.603	0.757	0.784	0.430	0.454	0.374	0.414
FACOT 16	0.827	0.852	0.955	1.000	0.379	0.379	0.339	0.333

Table 4.19: Δ_{0i} **and grey relation coefficients for 28 days of curing with respect to governing factors in FA-COT aggregates**

Trial No	Δ_{0i}				Grey relational coefficients			
	AIV (%)	ACV (%)	IPS (MPa)	WA (%)	AIV (%)	ACV (%)	IPS (MPa)	WA (%)
FACOT 1	0.477	0.521	0.486	0.441	0.512	0.490	0.507	0.531
FACOT 2	0.450	0.440	0.414	0.369	0.526	0.532	0.547	0.576
FACOT 3	0.462	0.506	0.468	0.387	0.520	0.497	0.516	0.564
FACOT 4	0.535	0.549	0.721	0.504	0.483	0.477	0.410	0.498
FACOT 5	0.031	0.000	0.000	0.000	0.942	1.000	1.000	1.000
FACOT 6	0.000	0.019	0.342	0.080	1.000	0.963	0.594	0.862
FACOT 7	0.142	0.113	0.414	0.243	0.778	0.816	0.547	0.673
FACOT 8	0.008	0.047	0.090	0.062	0.985	0.915	0.847	0.889
FACOT 9	0.442	0.455	0.505	0.333	0.531	0.523	0.498	0.600
FACOT 10	0.481	0.502	0.595	0.441	0.510	0.499	0.457	0.531
FACOT 11	0.465	0.486	0.523	0.423	0.518	0.507	0.489	0.542
FACOT 12	0.350	0.401	0.450	0.297	0.588	0.555	0.526	0.628
FACOT 13	1.000	1.000	1.000	0.982	0.333	0.333	0.333	0.337
FACOT 14	0.769	0.767	0.919	0.964	0.394	0.395	0.352	0.342
FACOT 15	0.615	0.603	0.757	0.784	0.448	0.453	0.398	0.390
FACOT 16	0.827	0.852	0.955	1.000	0.377	0.370	0.344	0.333

Table 4.20: Δ_{0i} **and grey relation coefficients for 100 days of curing with respect to governing factors in FA-COT aggregates**

Trial No	Δ_{0i}				Grey relational coefficients			
	AIV (%)	ACV (%)	IPS (MPa)	WA (%)	AIV (%)	ACV (%)	IPS (MPa)	WA (%)
FACOT 1	0.543	0.604	0.484	0.457	0.480	0.453	0.508	0.523
FACOT 2	0.461	0.448	0.355	0.348	0.520	0.527	0.585	0.590
FACOT 3	0.488	0.530	0.419	0.391	0.506	0.486	0.544	0.561
FACOT 4	0.589	0.626	0.677	0.576	0.459	0.444	0.425	0.465
FACOT 5	0.000	0.000	0.000	0.029	1.000	1.000	1.000	0.945
FACOT 6	0.016	0.122	0.306	0.070	0.970	0.804	0.620	0.878
FACOT 7	0.128	0.185	0.371	0.196	0.796	0.730	0.574	0.719
FACOT 8	0.043	0.041	0.113	0.000	0.921	0.925	0.816	1.000
FACOT 9	0.438	0.485	0.484	0.326	0.533	0.508	0.508	0.605
FACOT 10	0.504	0.585	0.581	0.239	0.498	0.461	0.463	0.676
FACOT 11	0.461	0.519	0.516	0.457	0.520	0.491	0.492	0.523
FACOT 12	0.326	0.404	0.435	0.283	0.606	0.553	0.534	0.639
FACOT 13	1.000	1.000	1.000	0.946	0.333	0.333	0.333	0.346
FACOT 14	0.798	0.800	0.887	0.891	0.385	0.385	0.360	0.359
FACOT 15	0.667	0.663	0.758	0.804	0.429	0.430	0.397	0.383
FACOT 16	0.826	0.837	0.903	1.000	0.377	0.374	0.356	0.333

4.4.3 Grey relational grade

The grey relational grade γ_i for pelletized FA-BT, FA-BL, FA-GGBS, FA-IOT and FA-COT aggregates at all the three curing ages was computed using Eqn. 3.4. The grey relational grade at all curing ages for all the respective governing factors in pelletized FA-BT, FA-BL, and FA-GGBS aggregates is presented in Tables 4.21, 4.22 and 4.23, respectively. Similarly, the grey relational grade at all curing ages for all the respective governing factors in pelletized FA-IOT and FA-COT aggregates is presented in Tables 4.24 and 4.25, respectively.

Table 4.21: Grey relational grades for three curing ages with respect to governing factors in FA-BT aggregates

Trial No	Grey relational grade		
	14 Days	28 Days	100 Days
FABT 1	0.424	0.406	0.426
FABT 2	0.361	0.343	0.359
FABT 3	0.333	0.335	0.337
FABT 4	0.541	0.513	0.546
FABT 5	0.564	0.495	0.540
FABT 6	0.454	0.412	0.438
FABT 7	0.642	0.597	0.566
FABT 8	0.606	0.572	0.652
FABT 9	1.000	1.000	1.000

Table 4.22: Grey relational grades for three curing ages with respect to governing factors in FA-BL aggregates

Trial No	Grey relational grade		
	14 Days	28 Days	100 Days
FABL 1	0.361	0.355	0.353
FABL 2	0.441	0.422	0.427
FABL 3	0.381	0.384	0.389
FABL 4	0.652	0.678	0.687
FABL 5	0.872	0.929	0.967
FABL 6	0.965	0.909	0.860
FABL 7	0.466	0.473	0.479
FABL 8	0.568	0.555	0.533
FABL 9	0.538	0.538	0.508

Table 4.23: Grey relational grades for three curing ages with respect to governing factors in FA-GGBS aggregates

Trial No	Grey relational grade		
	14 Days	28 Days	100 Days
FAGGBS 1	0.394	0.394	0.345
FAGGBS 2	0.425	0.422	0.377
FAGGBS 3	0.398	0.395	0.353
FAGGBS 4	0.562	0.555	0.524
FAGGBS 5	0.543	0.547	0.520
FAGGBS 6	0.633	0.657	0.601
FAGGBS 7	0.962	1.000	1.000
FAGGBS 8	0.774	0.735	0.656
FAGGBS 9	0.724	0.686	0.639

Table 4.24: Grey relational grades for three curing ages with respect to governing factors in FA-IOT aggregates

Trial No	Grey relational grade		
	14 Days	28 Days	100 Days
FAIOT 1	0.342	0.334	0.341
FAIOT 2	0.352	0.352	0.345
FAIOT 3	0.396	0.405	0.407
FAIOT 4	0.399	0.387	0.396
FAIOT 5	0.526	0.508	0.492
FAIOT 6	0.482	0.474	0.461
FAIOT 7	0.571	0.522	0.502
FAIOT 8	0.619	0.594	0.578
FAIOT 9	0.963	0.993	1.000
FAIOT 10	0.857	0.782	0.728
FAIOT 11	0.743	0.684	0.634
FAIOT 12	0.851	0.822	0.808
FAIOT 13	0.691	0.644	0.600
FAIOT 14	0.705	0.659	0.649

FAIOT 15	0.735	0.647	0.615
FAIOT 16	0.651	0.574	0.546

Table 4.25: Grey relational grades for three curing ages with respect to governing factors in FA-COT aggregates

Trial No	Grey relational grade		
	14 Days	28 Days	100 Days
FACOT 1	0.502	0.510	0.491
FACOT 2	0.525	0.545	0.556
FACOT 3	0.507	0.524	0.524
FACOT 4	0.478	0.467	0.448
FACOT 5	0.984	0.986	0.986
FACOT 6	0.791	0.854	0.818
FACOT 7	0.723	0.704	0.705
FACOT 8	0.943	0.909	0.915
FACOT 9	0.571	0.538	0.539
FACOT 10	0.528	0.499	0.524
FACOT 11	0.540	0.514	0.506
FACOT 12	0.606	0.574	0.583
FACOT 13	0.334	0.334	0.336
FACOT 14	0.374	0.371	0.372
FACOT 15	0.418	0.422	0.410
FACOT 16	0.358	0.356	0.360

Table 4.26: Response table for grey relational grade for three curing ages with respect to governing factors in FA-BT aggregates

Factors	Curing Ages	Mean grey Relational Grade			Maximum value – minimum value	Rank
		Level 1	Level 2	Level 3		
Na_2O content (%)	14 days	0.373	0.520	0.749	0.377	1
Water content (%)		0.536	0.510	0.596	0.086	3
BT (%)		0.495	0.634	0.513	0.139	2
Na_2O content (%)	28 days	0.361	0.473	0.723	0.362	1
Water content (%)		0.506	0.470	0.582	0.112	3
BT (%)		0.463	0.619	0.476	0.155	2

Na_2O content (%)	100 days	0.374	0.508	0.739	0.366	1
Water content (%)		0.513	0.517	0.592	0.079	3
BT (%)		0.505	0.635	0.481	0.154	2

Table 4.27: Response table for grey relational grade for three curing ages with respect to governing factors in FA-BL aggregates

Factors	Curing Ages	Mean grey Relational Grade			Maximum value – minimum value	Rank
		Level 1	Level 2	Level 3		
Na_2O content (%)	14 days	0.394	0.829	0.524	0.435	1
Water content (%)		0.493	0.627	0.628	0.135	2
BL (%)		0.631	0.543	0.573	0.088	3
Na_2O content (%)	28 days	0.387	0.839	0.522	0.452	1
Water content (%)		0.502	0.635	0.610	0.133	2
BL (%)		0.606	0.546	0.596	0.060	3
Na_2O content (%)	100 days	0.390	0.838	0.507	0.448	1
Water content (%)		0.507	0.642	0.586	0.136	2
BL (%)		0.582	0.541	0.612	0.071	3

Table 4.28: Response table for grey relational grade for three curing ages with respect to governing factors in FA-GGBS aggregates

Factors	Curing Ages	Mean grey Relational Grade			Maximum value – minimum value	Rank
		Level 1	Level 2	Level 3		
Na_2O content (%)	14 days	0.406	0.579	0.820	0.414	1
Water content (%)		0.639	0.581	0.585	0.059	3
GGBS (%)		0.600	0.570	0.634	0.064	2
Na_2O content (%)	28 days	0.404	0.586	0.807	0.404	1
Water content (%)		0.650	0.568	0.579	0.082	3
GGBS (%)		0.595	0.554	0.647	0.093	2
Na_2O content (%)	100 days	0.359	0.548	0.765	0.407	1
Water content (%)		0.623	0.518	0.531	0.106	3
GGBS (%)		0.534	0.513	0.624	0.111	2

Tables 4.26, 4.27 and 4.28 represent the average values of the response characteristics, levels, and the governing factors in pelletized FA-BT, FA-BL, and FA-GGBS aggregates, respectively. By observing the delta values or ranks obtained for pelletized FA-BT, FA-BL, and FA-GGBS aggregates, it can be inferred that the factor Na_2O content is having a significant impact among all the other factors considered in the production of FA-BT, FA-BL and FA-GGBS aggregates. The next most significant ones were found to be BT and GGBS content, followed by water content in the production of pelletized FA-BT and FA-GGBS aggregates, respectively. However, for pelletized FA-BL aggregates, water content

was found to be more significant than BL content. As a result of summarising this analysis, it is possible to generalise that the production as well as the characteristics of pelletized FA-BT, FA-BL, and FA-GGBS aggregates are highly susceptible to the factors considered in their manufacturing process (Sharath et al. 2022).

Table 4.29: Response table for grey relational grade for three curing ages with respect to governing factors in FA-IOT aggregates

Response Table for Means					
14 Days	**Level**	**Na_2O (%)**	**Water (%)**	**FA:IOT (%)**	**SiO_2/Na_2O**
	1	0.3722	0.6303	0.5542	0.6172
	2	0.5493	0.5988	0.6162	0.6013
	3	0.8534	0.6114	0.6705	0.6072
	4	0.6955	0.6297	0.6294	0.6446
	Max. value - Min. value	0.4812	0.0316	0.1163	0.0433
	Rank	1	4	2	3
Response Table for Means					
28 Days	**Level**	**Na_2O (%)**	**Water (%)**	**FA:IOT (%)**	**SiO_2/Na_2O**
	1	0.3697	0.6199	0.5166	0.5844
	2	0.5247	0.5666	0.5823	0.5684
	3	0.8204	0.5645	0.663	0.5675
	4	0.631	0.5946	0.5838	0.6255
	Max. value - Min. value	0.4507	0.0554	0.1464	0.058
	Rank	1	4	2	3
Response Table for Means					
100 Days	**Level**	**Na_2O (%)**	**Water (%)**	**FA:IOT (%)**	**SiO_2/Na_2O**
	1	0.372	0.6083	0.4955	0.5749
	2	0.5083	0.5458	0.5649	0.5393
	3	0.7925	0.5397	0.6585	0.5433
	4	0.6026	0.5818	0.5566	0.618
	Max. value - Min. value	0.4205	0.0686	0.1629	0.0787
	Rank	1	4	2	3

Table 4.30: Response table for grey relational grade for three curing ages with respect to governing factors in FA-COT aggregates

Response Table for Means					
14 Days	**Level**	**Na_2O (%)**	**Water (%)**	**FA:COT (%)**	**SiO_2/Na_2O**
	1	0.5031	0.5978	0.5479	0.5513
	2	0.8602	0.5548	0.6334	0.5858
	3	0.5615	0.5471	0.5989	0.5943
	4	0.3711	0.5663	0.5158	0.5847
	Max. value - Min. value	0.4891	0.0507	0.1176	0.043
	Rank	1	3	2	4
Response Table for Means					
28 Days	**Level**	**Na_2O (%)**	**Water (%)**	**FA:COT (%)**	**SiO_2/Na_2O**
	1	0.512	0.592	0.559	0.540
	2	0.863	0.567	0.632	0.576
	3	0.531	0.541	0.586	0.591
	4	0.371	0.577	0.501	0.570
	Max. value - Min. value	0.492	0.051	0.131	0.052
	Rank	1	4	2	3
Response Table for Means					
100 Days	**Level**	**Na_2O (%)**	**Water (%)**	**FA:COT (%)**	**SiO_2/Na_2O**
	1	0.505	0.588	0.544	0.538
	2	0.856	0.568	0.634	0.579
	3	0.538	0.536	0.588	0.599
	4	0.370	0.577	0.503	0.554
	Max. value - Min. value	0.486	0.052	0.130	0.061
	Rank	1	4	2	3

It is evident from the data presented in Table 4.29 that the grey relational grade is highest at Level 1 for water content%, Level 2 for ratio of FA:IOT mixture, Level 3 for Na_2O% and Level 4 for SiO_2/Na_2O at curing periods of 14 and 100 days. Thus, it can be inferred that simultaneous optimization in characteristics like AIV, ACV, IPS and WA can be carried out in aggregates made using lower water content%, lower FA:IOT ratio, high Na_2O % and high SiO_2/Na_2O ratio at varied curing periods. The higher the difference between maximum and minimum values of grey relational grade is an indication of high-level significance of thar particular factor. It is ranked according to the difference in the values

of grey relational grade which is presented above in Table 4.29. It can be observed that at 14, 28 and 100 days of curing the pelletized aggregates are influenced in order, first by Na_2O%, then FA:IOT ratio, SiO_2/Na_2O ratio and finally by water content %.

Table 4.30 represents the average of each response characteristic (here response means the tested engineering property of produced FA-COT aggregates) for each level of governing factor considered for producing pelletized FA-COT. The difference between maximum and minimum values of grey relational grade or the obtained ranks demonstrates that order of influence of the experimental parameters taken into consideration for producing pelletized FACOT aggregates, from which it can be clearly understood that dosage contents of Na_2O had the most significant influence among the other parameters followed by the blending ratio FA:COT, ratio of SiO_2/Na_2O, and water content dosages at all the three curing ages, represented as Na_2O % > FA:COT > SiO_2/Na_2O > water %. However, this order changed for 28 and 100 days curing periods that is Na_2O % > FA:COT > Water % > SiO_2/Na_2O, which signifies that the ratio of SiO_2/Na_2O became less significant over the period of time for the produced FA:COT aggregates.

CHAPTER – 5

RESULTS AND DISCUSSION ON MULTI-BLENDED PELLETIZED AGGREGATES

4.1 GENERAL

The section discusses the results obtained from the various tests performed on multi-blended pelletized aggregates cured at room temperature. Important observations obtained from advanced characterization techniques like SEM, TGA, and FTIR are also presented in this section.

5.2 ENGINEERING PROPERTIES OF MULTI-BLENDED PELLETIZED AGGREGATES

5.2.1 Aggregate impact value and aggregate crushing value

Figures 5.1(a-d) and 5.2(a-d) show the test results for the aggregate impact value and the aggregate crushing value of pelletized MMIOTBL, MMIOTGGBS, MMCOTBL, and MMCOTGGBS aggregates, respectively.

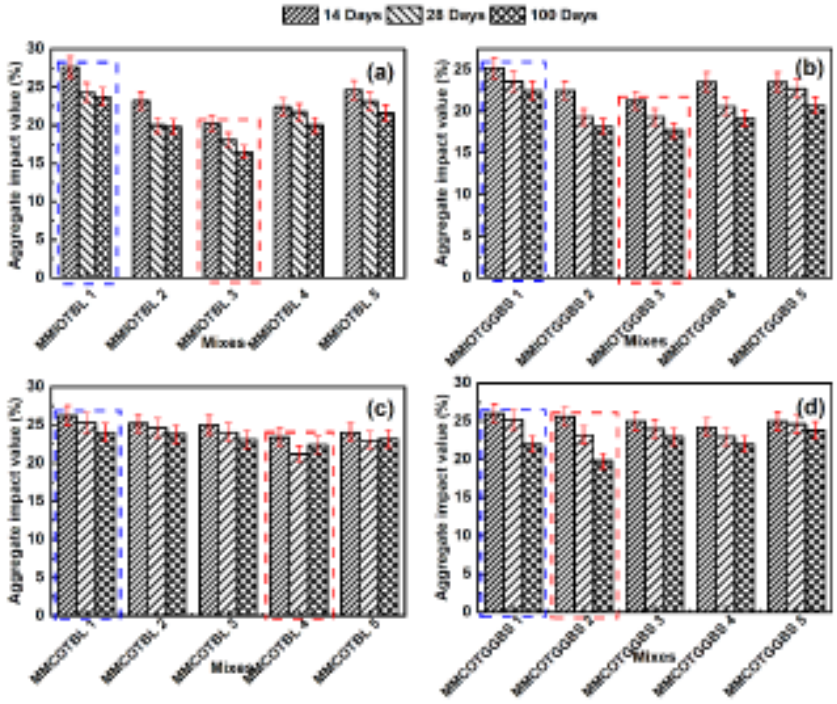

Figure 5.1: Obtained experimental results for aggregate impact value of pelletized (a) MMIOTBL; MMIOTGGBS and (b) MMCOTBL; MMCOTGGBS aggregates

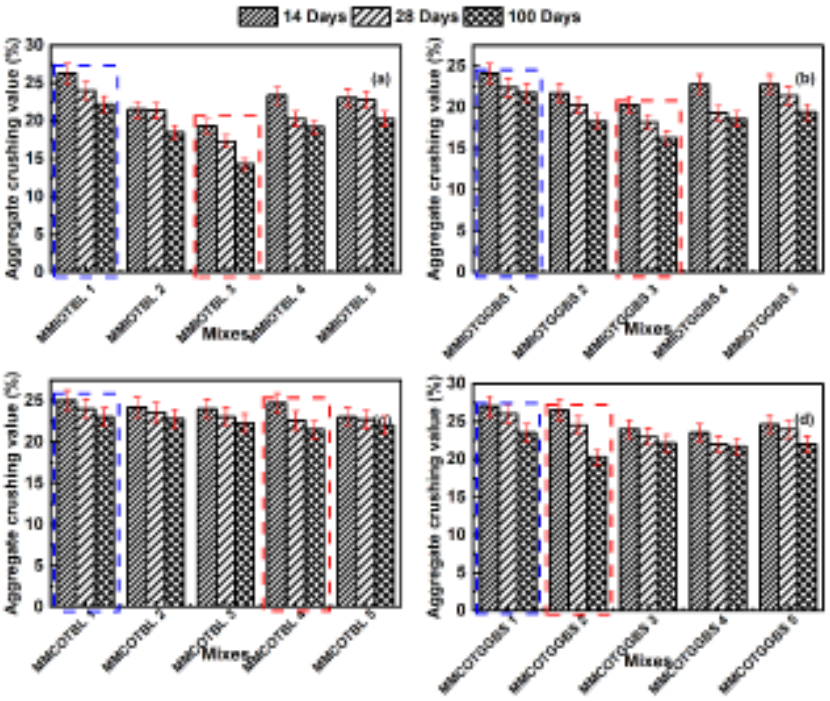

Figure 5.2: Obtained experimental results for aggregate crushing value of pelletized (a) MMIOTBL; MMIOTGGBS and (b) MMCOTBL; MMCOTGGBS aggregates

Figures 5.1(a), 5.2(a), 5.1(b) and 5.2(b) show that mix MMIOTBL 3 and MMIOTGGBS 3 (shown in red) had the best aggregate impact value and aggregate crushing value out of all MMIOTBL and MMIOTGGBS aggregates tested. MMIOTBL 3 can be attributed to the highest dosage of Na_2O content, i.e., 5% present in the mix proportion, followed by 30% of FA, 5% of UFA, 65% of IOT, and 15% of BL; MMIOTGGBS 3 can be attributed to highest dosage of Na_2O content, i.e., 5% present in the mix proportion, followed by 30% of FA, 5% of UFA, 65% of IOT, and 15% of GGBS.

5.2.2 Water absorption

Figure 5.3(a-d) shows the test results for the water absorption of pelletized MMIOTBL, MMIOTGGBS, MMCOTBL and MMCOTGGBS aggregates, respectively.

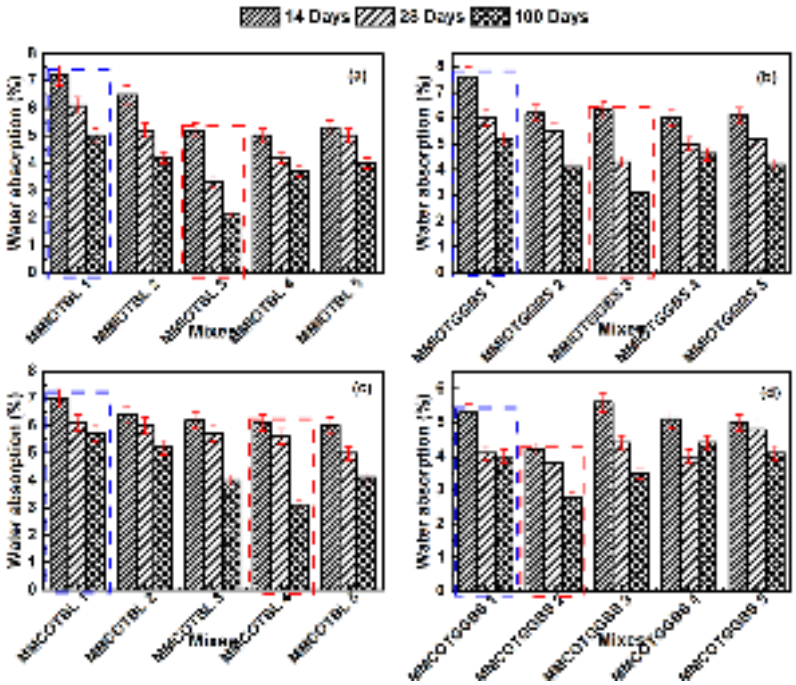

Figure 5.3: Obtained experimental results for water absorption of pelletized (a) MMIOTBL; MMIOTGGBS and (b) MMCOTBL; MMCOTGGBS aggregates

According to the results obtained on water absorption for produced MMIOTBL MMIOTGGBS and MMCOTBL, MMCOTGGBS aggregates [Figure 5.3(a-d), respectively], MMIOTBL 3 MMIOTGGBS 3, MMCOTBL 4, and MMCOTGGBS 2 (marked in red) had the lowest water absorption values, i.e., 3.1%, 2.1%, 3.1% and 2.8%, respectively.

5.2.3 Individual crushing strength of pellets

Figure 5.4(a-d) shows the test results for the water absorption of pelletized MMIOTBL, MMIOTGGBS, MMCOTBL and MMCOTGGBS aggregates, respectively.

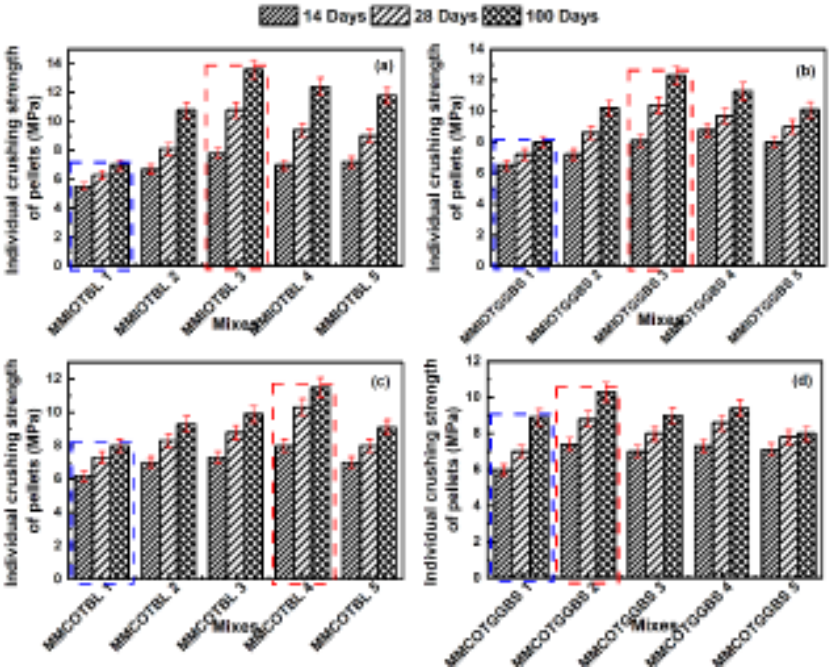

Figure 5.4: Obtained experimental results for individual crushing strength of pellets of pelletized (a) MMIOTBL; MMIOTGGBS and (b) MMCOTBL; MMCOTGGBS aggregates

As per the data presented in Figure 5.4a, the individual crushing strength of pellets measured for aggregate mix MMIOTBL 3 was found to be to 13.6 MPa at 100 days of curing. This mix consists of the highest dosage contents of Na_2O content, i.e., 5% present in the mix proportion, followed by 30% of FA, 5% of UFA, 65% of IOT, and 15% of BL. Based on the measured values of the crushing strengths of MMIOTGGBS (Figure 5.4b) aggregate mix had the highest crushing strength, at 12.3 MPa 6 MPa after 100 days of curing which is associated with to dosage contents of Na_2O (5%), followed by 30% of FA, 5% of UFA, 65% of IOT, and 15% of GGBS.

According to the results obtained on the individual crushing strength of pellets of pelletized MMCOTBL and MMCOTGGBS aggregate mixes, the highest crushing strength of pellets was attained by MMCOTBL 4 and MMCOTGGBS 2 aggregate mixes, which are associated with highest dosages of Na_2O (5%), followed by 20% of FA, 5% of UFA, 75% of COT, and 15% of BL; 5% of Na_2O, followed by 40% of FA, 5% of UFA, 55% of COT, and 15% of GGBS.

5.2.4 Specific gravity

The average specific gravity measured for multi-blended pelletized aggregates was found to be within the range of 2.4–2.6. As IOT and COT were denser than FA and UFA, their dosage influenced the specific gravity of the produced multi-blended pelletized aggregates. A detailed table showing the obtained values for the specific gravity of pelletized MMIOTBL, MMIOTGGBS, MMCOTBL and MMCOTGGBS aggregates is presented in Figure 5.5.

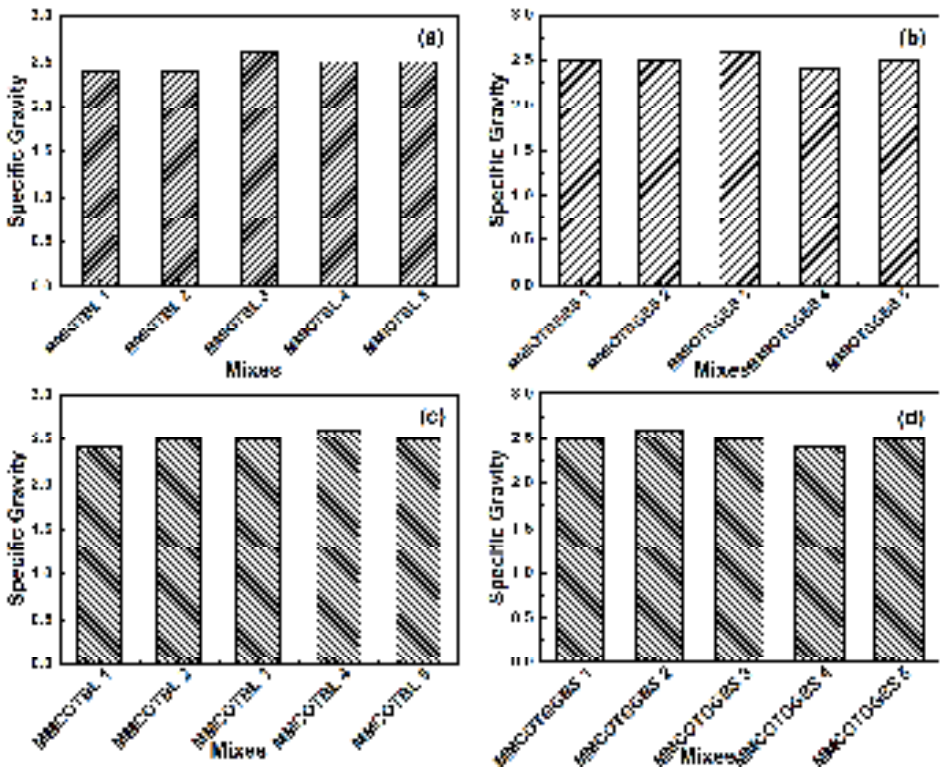

Figure 5.5: Specific gravity of pelletized (a) MMIOTBL (b) MMIOTGGBS (c) MMCOTBL and (d) MMCOTGGBS aggregates

5.3 ADVANCED CHARACTERIZATION STUDIES ON MULTI-BLENDED PELLETIZED AGGREGATES

The advanced characterization studies like SEM, TGA and FTIR was performed on the best-performing multi-blended pelletized aggregates (MMIOTBL 3, MMIOTGGBS 3, MMCOTBL 4, and MMCOTGGBS 2) which were identified based on the obtained engineering properties of multi-blended pelletized aggregates.

5.3.1 Morphology of the best performing multi-blended pelletized aggregates (SEM)

The microphotographs of best performing binary blended pelletized aggregates are presented in Figure 5.6.

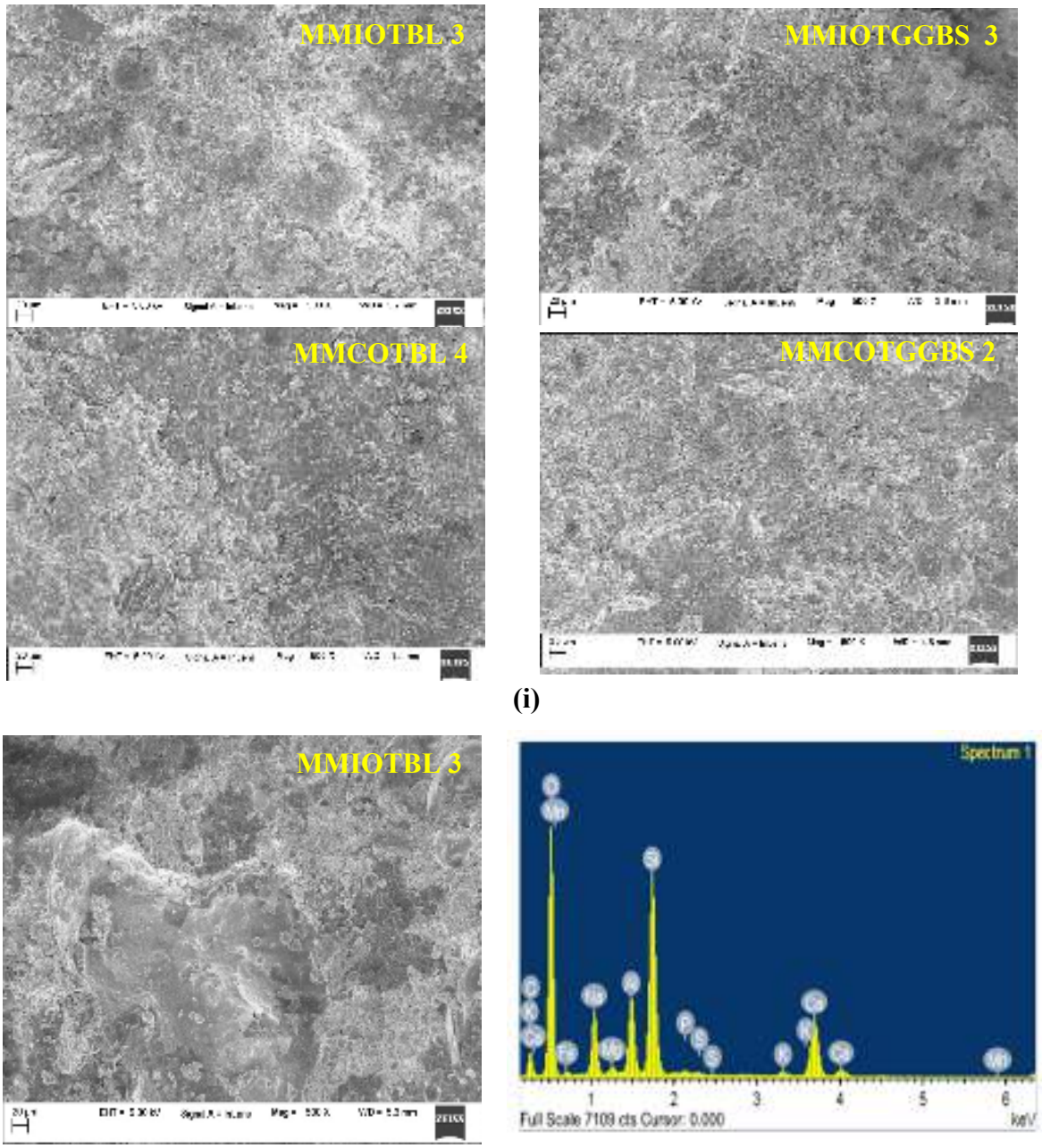

Figure 5.6: SEM micrographs of multi-blended pelletized (i) MMIOTBL 3, MMIOTGGBS 3, MMCOTBL 4 and MMCOTGGBS 2 and (ii) typical EDS graph of MMIOTBL 3

Table 5.1: Details of EDS analysis on pelletized MMIOTBL 3, MMIOTGGBS 3, MMCOTBL 4 and MMCOTGGBS 2 aggregate mixes

Mix Designation	Elemental Composition (%wt.)					Ca/Si	Al/Si
	O	Al	Si	Ca	Na		
MMIOTBL 3	17.09	1.52	3.49	3.50	2.02	1.00	0.43
MMIOTGGBS 3	17.87	1.47	2.48	2.74	1.97	0.90	0.59
MMCOTBL 4	13.94	1.92	3.45	2.98	2.76	0.86	0.55
MMCOTGGBS 2	14.00	1.98	4.61	5.28	2.55	0.87	0.43

From Figure 5.6, it can be understood that the microstructure of the multi-blended pelletized aggregate mixes of MMIOTBL 3, MMIOTGGBS 3, MMCOTBL 4 and MMCOTGGBS 2 depicted more compact and denser probably because of the increased amounts of N-A-S-H and C-A-S-H gel due to the involvement of UFA, IOT and COT wherein FA as the key precursor. From Table 5.1, EDS analysis on the said aggregate samples revealed that the reaction product comprised N-A-S-H/C-A-S-H gel as determined from major elements. This dissolution of ions resulted in an enhanced alkali activation with the inclusion of extra binding phases (C–S–H and N–A–S–H/C–A–S–H) which are responsible for increased strengths results, as observed from attained results presented in Table 5.1.

5.3.2 Thermogravimetric analysis (TGA) of best performing multi-blended pelletized aggregates

The TG-DTG plot of best performing binary blended pelletized aggregates (MMIOTBL 3, MMIOTGGBS 3, MMCOTBL 4, and MMCOTGGBS 2) is presented in Figure 5.7. Commonly, in this figure, the TG curve represents the occurrence of thermogravimetric mass loss for binary blended pelletized aggregates during the process of heating from the temperature range of 25°C–825°C, whereas the DTG curve signifies the temperature boundaries for the decomposition of specific compounds that are discussed in the subsequent sections.

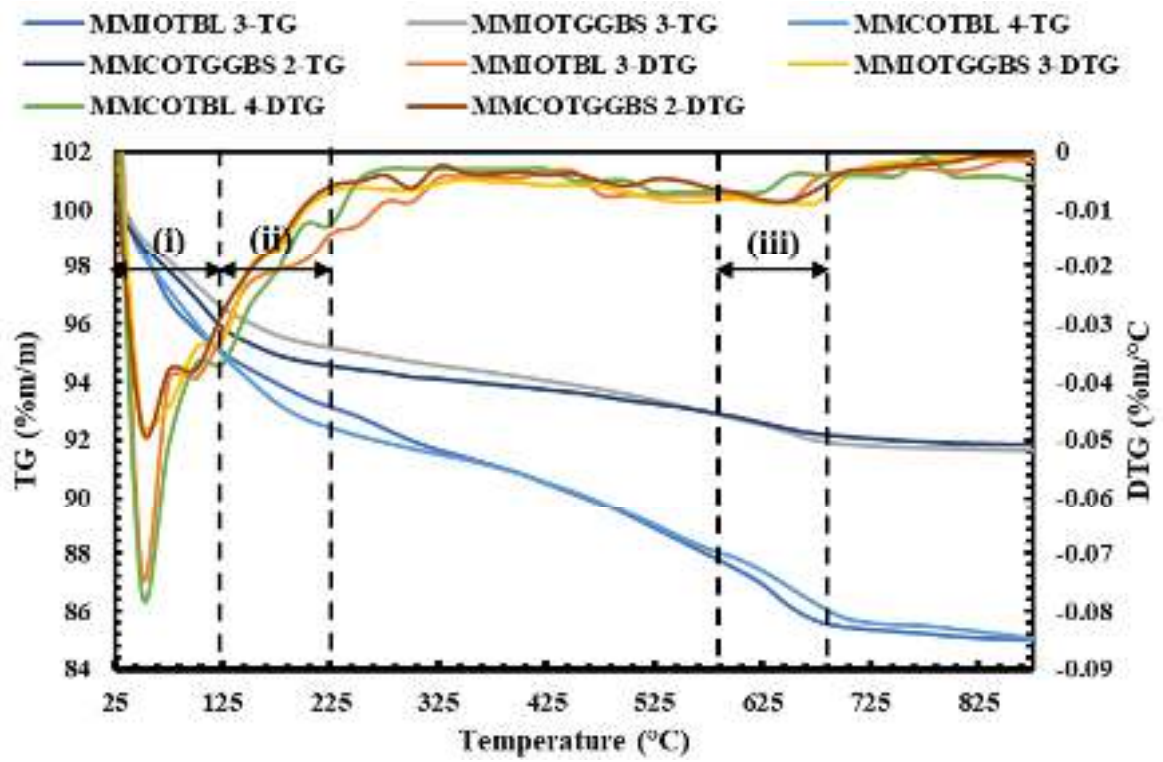

Figure 5.7: TG/DTG curves of multi-blended pelletized aggregates

From TGA results and Figure 5.7, it can be observed that significant weight losses took place in pelletized MMIOTBL 3, MMIOTGGBS 3, MMCOTBL 4 and MMCOTGGBS 2 aggregate mixes between various temperature ranges of (i) 25–120°C: signifies the loss of physically absorbed free water molecules on the pores and surfaces of the samples (Adriano et al. 2013; Longhi et al. 2019; Wuddivira et al. 2012), (ii) 120-225°C: signifies with the thermal degradation of chemically bound water from N-A-S-H/C-A-S-H (Adesanya et al. 2018; Ismail et al. 2014; Palomo et al. 2015), (iii) 600-700°C: signifies decomposition of carbonates (Abdullah et al. 2018; Cornejo et al. 2018; Everaert et al. 2017). The quantification of the amounts of N-A-S-H/C-A-S-H in these multi-blended pelletized aggregate mixes was conducted using a proposed equation (equation 5.1) and the same is presented in Figure 5.8.

$$\Delta M_{N-A-S-H/C-A-S-H}\,\% = M_{120°C} - M_{225°C} \qquad \text{Eqn. 5.1}$$

where, $\Delta M_{N-A-S-H/C-A-S-H}$ is change in mass loss percentage of N-A-S-H/C-A-S-H and $M_{120°C}$, $M_{225°C}$ is the mass loss at the temperatures of 120 and 225 °C.

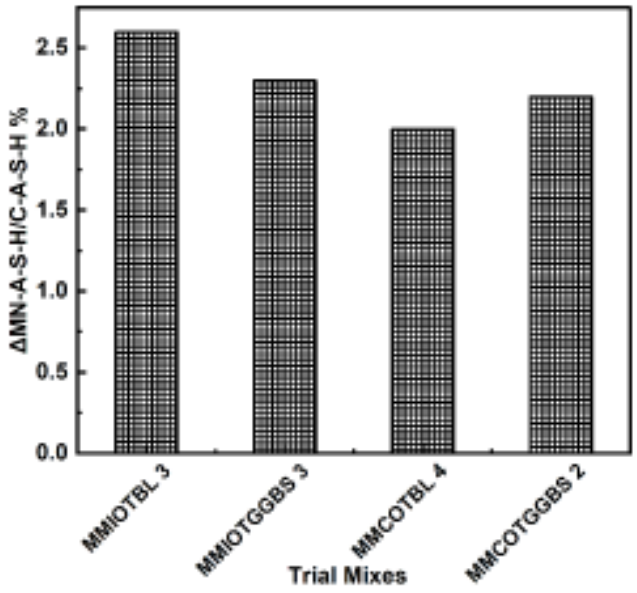

Figure 5.8: Quantification of N-A-S-H/C-A-S-H in multi-blended pelletized aggregates

From Figure 5.8, it can be witnessed that in the produced multi-blended pelletized aggregate mixes, the major reaction product that is N-A-S-H found to incremented in proportion to Na_2O and IOT/COT dosages in these aggregate mixes.

5.3.3 Fourier Transform Infrared Spectroscopy (FTIR) analysis of best performing multi-blended pelletized aggregates

FTIR spectra of best performing multi-blended pelletized aggregate mixes (MMIOTBL 3, MMIOTGGBS 3, MMCOTBL 4 and MMCOTGGBS 2) are presented In Figure 5.9, respectively.

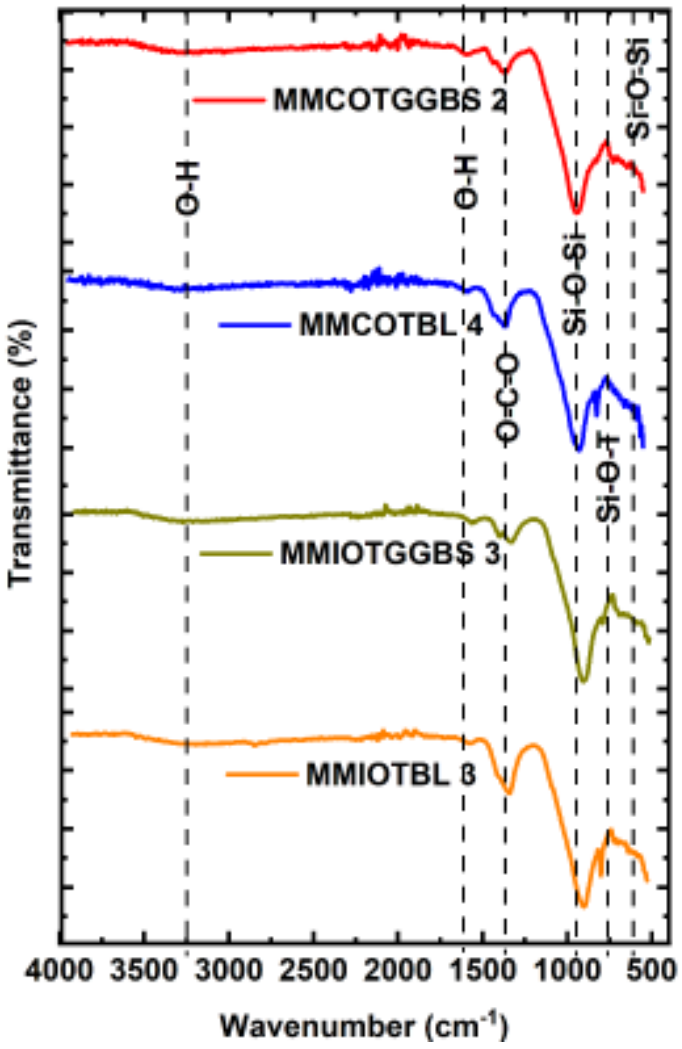

Figure 5.8: FTIR spectra of multi-blended pelletized aggregates

In the Figure 5.9, the existence of O-H bond (marked at ~3300 cm^{-1} and ~1650 cm^{-1}) is due the presence of residual water present in the multi-blended pelletized aggregates. The existence/formation of carbonates (O-C-O) region marked at (~1363 cm^{-1}) could be attributed due to the reaction between Na and atmospheric CO_2, as these produced aggregates were cured under ambient temperature conditions. The peaks marked at ~889.2, 890.1, 938.1 and 952.4 cm^{-1} indicate the peaks of Si-O-Si in pelletized MMIOTBL 3, MMIOTGGBS 3, MMCOTBL 4 and MMCOTGGBS 2 aggregate mixes, respectively. The formation of Si-O-Si in these mixes can contribute to towards the strength achievement in the respective aggregate mixes/produced aggregates. Moreover, it is one the primary indicators of geopolymerization (Davidovits 2008). The existence of the region of Si-O-T (marked at ~747 cm^{-1}) can be attributed due to the presence of quartz in the substituted materials, might have contributed to the formation of tetrahedron SiO_4 (Krivoshein et al. 2020). However, the peaks of Si-O-Si (marked at ~671.6 cm^{-1}) indicates the presence of

products formed during the polycondensation phase of geopolymerization reaction, before the initiation of geopolymer matrix formation (Davidovits 2008; Krivoshein et al. 2020). Furthermore, it is important to note the peaks of MMIOTBL 3, MMIOTGGBS 3, MMCOTBL 4 and MMCOTGGBS 2 slightly shifted to lower frequencies is in indicative of the difference in the strength attained in the produced aggregates under these mixes.

CHAPTER – 6

CONCLUSIONS AND SCOPE FOR FURTHER STUDIES

6.1 GENERAL

In this chapter, the major findings and conclusions of FA based pelletized aggregates cured in ambient temperature conditions are presented. Further scope for further studies is also included in this chapter.

6.2 CONCLUSIONS

The underlying conclusions are made based on the experimental investigations on the influence of incorporated raw materials like FA, IOT, COT, UFA and binding agents like bentonite, burnt lime, and GGBS in conjunction with alkaline activators for producing ambiently cured pelletized aggregates, hence making it as a sustainable and cost-reductive option. The subsequent sections present the conclusions from individual phases of this experimental research work.

Production of binary blended pelletized aggregates and its engineering properties

- The fly ash based pelletized aggregates can be effectively produced with a joint conjuncture of materials like bentonite, burnt lime, ground granulated blast furnace slag, iron ore tailings and copper ore tailings with the alkaline solutions.
- Among the governing factors taken into consideration for producing pelletized FA-BT and FA-GGBS aggregates, all the characteristics of FA-BT and FA-GGBS aggregates like AIV, ACV, WA and IPS were majorly influenced by dosage contents of Na_2O followed by doses of BT and GGBS, respectively. The dosage contents of water were found to be less significant in the production of FA-BT and FA-GGBS aggregates. However, for FA-BL aggregates, the characteristics were greatly influenced by doses of Na_2O and water wherein the BL dose was found to be less influential in the production of FA-BL aggregates.
- Among the nine FA-BT aggregate mixes, the mix FABT 9 (consisting of 5% Na_2O, 21% water and 10% BT) obtained of aggregate impact value, aggregate crushing value, water absorption and individual crushing strength at 100 days as 25%, 23%, 15.3% and 7.2 MPa, respectively. Among the FA-BT aggregates mixes, the mix FABL 5

(consisting of 5% Na_2O, 20% water and 15% BL) obtained the characteristics at 100 days as 17.4%, 15.5%, 14.1% and 11.6 MPa, respectively. In FA-GGBS aggregate mixes, the mix FAGGBS 7 (consisting of 5% Na_2O, 19% water and 15% GGBS) obtained the aggregate impact value, aggregate crushing value, water absorption and individual crushing strength at 100 days as 23.5%, 22.3%, 11.3% and 6.2 MPa, respectively.

From these observations, it can be concluded that FABT 9, FABL 5, FAGGBS 7 were found to be to the best performing mixes among all.

- The average specific gravity of FA-BT, FA-BL and FA-GGBS aggregates was found to be in the range of 2.0-2.2.
- From the production of FA-BT, FA-BL and FA-GGBS aggregates, it can be concluded that a dose of 5% as Na_2O serves to be first optimized value among the key parameters of geopolymerization involved in the production methodology of pelletized aggregates. Second, the optimized doses of water are 21% for FA-BT, 20% for FA-BL and 19% for FA-GGBS aggregates. Third, the optimized doses of additive admixtures stood as 10% for FA-BT, 15% for both FA-BL and FA-GGBS aggregates.
- Among the governing factors taken into consideration for producing pelletized FA-IOT and FA-COT aggregates, the obtained characteristics of FA-IOT and FA-COT aggregates were majorly influenced by the dosage contents of Na_2O followed by blending proportion of FA with IOT (FA:IOT) and FA with COT (FA:COT). However, the doses of water and ratio of SiO_2/Na_2O had a relatively lesser impact on characteristics of FA-IOT and FA-COT aggregates.
- Among the sixteen FA-IOT aggregate mixes, the mix FAIOT 9 (consisting of 5% Na_2O, 13.5% water, 30:70 FA:IOT proportion and 0.3 SiO_2/Na_2O ratio) obtained aggregate impact value, aggregate crushing value, water absorption and individual crushing strength at 100 days as 21.2%, 20.3%, 2.5% and 10.5 MPa, respectively. In FA-COT aggregate mixes, the mix FACOT 5 (consisting of 4% Na_2O, 13.5% water, 40:60 FA:COT proportion and 0.27 SiO_2/Na_2O ratio) achieved 25.6%, 24.1%, 5.2% and 8.9 MPa, respectively.

  From these observations, it can be concluded that FAIOT 9 and FACOT 5 were found to be to the best performing mixes among all.
- The produced fly ash based pelletized aggregates admixed with IOT and COT were found to have a specific gravity value ranging from 2.4 to 2.6 indicates the

advantageous incorporation of IOT/COT in production of pelletized FA-IOT and FA-COT aggregates.

- From the production of FA-IOT aggregates, it can be concluded that a dose of 5% as Na_2O serves to be first optimized value among the key parameters of geopolymerization involved in the production methodology of pelletized aggregates. Second, the optimized dose of water stands as 13.5%, Third, the optimized dose of FA:IOT proportion is 30:70. Fourth, the optimized ratio of SiO_2/Na_2O comes out as 0.3. For FA-COT aggregates, it can be stated that the optimized doses of governing factors are 4% Na_2O, 13.5% water, 40:60 FA:COT and 0.27 as SiO_2/Na_2O ratio, respectively.
- The morphological studies conducted on binary blended pelletized aggregates revealed that aggregates produced with higher dosages of Na_2O followed by incorporation of BT, BL, GGBS, IOT, and COT possess a more homogenous and denser microstructure.
- From TGA analysis performed on pelletized FA-BT, FA-BL and FA-GGBS aggregates, it can be revealed that the quantified amount of geopolymerization products (N-A-S-H/C-A-S-H) was found to be the maximum for aggregates produced with 5% Na_2O content and 15% BL content. However, mass loss associated with N-A-S-H/C-A-S-H was found to be intensified for aggregates admixed with calcium-rich minerals, i.e., BT and GGBS. Furthermore, mass loss studies performed on FA-IOT and FA-COT aggregates showed that the quantified C-S-H and $Ca(OH)_2$ contents are susceptible to dosages of Na_2O and blending ratios of FA with IOT; COT.
- FTIR analysis on binary blended pelletized aggregates concluded that there exists an occurrence of shifting of major bands of Si–O–T and Si–O–Si happens towards lower wavenumbers with the progression in time.

Production of multi-blended pelletized aggregates and its engineering properties

- Production of multi-blended pelletized aggregates with the incorporation of ultrafine fly ash with fly ash, bentonite, burnt lime, GGBS, iron ore and copper ore tailings were found to have pronounced effect on the engineering properties like aggregate impact value, aggregate crushing value, water absorption and individual crushing strength of pellets of produced MMIOTBL, MMIOTGGBS, MMCOTBL and MMCOTGGBS aggregates.
- Among the five MMIOTBL, MMIOTGGBS, MMCOTBL and MMCOTGGBS aggregate mixes, the mix MMIOTBL 3 (consisting of 5% Na_2O, 30:5:65 as

FA:UFA:IOT proportion, 20% water and 15% BL) achieved the aggregate impact value, aggregate crushing value, water absorption and individual crushing strength at 100 days as 16.5%, 17.7%, 2.1% and 13.6 MPa, respectively. In MMIOTGGS aggregate mixes, the mix MMIOTGGBS 3 (consisting of 5% Na_2O, 30:5:65 as FA:UFA:IOT proportion, 20% water and 15% GGBS) achieved the characteristics at 100 days as 17.7%, 16.3%, 3.1% and 12.3 MPa, respectively.

From these observations, it can be concluded that MMIOTBL 3 and MMIOTGGBS 3 were found to be to the best performing mixes among all.

- Among the five MMCOTBL aggregate mixes, the MMCOTBL 4 mix (consisting of consisting of 5% Na_2O, 20:5:75 as FA:UFA:COT proportion, 20% water, 15% BL) obtained the aggregate impact value, aggregate crushing value, water absorption and individual crushing strength at 100 days as 22.4%, 21.5%, 3.1% and 11.5 MPa, respectively. In MMCOTGGBS aggregate mixes, the MMCOTGGBS 2 aggregate mix (consisting of 5% Na_2O, 40:5:65 as FA:UFA:COT proportion, 20% water, 15% GGBS) obtained the characteristics at 100 days as 19.8%, 20.3%, 2.8% and 10.3 MPa, respectively.
- The produced fly ash based multi-blended pelletized aggregates were found to have a specific gravity value ranging from 2.4 to 2.6
- Morphological and EDS analysis performed on multi-blended pelletized aggregates have revealed that the produced aggregates possess a more homogenous and denser microstructure, wherein the reactions products were found to be N-A-S-H/C-A-S-H.
- TGA analysis performed on multi-blended pelletized aggregates concluded the major reaction product that is N-A-S-H/C-A-S-H is dependent on the combinations of Na_2O and UFA, BL, GGBS, IOT and COT dosages.
- FTIR studies concluded there exists a slight occurrence of shifting of major bands of Si– O–T and Si–O–Si towards lower wavenumbers in the pelletized MMIOTBL 3, MMIOTGGBS 3, MMCOTBL 4 and MMCOTGGBS 2, indicating the attainment of superior engineering properties in the produced aggregates.
- From the production multi-blended pelletized aggregates, it can be concluded that the incorporation of optimized doses of Na_2O, water, bentonite, GGBS with ultrafine fly ash and other two mine tailings had significantly influenced all the characteristics of the multi-blended pelletized aggregates.

Comparative remarks from binary blended and multi-blended pelletized aggregates

- While comparing the binary blended pelletized aggregates with multi-blended pelletized aggregates, it can be concluded that the multi-blended pelletized aggregates were found to be superior in light with the various engineering characteristics such as aggregate impact value, aggregate crushing value, water absorption, specific gravity and individual crushing strength.
- It can be concluded that the inclusion of ultrafine fly ash with iron and copper ore tailings, burnt lime and GGBS greatly influenced some specific characteristics of fly ash based pelletized aggregates like specific gravity, water absorption and individual crushing strength.

6.3 SCOPE FOR FURTHER RESEARCH

- Mass-scale production of FA based pelletized aggregates with the incorporation of additional supplementary cementitious materials can be explored for increasing the interaction with the mine tailings-based geopolymer system in order to efficiently tune and improve the characteristics of the produced aggregates.
- The properties of fly ash based pelletized aggregates still be can be improved either by treating their surface by adopting encapsulation methodology etc., or by incorporating suitable additives in conjunction with other types of alkaline activators into the production process.
- A huge scope is available to find out the possible utilization of pelletized fly ash-based aggregates in concrete production with partial or full replacement with the natural aggregates.
- Additional studies can be taken up further for understanding the behaviour of structural members under various stress that are made up of concrete with pelletized fly ash-based aggregates.
- Various types of pre-treatment techniques for mine tailings are needed for boosting their interaction with other precursors for producing pelletized aggregates.

REFERENCES

Abdul Rahim, R. H., Azizli, K. A., Man, Z., Rahmiati, T., and Ismail, L. (2014). "Effect of solid to liquid ratio on the mechanical and physical properties of fly ash geopolymer without sodium silicate." *Applied mechanics and materials*, Trans Tech Publ, 46–49.

Abdullah, M. M. A., Hussin, K., Bnhussain, M., Ismail, K. N., and Ibrahim, W. M. W. (2011). "Mechanism and chemical reaction of fly ash geopolymer cement-a review." *Int. J. Pure Appl. Sci. Technol*, 6(1), 35–44.

Abdullah, M., Ming, L. Y., Yong, H. C., and Tahir, M. F. M. (2018). "Cement Based Materials." InTechOpen London, UK:

Adesanya, E., Ohenoja, K., Luukkonen, T., Kinnunen, P., and Illikainen, M. (2018). "One-part geopolymer cement from slag and pretreated paper sludge." *Journal of Cleaner Production*, 185, 168–175.

Adriano, A., Soriano, G., and Duque, J. (2013). "Characterization of water absorption and desorption properties of natural zeolites in Ecuador." *Fifth International Symposium on Energy*, 1–9.

Ahmari, S., and Zhang, L. (2012). "Production of eco-friendly bricks from copper mine tailings through geopolymerization." *Construction and building materials*, 29, 323–331.

Ahmari, S., Zhang, L., and Zhang, J. (2012). "Effects of activator type/concentration and curing temperature on alkali-activated binder based on copper mine tailings." *Journal of Materials Science*, 47(16), 5933–5945.

Ahmaruzzaman, M. (2010). "A review on the utilization of fly ash." *Progress in energy and combustion science*, 36(3), 327–363.

Asadizadeh, M., Clements, C., Hedayat, A., Tunstall, L., Gonzalez, J. A. V., Alvarado, J. W. V., and Neira, M. T. (2023a). "The effect of class F fly ash on the geopolymerization and compressive strength of lightweight aggregates made from alkali-activated mine tailings." *Construction and Building Materials*, 395, 132275.

Asadizadeh, M., Hedayat, A., Tunstall, L., Gonzalez, J. A. V., Alvarado, J. W. V., and Neira, M. T. (2024). "The impact of slag on the process of geopolymerization and the mechanical performance of mine-tailings-based alkali-activated lightweight aggregates." *Construction and Building Materials*, 411, 134347.

Asadizadeh, M., Hedayat, A., Tunstall, L., Taboada Neira, M., Vega González, J. A., and Verá Alvarado, J. W. (2023b). "Mechanical properties of lightweight aggregates produced from mine tailings via alkali-activation." *ARMA US Rock Mechanics/Geomechanics Symposium*, ARMA, ARMA-2023.

Aseniero, J. P. J., Opiso, E. M., Banda, M. H. T., and Tabelin, C. B. (2019). "Potential utilization of artisanal gold-mine tailings as geopolymeric source material: preliminary investigation." *SN Applied Sciences*, 1, 1–9.

Atiş, C. D., Görür, E. B., Karahan, O., Bilim, C., İlkentapar, S., and Luga, E. (2015). "Very high strength (120 MPa) class F fly ash geopolymer mortar activated at different NaOH amount, heat curing temperature and heat curing duration." *Construction and building materials*, 96, 673–678.

Azhar, N. S. D. M., Zainal, F. F., and Abdullah, M. M. A. B. (2020). "Bonding and Phases Analysis of Geopolymer Materials." *IOP Conference Series: Materials Science and Engineering*, IOP Publishing, 12052.

Bakri, A. M. M. Al, Kamarudin, H., Bnhussain, M., Rafiza, A. R., and Zarina, Y. (2012). "Effect of Na^ sub 2^ SiO^ sub 3^/NaOH Ratios and NaOH Molarities on Compressive Strength of Fly-Ash-Based Geopolymer." *ACI Materials Journal*, 109(5), 503.

Barbosa, V. F. F., MacKenzie, K. J. D., and Thaumaturgo, C. (2000). "Synthesis and characterisation of materials based on inorganic polymers of alumina and silica: sodium polysialate polymers." *International journal of inorganic materials*, 2(4), 309–317.

Baykal, G., and Döven, A. G. (2000). "Utilization of fly ash by pelletization process; theory, application areas and research results." *Resources, Conservation and Recycling*, 30(1), 59–77.

Bernal, S. A., Rodríguez, E. D., Mejia de Gutiérrez, R., Provis, J. L., and Delvasto, S. (2012). "Activation of metakaolin/slag blends using alkaline solutions based on chemically modified silica fume and rice husk ash." *Waste and Biomass Valorization*, 3(1), 99–108.

Bijen, J. M. J. M. (1986a). "Manufacturing processes of artificial lightweight aggregates from fly ash." *International Journal of Cement Composites and Lightweight Concrete*, 8(3), 191–199.

Bijen, J. M. J. M. (1986b). "Manufacturing processes of artificial lightweight aggregates from fly ash." *International Journal of Cement Composites and Lightweight Concrete*,

8(3), 191–199.

Borges, P. H. R., Ramos, F. C. R., Caetano, T. R., Panzerra, T. H., and Santos, H. (2019). “Reuse of iron ore tailings in the production of geopolymer mortars.” *REM-International Engineering Journal*, 72, 581–587.

Brinkman, L., and Miller, S. A. (2021). “Environmental impacts and environmental justice implications of supplementary cementitious materials for use in concrete.” *Environmental Research: Infrastructure and Sustainability*, 1(2), 25003.

Bui, L. A., Hwang, C., Chen, C., Lin, K., and Hsieh, M. (2012a). “Manufacture and performance of cold bonded lightweight aggregate using alkaline activators for high performance concrete.” *Construction and Building Materials*, 35, 1056–1062.

Bui, L. A. T., Hwang, C. L., Chen, C. T., and Hsieh, M. Y. (2012b). “Characteristics of cold-bonded lightweight aggregate produced with different mineral admixtures.” *Applied mechanics and materials*, Trans Tech Publ, 978–983.

Bui, L. A. T., Hwang, C. L., Chen, C. T., Lin, K. L., and Hsieh, M. Y. (2012c). “Manufacture and performance of cold bonded lightweight aggregate using alkaline activators for high performance concrete.” *Construction and Building Materials*.

Bureau of Indian Standards (BIS). (2002). “IS : 2366 (Part IV)-1963-Methods of test for Aggregates for Concrete, part 4 : Mechanical properties.” *Indian Standards*, 1–37.

Caballero, E., Sánchez, W., and Ríos, C. A. (2014). “Synthesis of geopolymers from alkaline activation of gold mining wastes.” *Ingeniería y competitividad*, 16(1), 317–330.

Cavazzuti, M. (2013a). “Design of experiments.” *Optimization methods*, Springer, 13–42.

Cavazzuti, M. (2013b). “Design of Experiments BT - Optimization Methods: From Theory to Design Scientific and Technological Aspects in Mechanics.” M. Cavazzuti, ed., Berlin, Heidelberg: Springer Berlin Heidelberg, 13–42.

Chau-Khun, M., Zawawi, A. A., and Wahid, O. (2018). “Structural and material performance of geopolymer concrete 2018.” *ELSEVIER*.

Chi, J. M., Huang, R., Yang, C.-C., and Chang, J. J. (2003). “Effect of aggregate properties on the strength and stiffness of lightweight concrete.” *Cement and Concrete Composites*, 25(2), 197–205.

Chiou, J., Wang, K.-S., Chen, C.-H., and Lin, Y.-T. (2006). “Lightweight aggregate made

from sewage sludge and incinerated ash." *Waste Management*, 26(12), 1453–1461.

Cioffi, R., Colangelo, F., Montagnaro, F., and Santoro, L. (2011). "Manufacture of artificial aggregate using MSWI bottom ash." *Waste Management*, 31(2), 281–288.

Colangelo, F., and Cioffi, R. (2013). "Use of cement kiln dust, blast furnace slag and marble sludge in the manufacture of sustainable artificial aggregates by means of cold bonding pelletization." *Materials*, 6(8), 3139–3159.

Colangelo, F., Messina, F., and Cioffi, R. (2015). "Recycling of MSWI fly ash by means of cementitious double step cold bonding pelletization: Technological assessment for the production of lightweight artificial aggregates." *Journal of hazardous materials*, 299, 181–191.

Cornejo, M. H., Elsen, J., Togra, B., Baykara, H., Soriano, G., and Paredes, C. (2018). "Effect of calcium hydroxide and water to solid ratio on compressive strength of mordenite-based geopolymer and the evaluation of its thermal transmission property." *ASME International Mechanical Engineering Congress and Exposition*, American Society of Mechanical Engineers, V012T11A022.

Csavina, J., Field, J., Taylor, M. P., Gao, S., Landázuri, A., Betterton, E. A., and Sáez, A. E. (2012). "A review on the importance of metals and metalloids in atmospheric dust and aerosol from mining operations." *Science of the Total Environment*, 433, 58–73.

Davidovits, J. (1991). "Geopolymers: inorganic polymeric new materials." *Journal of Thermal Analysis and calorimetry*, 37(8), 1633–1656.

Davidovits, J. (1999). "Chemistry of Geopolymeric Systems, Terminology In: Proceedings of 99 International Conference." *eds. Joseph Davidovits, R. Davidovits & C. James, France*.

Davidovits, J. G. (2008). "Chemistry and applications." *Saint-Quentin: Institute Geopolymer*, 592.

DIN, E. N. (2013). "1097-6: Prüfverfahren für mechanische und physikalische Eigenschaften von Gesteinskörnungen–Teil 6: Bestimmung der Rohdichte und der Wasseraufnahme." *Deutsches Institut für Normung eV, Ausgabe*.

DIN, E. N. (2015). "13055: 2015-11: Leichte Gesteinskörnungen." *Deutsche und Englische Fassung FprEN*, 13055.

Divvala, S. (2021). “Early strength properties of geopolymer concrete composites: an experimental study.” *Materials Today: Proceedings*, 47, 3770–3777.

Dold, B. (2020). “Sourcing of critical elements and industrial minerals from mine waste–The final evolutionary step back to sustainability of humankind?” *Journal of Geochemical Exploration*, 219, 106638.

Dong, L., Tong, X., Li, X., Zhou, J., Wang, S., and Liu, B. (2019). “Some developments and new insights of environmental problems and deep mining strategy for cleaner production in mines.” *Journal of Cleaner Production*, 210, 1562–1578.

Duan, P., Yan, C., Luo, W., and Zhou, W. (2016a). “A novel surface waterproof geopolymer derived from metakaolin by hydrophobic modification.” *Materials Letters*, 164, 172–175.

Duan, P., Yan, C., Zhou, W., and Ren, D. (2016b). “Fresh properties, compressive strength and microstructure of fly ash geopolymer paste blended with iron ore tailing under thermal cycle.” *Construction and Building Materials*, 118, 76–88.

Duxson, P., Fernández-Jiménez, A., Provis, J. L., Lukey, G. C., Palomo, A., and Deventer, J. S. J. van. (2007). “Geopolymer technology: the current state of the art.” *Journal of materials science*, 42(9), 2917–2933.

Eugênio, T. M. C., Fagundes, J. F., Viana, Q. S., Vilela, A. P., and Mendes, R. F. (2021). “Study on the feasibility of using iron ore tailing (iot) on technological properties of concrete roof tiles.” *Construction and Building Materials*, 279, 122484.

Everaert, C., Luypaert, M., Maag, J. L. V, Cheng, Q. X., Dinger, M. E., Hellemans, J., and Mestdagh, P. (2017). “Benchmarking of RNA-sequencing analysis workflows using whole-transcriptome RT-qPCR expression data.” *Scientific reports*, 7(1), 1–11.

Fernández-Jiménez, A., and Palomo, A. (2005). “Composition and microstructure of alkali activated fly ash binder: Effect of the activator.” *Cement and concrete research*, 35(10), 1984–1992.

Fernández-Jiménez, A., Palomo, A., Sobrados, I., and Sanz, J. (2006). “The role played by the reactive alumina content in the alkaline activation of fly ashes.” *Microporous and Mesoporous materials*, 91(1–3), 111–119.

Fifinatasha, S. N., Bakri, A. M. M. Al, Kamarudin, H., Zarina, Y., Rafiza, A. R., and Liyana, J. (2013). “Reviews on the different sources materials to the geopolymer

performance.” *Advances in Environmental Biology*, 7(12 S2), 3835–3843.

Gao, X., Yu, Q. L., and Brouwers, H. J. H. (2015). “Properties of alkali activated slag–fly ash blends with limestone addition.” *Cement and Concrete Composites*, 59, 119–128.

Garg, N., Özçelik, V. O., Skibsted, J., and White, C. E. (2019). “Nanoscale ordering and depolymerization of calcium silicate hydrates in the presence of alkalis.” *The Journal of Physical Chemistry C*, 123(40), 24873–24883.

Geetha, S., and Ramamurthy, K. (2010a). “Reuse potential of low-calcium bottom ash as aggregate through pelletization.” *Waste management*, 30(8–9), 1528–1535.

Geetha, S., and Ramamurthy, K. (2010b). “Environmental friendly technology of cold-bonded bottom ash aggregate manufacture through chemical activation.” *Journal of cleaner production*, 18(15), 1563–1569.

Geetha, S., and Ramamurthy, K. (2011). “Properties of sintered low calcium bottom ash aggregate with clay binders.” *Construction and Building Materials*, 25(4), 2002–2013.

Geetha, S., and Ramamurthy, K. (2013). “Properties of geopolymerised low-calcium bottom ash aggregate cured at ambient temperature.” *Cement and Concrete Composites*, 43, 20–30.

Gesoĝlu, M., Güneyisi, E., and Mahmood, S. F. (2012). “H. öznur öz, K. Mermerdaş," Recycling ground granulated blast furnace slag as cold bonded artificial aggregate partially used in self-compacting concrete.” *J. Hazard. Mater*, 235–236.

Gesoğlu, M., Güneyisi, E., and Öz, H. Ö. (2012). “Properties of lightweight aggregates produced with cold-bonding pelletization of fly ash and ground granulated blast furnace slag.” *Materials and structures*, 45(10), 1535–1546.

Gesoğlu, M., Özturan, T., and Güneyisi, E. (2007). “Effects of fly ash properties on characteristics of cold-bonded fly ash lightweight aggregates.” *Construction and Building Materials*, 21(9), 1869–1878.

Gomathi, P., and Sivakumar, A. (2012). “Characterization on the strength properties of pelletized fly ash aggregate.” *ARPN Journal of Engineering and Applied Sciences*, 7(11), 1523–1532.

Gomathi, P., and Sivakumar, A. (2014a). “Fly ash based lightweight aggregates incorporating clay binders.” *Indian Journal of Engineering and Materials Sciences*, 21(2),

227–232.

Gomathi, P., and Sivakumar, A. (2014b). “Synthesis of geopolymer based class-F fly ash aggregates and its composite properties in Concrete.” *Archives of Civil Engineering*, 60(1), 55–75.

Gomathi, P., and Sivakumar, A. (2015a). “Accelerated curing effects on the mechanical performance of cold bonded and sintered fly ash aggregate concrete.” *Construction and Building Materials*, 77, 276–287.

Gomathi, P., and Sivakumar, A. (2015b). “Accelerated curing effects on the mechanical performance of cold bonded and sintered fly ash aggregate concrete.” *Construction and Building Materials*, 77, 276–287.

Gomathi, P., Sivakumar, A., Singh, D., Rajaraman, A., and Sounthararajan, V. M. (2013). “Crushing strength properties of furnace slag-fly ash blended lightweight aggregates.” *ARPN Journal Engineering and Applied Sciences*, 8(4), 246–251.

Görhan, G., and Kürklü, G. (2014). “The influence of the NaOH solution on the properties of the fly ash-based geopolymer mortar cured at different temperatures.” *Composites part b: engineering*, 58, 371–377.

Güneyisi, E., Gesoğlu, M., Altan, I., and Öz, H. Ö. (2015). “Utilization of cold bonded fly ash lightweight fine aggregates as a partial substitution of natural fine aggregate in self-compacting mortars.” *Construction and Building Materials*, 74, 9–16.

Hageman, P. L., and Briggs, P. H. (2000). *A simple field leach test for rapid screening and qualitative characterization of mine waste dump material on abandoned mine lands*. US Dept. of the Interior, US Geological Survey,.

Hanrahan, G., and Lu, K. (2006). “Application of factorial and response surface methodology in modern experimental design and optimization.” *Critical Reviews in Analytical Chemistry*, 36(3–4), 141–151.

Hardjito, D., Cheak, C. C., and Ing, C. H. L. (2008). “Strength and setting times of low calcium fly ash-based geopolymer mortar.” *Modern applied science*, 2(4), 3–11.

Hardjito, D., and Rangan, B. V. (2005). “Development and properties of low-calcium fly ash-based geopolymer concrete.”

Harikrishnan, K. I., and Ramamurthy, K. (2006). “Influence of pelletization process on the

properties of fly ash aggregates." *Waste management*, 26(8), 846–852.

Hertel, T., Blanpain, B., and Pontikes, Y. (2016). "A proposal for a 100% use of bauxite residue towards inorganic polymer mortar." *Journal of Sustainable Metallurgy*, 2, 394–404.

Holm, T. A., and Ries, J. P. (2006). "Lightweight concrete and aggregates." *Significance of tests and properties of concrete and concrete-making materials*, ASTM International.

Huang, B., Feng, Q., An, D., and Zhang, J. (2020). "Use of mine tailings as precast construction materials through alkali activation." *Mining, Metallurgy & Exploration*, 37, 251–265.

Hwang, C.-L., and Tran, V.-A. (2015). "A study of the properties of foamed lightweight aggregate for self-consolidating concrete." *Construction and Building Materials*, 87, 78–85.

Insights, F. B. (2021). "Market research report." *Fortune Business Insights*, 2021–2028.

IS:383-2016. (2016). "Indian Standard Coarse and Fine aggregate for Concrete-Specification." *Bureau of Indian Standards, New Delhi, India*, (January), 1–21.

Ismail, I., Bernal, S. A., Provis, J. L., San Nicolas, R., Hamdan, S., and Deventer, J. S. J. van. (2014). "Modification of phase evolution in alkali-activated blast furnace slag by the incorporation of fly ash." *Cement and Concrete Composites*, 45, 125–135.

Jang, J. G., Lee, N. K., and Lee, H.-K. (2014). "Fresh and hardened properties of alkali-activated fly ash/slag pastes with superplasticizers." *Construction and Building Materials*, 50, 169–176.

Jiao, X., Zhang, Y., Chen, T., Bao, S., Liu, T., and Huang, J. (2011). "Geopolymerisation of a silica-rich tailing." *Minerals Engineering*, 24(15), 1710–1712.

Kang, X., Kang, G.-C., Chang, K.-T., and Ge, L. (2015). "Chemically stabilized soft clays for road-base construction." *Journal of Materials in Civil Engineering*, 27(7), 4014199.

Kastiukas, G., Zhou, X., and Castro-Gomes, J. (2016). "Development and optimisation of phase change material-impregnated lightweight aggregates for geopolymer composites made from aluminosilicate rich mud and milled glass powder." *Construction and Building Materials*, 110, 201–210.

Kaze, C. R., Adesina, A., Lecomte-Nana, G. L., Metekong, J. V. S., Samen, L. V. E. K.,

Kamseu, E., and Melo, U. C. (2021). “Synergetic effect of rice husk ash and quartz sand on microstructural and physical properties of laterite clay based geopolymer.” *Journal of Building Engineering*, 43, 103229.

Khale, D., and Chaudhary, R. (2007). “Mechanism of geopolymerization and factors influencing its development: a review.” *Journal of materials science*, 42(3), 729–746.

Kinnunen, P., Ismailov, A., Solismaa, S., Sreenivasan, H., Räisänen, M.-L., Levänen, E., and Illikainen, M. (2018). “Recycling mine tailings in chemically bonded ceramics–a review.” *Journal of cleaner production*, 174, 634–649.

Kiventerä, J., Golek, L., Yliniemi, J., Ferreira, V., Deja, J., and Illikainen, M. (2016). “Utilization of sulphidic tailings from gold mine as a raw material in geopolymerization.” *International Journal of Mineral Processing*, 149, 104–110.

Kiventerä, J., Perumal, P., Yliniemi, J., and Illikainen, M. (2020). “Mine tailings as a raw material in alkali activation: A review.” *International Journal of Minerals, Metallurgy and Materials*, 27(8), 1009–1020.

Kockal, N. U., and Ozturan, T. (2011). “Characteristics of lightweight fly ash aggregates produced with different binders and heat treatments.” *Cement and Concrete Composites*, 33(1), 61–67.

Komljenovic, M., Bascarevic, Z., and Bradic, V. (2010). “Mechanical and microstructural properties of alkali-activated fly ash Geopolymers Journal of Hazardous Materials.” *vol*, 181, 1–3.

Kong, D. L. Y., Sanjayan, J. G., and Sagoe-Crentsil, K. (2007). “Comparative performance of geopolymers made with metakaolin and fly ash after exposure to elevated temperatures.” *Cement and concrete research*, 37(12), 1583–1589.

Krishnan, T., and Purushothaman, R. (2017). “Optimization and influence of parameter affecting the compressive strength of geopolymer concrete containing recycled concrete aggregate: using full factorial design approach.” *IOP Conference Series: Earth and Environmental Science*, IOP Publishing, 12013.

Krivoshein, P. K., Volkov, D. S., Rogova, O. B., and Proskurnin, M. A. (2020). “FTIR photoacoustic spectroscopy for identification and assessment of soil components: Chernozems and their size fractions.” *Photoacoustics*, 18, 100162.

Kuranchie, F. A., Shukla, S. K., and Habibi, D. (2016). “Utilisation of iron ore mine tailings

for the production of geopolymer bricks." *International Journal of Mining, Reclamation and Environment*, 30(2), 92–114.

Lazorenko, G., Kasprzhitskii, A., Kruglikov, A., Mischinenko, V., and Yavna, V. (2020a). "Sustainable geopolymer composites reinforced with flax tows." *Ceramics International*, 46(8), 12870–12875.

Lazorenko, G., Kasprzhitskii, A., Shaikh, F., Krishna, R. S., and Mishra, J. (2021). "Utilization potential of mine tailings in geopolymers: Physicochemical and environmental aspects." *Process Safety and Environmental Protection*, 147, 559–577.

Lazorenko, G., Kasprzhitskii, A., Yavna, V., Mischinenko, V., Kukharskii, A., Kruglikov, A., Kolodina, A., and Yalovega, G. (2020b). "Effect of pre-treatment of flax tows on mechanical properties and microstructure of natural fiber reinforced geopolymer composites." *Environmental Technology & Innovation*, 20, 101105.

Leong, H. Y., Ong, D. E. L., Sanjayan, J. G., and Nazari, A. (2016). "The effect of different Na2O and K2O ratios of alkali activator on compressive strength of fly ash based-geopolymer." *Construction and Building Materials*, 106, 500–511.

Li, Y., Wu, D., Zhang, J., Chang, L., Wu, D., Fang, Z., and Shi, Y. (2000). "Measurement and statistics of single pellet mechanical strength of differently shaped catalysts." *Powder technology*, 113(1–2), 176–184.

Li, Z., Wang, L., and Ma, G. (2019). "Method for the enhancement of buildability and bending resistance of three-dimensional-printable tailing mortar." *3D Concrete printing technology*, Elsevier, 161–180.

Longhi, M. A., Zhang, Z., Rodríguez, E. D., Kirchheim, A. P., and Wang, H. (2019). "Efflorescence of alkali-activated cements (geopolymers) and the impacts on material structures: A critical analysis." *Frontiers in Materials*, 6, 89.

Lottermoser, B. G. (2011). "Recycling, reuse and rehabilitation of mine wastes." *Elements*, 7(6), 405–410.

Manikandan, R., and Ramamurthy, K. (2007). "Influence of fineness of fly ash on the aggregate pelletization process." *Cement and Concrete Composites*.

Manikandan, R., and Ramamurthy, K. (2008). "Effect of curing method on characteristics of cold bonded fly ash aggregates." *Cement and concrete composites*, 30(9), 848–853.

Manikandan, R., and Ramamurthy, K. (2009). “Swelling characteristic of bentonite on pelletization and properties of fly ash aggregates.” *Journal of materials in civil engineering*, 21(10), 578–586.

Manjarrez, L., Nikvar-Hassani, A., Shadnia, R., and Zhang, L. (2019). “Experimental study of geopolymer binder synthesized with copper mine tailings and low-calcium copper slag.” *Journal of Materials in Civil Engineering*, 31(8), 4019156.

Manjarrez, L., and Zhang, L. (2018). “Utilization of copper mine tailings as road base construction material through geopolymerization.” *J. Mater. Civ. Eng*, 30(9), 4018201.

Mannan, M. A., and Neglo, K. (2010). “Mix design for oil-palm-boiler clinker (OPBC) concrete.” *Journal of Science and Technology (Ghana)*, 30(1).

Mishra, A., Choudhary, D., Jain, N., Kumar, M., Sharda, N., and Dutt, D. (2008). “Effect of concentration of alkaline liquid and curing time on strength and water absorption of geopolymer concrete.” *ARPN Journal of engineering and Applied Sciences*, 3(1), 14–18.

Montgomery, D. C. (2017). *Design and analysis of experiments*. John wiley & sons.

Moradi, M., You, Y., Hung, H., Li, J., Park, R., Alexandrou, N., Moussa, S. G., Jantunen, L., Robitaille, R., and Staebler, R. M. (2021). “Fugitive emissions of polycyclic aromatic compounds from an oil sands tailings pond based on fugacity and inverse dispersion flux calculations.” *Environmental Pollution*, 269, 116115.

Morsy, M. S., Alsayed, S. H., Al-Salloum, Y., and Almusallam, T. (2014). “Effect of sodium silicate to sodium hydroxide ratios on strength and microstructure of fly ash geopolymer binder.” *Arabian journal for science and engineering*, 39(6), 4333–4339.

Mustafa Al Bakri, A. M., Kamarudin, H., Bnhussain, M., Rafiza, A. R., and Zarina, Y. (2012). “Effect of Na 2 SiO 3/NaOH Ratios and NaOH Molarities on Compressive Strength of Fly-Ash-Based Geopolymer.” *ACI Materials Journal*, 109(5).

Nagaraj, D. R. (2000). “Minerals recovery and processing.” *Kirk-Othmer Encyclopedia of Chemical Technology*.

Nath, P., Sarker, P. K., and Rangan, V. B. (2015). “Early age properties of low-calcium fly ash geopolymer concrete suitable for ambient curing.” *Procedia Engineering*, 125, 601–607.

Nguyen, T. A. H., Liu, Y., Wu, S., and Huang, L. (2022). “Unravelling in-situ hardpan

properties and functions in capping sulfidic Cu-Pb-Zn tailings and forming a duplex soil system cover." *Journal of Hazardous Materials*, 425, 127943.

Nikolić, V., Komljenović, M., Baščarević, Z., Marjanović, N., Miladinović, Z., and Petrović, R. (2015). "The influence of fly ash characteristics and reaction conditions on strength and structure of geopolymers." *Construction and Building materials*, 94, 361–370.

Niu, F. S., Zhou, S. S., Liu, S. X., and Zhang, J. X. (2011). "Study of manufacture process and properties of tailings and slag based geopolymers." *Advanced Materials Research*, 156, 803–807.

Nor, A. M., Yahya, Z., Abdullah, M. M. A. B., Razak, R. A., Ekaputri, J. J., Faris, M. A., and Hamzah, H. N. (2016). "A Review on the Manufacturing of Lightweight Aggregates Using Industrial By-Product." *MATEC Web of Conferences*, EDP Sciences, 1067.

Nurcholis, M., Yudiantoro, D. F., Haryanto, D., and Mirzam, A. (2017). "Heavy metals distribution in the artisanal gold mining area in Wonogiri." *Indonesian Journal of Geography*, 49(2), 133–144.

Obenaus-Emler, R., Falah, M., and Illikainen, M. (2020). "Assessment of mine tailings as precursors for alkali-activated materials for on-site applications." *Construction and Building Materials*, 246, 118470.

Oktay, H., Yumrutaş, R., and Akpolat, A. (2015). "Mechanical and thermophysical properties of lightweight aggregate concretes." *Construction and Building Materials*, 96, 217–225.

Osinubi, K. J., Yohanna, P., and Eberemu, A. O. (2015). "Cement modification of tropical black clay using iron ore tailings as admixture." *Transportation Geotechnics*, 5, 35–49.

Palmer, M. A., Bernhardt, E. S., Schlesinger, W. H., Eshleman, K. N., Foufoula-Georgiou, E., Hendryx, M. S., Lemly, A. D., Likens, G. E., Loucks, O. L., and Power, M. E. (2010). "Mountaintop mining consequences." *Science*, 327(5962), 148–149.

Palomo, A., Grutzeck, M. W., and Blanco, M. T. (1999). "Alkali-activated fly ashes: A cement for the future." *Cement and concrete research*, 29(8), 1323–1329.

Palomo, Á., Kavalerova, E., Fernández-Jiménez, A., Krivenko, P., García-Lodeiro, I., and Maltseva, O. (2015). "A review on alkaline activation: new analytical perspectives."

Panagiotopoulou, C., Kontori, E., Perraki, T., and Kakali, G. (2007). "Dissolution of

aluminosilicate minerals and by-products in alkaline media." *Journal of Materials Science*, 42(9), 2967–2973.

Patankar, S. V, Ghugal, Y. M., and Jamkar, S. S. (2014). "Effect of concentration of sodium hydroxide and degree of heat curing on fly ash-based geopolymer mortar." *Indian Journal of Materials Science*, 2014.

Phoo-ngernkham, T., Maegawa, A., Mishima, N., Hatanaka, S., and Chindaprasirt, P. (2015). "Effects of sodium hydroxide and sodium silicate solutions on compressive and shear bond strengths of FA–GBFS geopolymer." *Construction and Building Materials*, 91, 1–8.

Priyadharshini, P., Ganesh, G. M., and Santhi, A. S. (2012). "A review on artificial aggregates." *International Journal of Earth Sciences and Engineering*, 5(3), 540–546.

Priyadharshini, P., Ganesh, M. G., and Santhi, A. S. (2011). "Experimental study on cold bonded fly ash aggregates." *International journal of Civil and Structural engineering*, 2(2), 493.

Provis, J. L., and Deventer, J. S. J. Van. (2009). *Geopolymers: structures, processing, properties and industrial applications*. Elsevier.

Qaidi, S. M. A., Tayeh, B. A., Zeyad, A. M., Azevedo, A. R. G. de, Ahmed, H. U., and Emad, W. (2022). "Recycling of mine tailings for the geopolymers production: A systematic review." *Case Studies in Construction Materials*, 16, e00933.

Qi, C., and Fourie, A. (2019). "Cemented paste backfill for mineral tailings management: Review and future perspectives." *Minerals Engineering*, 144, 106025.

Rafeet, A., Vinai, R., Soutsos, M., and Sha, W. (2019). "Effects of slag substitution on physical and mechanical properties of fly ash-based alkali activated binders (AABs)." *Cement and Concrete Research*, 122, 118–135.

Ramamurthy, K., and Harikrishnan, K. I. (2006). "Influence of binders on properties of sintered fly ash aggregate." *Cement and Concrete Composites*, 28(1), 33–38.

Rangan, B. V., Hardjito, D., Wallah, S. E., and Sumajouw, D. M. J. (2005). "Studies on fly ash-based geopolymer concrete." *Proceedings of the World Congress Geopolymer, Saint Quentin, France*, 133–137.

Rao, P. V. T. (1994). "Agglomeration and prereduction of ores."

Rattanasak, U., and Chindaprasirt, P. (2009). “Influence of NaOH solution on the synthesis of fly ash geopolymer.” *Minerals Engineering*, 22(12), 1073–1078.

Rattanasak, U., Pankhet, K., and Chindaprasirt, P. (2011). “Effect of chemical admixtures on properties of high-calcium fly ash geopolymer.” *International Journal of Minerals, Metallurgy, and Materials*, 18(3), 364–369.

Reddy, M. V. S., Nataraja, M., Sindhu, K., Harani, V., and Madhuralalasa, K. (2016). “Performance of light weight concrete using fly ash pellets as coarse aggregate replacement.” *International Journal of Engineering Research Technology*, 9, 95–104.

Rico, M., Benito, G., Salgueiro, A. R., Díez-Herrero, A., and Pereira, H. G. (2008). “Reported tailings dam failures: a review of the European incidents in the worldwide context.” *Journal of hazardous materials*, 152(2), 846–852.

Ridtirud, C., Chindaprasirt, P., and Pimraksa, K. (2011). “Factors affecting the shrinkage of fly ash geopolymers.” *International Journal of Minerals, Metallurgy, and Materials*, 18(1), 100–104.

Risdanareni, P., Ekaputri, J. J., and Triwulan. (2015). “The influence of alkali activator concentration to mechanical properties of geopolymer concrete with trass as a filler.” *Materials Science Forum*, Trans Tech Publ, 125–134.

Rosas-Casarez, C. A., Arredondo-Rea, S. P., Gómez-Soberón, J. M., Alamaral-Sánchez, J. L., Corral-Higuera, R., Chinchillas-Chinchillas, M. de J., and Acuña-Agüero, O. H. (2014). “Experimental study of XRD, FTIR and TGA techniques in geopolymeric materials.” *Int. J. Adv. Comput. Sci. Appl*, 4(4), 221–226.

Sadat, M. R., Bringuier, S., Asaduzzaman, A., Muralidharan, K., and Zhang, L. (2016). “A molecular dynamics study of the role of molecular water on the structure and mechanics of amorphous geopolymer binders.” *The Journal of chemical physics*, 145(13), 134706.

Sahoo, S., Das, B. B., and Mustakim, S. (2017). “Acid, alkali, and chloride resistance of concrete composed of low-carbonated fly ash.” *Journal of Materials in Civil Engineering*, 29(3), 4016242.

Salam, A. M., Örmeci, B., and Simms, P. H. (2021). “Determination of optimum polymer dosage for dewatering of oil sands tailings using torque rheology.” *Journal of Petroleum Science and Engineering*, 197, 107986.

Santos, L. F. dos, Carvalho, J. M. F. de, Peixoto, R. A. F., and Brigolini, G. J. (2019). “Iron

ore tailing-based geopolymer containing glass wool residue: A study of mechanical and microstructural properties." *Construction and Building Materials*, 220, 375–385.

Sastry, K. V. S. G. K., Sahitya, P., and Ravitheja, A. (2021). "Influence of nano TiO2 on strength and durability properties of geopolymer concrete." *Materials Today: Proceedings*, 45, 1017–1025.

Sedira, N., and Castro-Gomes, J. (2019). "Effects of EAF-Slag on alkali-activation of tungsten mining waste: mechanical properties." *MATEC Web of Conferences*, EDP Sciences, 1003.

Sedira, N., Castro-Gomes, J., and Magrinho, M. (2018). "Red clay brick and tungsten mining waste-based alkali-activated binder: Microstructural and mechanical properties." *Construction and Building Materials*, 190, 1034–1048.

Sharath, B. P., and Das, B. B. (2021). "Production of Artificial Aggregates Using Industrial By-Products Admixed with Mine Tailings—A Sustainable Solution." *Recent Trends in Civil Engineering*, Springer, 383–397.

Sharath, B. P., K, S., and Das, B. B. (2022). "Influence of Geopolymerization Factors on Sustainable Production of Pelletized Fly Ash Based Aggregates Admixed with Bentonite, Lime and Ggbs." *Journal of materials in civil engineering*, 35(11).

Sharath, B. P., Nikunj, P., and Das, B. B. (2023a). "Influence of Integration of Iron Ore Tailings on the Physio-mechanical and Microstructure Properties of Fly Ash–Based Coarse Aggregates." *Journal of Testing and Evaluation*, 51(5).

Sharath, B. P., Shivaprasad, K. N., Athikkal, M. M., and Das, B. B. (2018). "Some studies on sustainable utilization of iron ore tailing (IOT) as fine aggregates in fly ash based geopolymer mortar." *IOP conference series: materials science and engineering*, IOP Publishing, 92010.

Sharath, B. P., Snehal, K., Das, B. B., and Barbhuiya, S. (2023b). "Influence of Geopolymerization Factors on Sustainable Production of Pelletized Fly Ash–Based Aggregates Admixed with Bentonite, Lime, and GGBS." *Journal of Materials in Civil Engineering*, 35(11), 4023423.

Shivaprasad, K. N., and Das, B. B. (2017). "Influence of alkali binder dosage on the efficiency of pelletization of aggregates from iron ore tailing and fly ash." *Int J Eng Res Mechan Civil Eng*, 2(3), 388–392.

Shivaprasad, K. N., and Das, B. B. (2018). "Determination of optimized geopolymerization factors on the properties of pelletized fly ash aggregates." *Construction and Building Materials*, 163, 428–437.

Shuaibu, R. A. (2014). "Compressive strength of low calcium fly ash geopolymer concrete-A Review." *International Journal of Emerging Technology and Advanced Engineering*, 4(4).

Singh, J., and Singh, S. P. (2019). "Development of alkali-activated cementitious material using copper slag." *Construction and building materials*, 211, 73–79.

Singh, L. P., Goel, A., Bhattacharyya, S. K., Sharma, U., and Mishra, G. (2015). "Hydration studies of cementitious material using silica nanoparticles." *Journal of Advanced Concrete Technology*, 13(7), 345–354.

Singh, P. S., Trigg, M., Burgar, I., and Bastow, T. (2005). "Geopolymer formation processes at room temperature studied by 29Si and 27Al MAS-NMR." *Materials Science and Engineering: A*, 396(1–2), 392–402.

Sivakumar, A., and Gomathi, P. (2012). "Pelletized fly ash lightweight aggregate concrete: A promising material." *Journal of Civil Engineering and Construction Technology*, 3(2), 42–48.

Snehal, K., Das, B. B., and Akanksha, M. (2020). "Early age, hydration, mechanical and microstructure properties of nano-silica blended cementitious composites." *Construction and Building Materials*, 233, 117212.

Snehal, K., Das, B. B., and Barbhuiya, S. (2022). "Influence of aggressive exposure on the degradation of nano-silica admixed cementitious mortar integrated with phase change materials." *Construction and Building Materials*, 335, 127467.

Somna, K., Jaturapitakkul, C., Kajitvichyanukul, P., and Chindaprasirt, P. (2011). "NaOH-activated ground fly ash geopolymer cured at ambient temperature." *Fuel*, 90(6), 2118–2124.

Soudki, K. A., El-Salakawy, E. F., and Elkum, N. B. (2001). "Full factorial optimization of concrete mix design for hot climates." *Journal of materials in civil engineering*, 13(6), 427–433.

Sumer, M. (2012). "Compressive strength and sulfate resistance properties of concretes containing Class F and Class C fly ashes." *Construction and Building Materials*, 34, 531–

536.

Sunil, B. M., Manjunatha, L. S., Ravi, L., and Yaragal, S. C. (2015). “Potential use of mine tailings and fly ash in concrete.” *Advances in concrete construction*, 3(1), 55.

Tajra, F., Abd Elrahman, M., Chung, S.-Y., and Stephan, D. (2018). “Performance assessment of core-shell structured lightweight aggregate produced by cold bonding pelletization process.” *Construction and Building Materials*, 179, 220–231.

Tajra, F., Abd Elrahman, M., and Stephan, D. (2019). “The production and properties of cold-bonded aggregate and its applications in concrete: A review.” *Construction and Building Materials*, 225, 29–43.

Tang, P., and Brouwers, H. J. H. (2018). “The durability and environmental properties of self-compacting concrete incorporating cold bonded lightweight aggregates produced from combined industrial solid wastes.” *Construction and Building Materials*, 167, 271–285.

Tang, P., Florea, M. V. A., and Brouwers, H. J. H. (2017). “Employing cold bonded pelletization to produce lightweight aggregates from incineration fine bottom ash.” *Journal of cleaner production*, 165, 1371–1384.

Teixeira-Pinto, A., Fernandes, P., and Jalali, S. (2002). “Geopolymer manufacture and application-Main problems when using concrete technology.” *Geopolymers 2002 International Conference, Melbourne, Australia, Siloxo Pty. Ltd*.

Terzić, A., Pezo, L., Mitić, V., and Radojević, Z. (2015). “Artificial fly ash based aggregates properties influence on lightweight concrete performances.” *Ceramics international*, 41(2), 2714–2726.

Thejas, H. K., and Hossiney, N. (2022). “Alkali-activated bricks made with mining waste iron ore tailings.” *Case Studies in Construction Materials*, 16, e00973.

Thomas, J., and Harilal, B. (2015). “Properties of cold bonded quarry dust coarse aggregates and its use in concrete.” *Cement and Concrete Composites*, 62, 67–75.

Vargas, A. S. de, Dal Molin, D. C. C., Masuero, Â. B., Vilela, A. C. F., Castro-Gomes, J., and Gutierrez, R. M. de. (2014). “Strength development of alkali-activated fly ash produced with combined NaOH and Ca (OH) 2 activators.” *Cement and Concrete Composites*, 53, 341–349.

Vasugi, V., and Ramamurthy, K. (2014). “Identification of design parameters influencing

manufacture and properties of cold-bonded pond ash aggregate." *Materials & Design (1980-2015)*, 54, 264–278.

Vickers, N. J. (2017). "Animal communication: when i'm calling you, will you answer too?" *Current biology*, 27(14), R713–R715.

Videla, C., and Martinez, P. M. (2002). "Fly ash lightweight aggregates produced by cold bonding for sustainable concrete construction." *Challenges of Concrete Construction: Volume 5, Sustainable Concrete Construction: Proceedings of the International Conference held at the University of Dundee, Scotland, UK on 9–11 September 2002*, Thomas Telford Publishing, 363–372.

Vijay, P. (2015). "Use of fly ash aggregates in concrete and its applications in structures." *Int. J. Re. Devel. Eng. Technol*, 4(7).

Wang, A., Liu, H., Hao, X., Wang, Y., Liu, X., and Li, Z. (2019). "Geopolymer synthesis using garnet tailings from molybdenum mines." *Minerals*, 9(1), 48.

Wang, H., Li, H., and Yan, F. (2005). "Synthesis and mechanical properties of metakaolinite-based geopolymer." *Colloids and Surfaces A: Physicochemical and Engineering Aspects*, 268(1–3), 1–6.

Wasserman, R., and Bentur, A. (1997). "Effect of lightweight fly ash aggregate microstructure on the strength of concretes." *Cement and Concrete Research*, 27(4), 525–537.

Wei, B., Zhang, Y., and Bao, S. (2017). "Preparation of geopolymers from vanadium tailings by mechanical activation." *Construction and Building Materials*, 145, 236–242.

Wuddivira, M. N., Robinson, D. A., Lebron, I., Bréchet, L., Atwell, M., Caires, S. De, Oatham, M., Jones, S. B., Abdu, H., and Verma, A. K. (2012). "Estimation of soil clay content from hygroscopic water content measurements." *Soil Science Society of America Journal*, 76(5), 1529–1535.

Yang, K.-H., Mun, J.-H., Sim, J.-I., and Song, J.-K. (2011). "Effect of water content on the properties of lightweight alkali-activated slag concrete." *Journal of materials in civil engineering*, 23(6), 886–894.

Yao, G., Wang, Q., Wang, Z., Wang, J., and Lyu, X. (2020). "Activation of hydration properties of iron ore tailings and their application as supplementary cementitious materials in cement." *Powder Technology*, 360, 863–871.

Ye, J., Zhang, W., and Shi, D. (2017). “Properties of an aged geopolymer synthesized from calcined ore-dressing tailing of bauxite and slag.” *Cement and Concrete Research*, 100, 23–31.

Zhai, Q., Liu, R., Wang, C., Wen, X., Li, X., and Sun, W. (2022). “A novel scheme for the utilization of Cu slag flotation tailings in preparing internal electrolysis materials to degrade printing and dyeing wastewater.” *Journal of Hazardous Materials*, 424, 127537.

Zhang, C., Wang, X., Hu, Z., Wu, Q., Zhu, H., and Lu, J. (2021). “Long-term performance of silane coupling agent/metakaolin based geopolymer.” *Journal of Building Engineering*, 36, 102091.

Zhang, J. X., Liu, S. X., and Xie, J. (2013). “Study of Manufacture Process and Properties of Tailings and Slag Based Mine Filling Cementitious Materials.” *Advanced Materials Research*, Trans Tech Publ, 1077–1081.

Zhang, L., Ahmari, S., and Zhang, J. (2011). “Synthesis and characterization of fly ash modified mine tailings-based geopolymers.” *Construction and Building Materials*, 25(9), 3773–3781.

Zhang, W., Long, J., Zhang, X., Shen, W., and Wei, Z. (2020). “Pollution and ecological risk evaluation of heavy metals in the soil and sediment around the HTM tailings pond, Northeastern China.” *International journal of environmental research and public health*, 17(19), 7072.

Zhao, S., Xia, M., Yu, L., Huang, X., Jiao, B., and Li, D. (2021). “Optimization for the preparation of composite geopolymer using response surface methodology and its application in lead-zinc tailings solidification.” *Construction and Building Materials*, 266, 120969.

Zhao, X., Liu, C., Zuo, L., Wang, L., Zhu, Q., and Wang, M. (2019). “Investigation into the effect of calcium on the existence form of geopolymerized gel product of fly ash based geopolymers.” *Cement and Concrete Composites*, 103, 279–292.

Zhou, W., Wang, Y., Lian, Z., Yang, T., Zeng, Q., Feng, S., Fang, Z., Shu, W., Huang, L., and Ye, Z. (2020). “Revegetation approach and plant identity unequally affect structure, ecological network and function of soil microbial community in a highly acidified mine tailings pond.” *Science of the Total Environment*, 744, 140793.

PATENTS AND PUBLICATIONS BASED ON THE PRESENT RESEARCH WORK

PATENTS FILED AT INDIAN PATENT OFFICE

1. Patent filed titled "Optimized Proportion for Producing Fly ash Based Coarse Aggregates Integrated with Iron Ore Tailings" bearing **Application no**: 202341052223
   Status: Application in Hearing
2. Patent filed titled "A Composition for Production of Fly ash Based Pelletized Aggregates with Burnt Lime" bearing **Application no**: 202341058070
   Status: Application referred u/s 12 for examination.
3. Patent filed titled "Optimized Proportion for Production of Fly ash Based Pelletized Aggregates Integrated with Copper ore Tailings" bearing **Application no**: 202341058070
   Status: Application referred u/s 12 for examination

INTERNATIONAL JOURNALS (SCI/SCOPUS Indexed)

B. P. Sharath, Snehal K, B. B. Das and Salim Barbhuiya, "Influence of Geopolymerization Factors on Sustainable Production of Pelletized Fly Ash–Based Aggregates Admixed with Bentonite, Lime, and GGBS", *Journal of Materials in Civil Engineering*, ASCE Publications., 35, no.11 (2023)
DOI: https://10.1061/JMCEE7.MTENG-15200

B.P. Sharath, P. Nikunj, and B. B. Das. "Influence of Integration of Iron Ore Tailings on the Physio-mechanical and Microstructure Properties of Fly Ash–Based Coarse Aggregates." *Journal of Testing and Evaluation*, ASTM Publications 51, no. 5 (2023).
DOI: https://doi.org/10.1520/JTE20220466

BOOK CHAPTERS (SCOPUS INDEXED)

B. P. Sharath, A. R. Akhliesh Kumar and B. B. Das, "Comparison of multi criterion decision making approaches (MCDM) on produced fly ash based pelletized geopolymer coarse aggregates integrated with iron ore tailings", In Indian Concrete Journal, 2024.

B. P. Sharath and B. B. Das, "Production of artificial aggregates using industrial by-products admixed with mine tailings—a sustainable solution." In *Recent Trends in Civil Engineering: Select Proceedings of TMSF 2019*, pp. 383-397. Springer Singapore, 2021.

DOI: https://doi.org/10.1007/978-981-15-8293-6_33

B. P. Sharath, and B. B. Das. "Engineering Properties of Heavyweight Concrete—A Review." Smart Technologies for Sustainable Development: Select Proceedings of SMTS 2019 (2021): 297-314.
DOI: https://doi.org/10.1007/978-981-15-5001-0_25

B. P. Sharath, K. N. Shivaprasad, M. M. Athikkal, and B. B. Das. "Some studies on sustainable utilization of iron ore tailing (IOT) as fine aggregates in fly ash based geopolymer mortar." In IOP conference series: materials science and engineering, vol. 431, no. 9, p. 092010. IOP Publishing, 2018.
DOI: https://doi.org/10.1088/1757-899X/431/9/092010

OTHER PUBLICATIONS

Prasanna, K. M., **B. P. Sharath**, Himanshu Choukade, K. N. Shivaprasad, B. B. Das, and Gangadhar Mahesh. "Research on Setting Time, Compressive Strength and Microstructure of Fly Ash-Based Geopolymer Mixture Containing Slag." *Iranian Journal of Science and Technology, Transactions of Civil Engineering* (2022): 1-15.
DOI: https://doi.org/10.1007/s40996-022-01010-9

K N Shivaprasad, B. B. Das and **B. P. Sharath**, "Pelletization Factors on the Production of Fly ash Aggregates and its Performance in Cement Concrete, *Proceedings of the Institution of Civil Engineers - Construction Materials*, ICE Publications (2020) 1–57.
DOI: https://doi.org/10.1680/jcoma.19.00053

CURRICULUM VITAE

PERSONAL DETAILS:

Name	:	**B. P. SHARATH**
Father's Name	:	B. V. PRAKASH
Mother's Name	:	A. B. SAROJA
Date of Birth	:	29-03-1993
E-Mail ID	:	bpsharath1993@gmail.com
Contact Number	:	Mobile: +91-7019501664; 8951352236

EDUCATIONCAL QUALIFICATION:

Course	Institution/University	Year of Passing	Class obtained	Percentage of Marks
B.E. (Civil Engineering)	NITTE University	2014	First Class	67%
M.Tech (Construction Technology and Management)	SDIT, Mangalore	2016	First Class with Distinction	75%

WORK EXPERIENCE:

ORGANIZATION	POSTS HELD	DURATION
National Institute of Technology, Tiruchirappalli, Tamil Nadu	Contract Faculty	Stared in November 2023
National Institute of Technology Karnataka, Surathkal, Mangalore	Research Scholar	July 2018 till Date
National Institute of Technology Karnataka, Surathkal, Mangalore	Junior Research Fellow	January 2018 till Date
Pinnacle Prime Constructions Pvt. Ltd., Bangalore	Quality Controller	March 2017 to January 2018

RESEARCH PUBLICATIONS:

Type of Publication	Number of Publications
Patents Filed	3
International Journal Publications	4
Book Chapters	4